CONDITION MONITORING BASED ON A WIRELESS, DISTRIBUTED AND SCALABLE PLATFORM

ER POI VOON

(*B. ENG. (EE), NUS*)

A THESIS SUBMITTED

FOR THE DEGREE OF DOCTOR OF PHILOSOPHY

DEPARTMENT OF ELECTRICAL AND COMPUTER ENGINEERING

NATIONAL UNIVERSITY OF SINGAPORE

2016

DECLARATION

I hereby declare that the thesis is my original work and it has been written by me in its entirety. I have duly acknowledged all the sources of information which have been used in the thesis.

This thesis has also not been submitted for any degree in any university previously.

Er Poi Voon

25-Aug-2016

Acknowledgments

First and foremost, I would like to take this opportunity to express my heartfelt gratitude to my supervisor, Prof. Tan Kok Kiong, for his guidance, inspiration and encouragement throughout the course of my Ph.D studies. He has been instrumental in guiding me in the right path whenever I seemed to deviate or lose focus in the research direction. This thesis cannot be completed without his invaluable advice and support throughout my research project.

I shall extend my gratitude to the National University of Singapore for subsidizing my course fees during my tenured as a Research Engineer in the NUS-SIMTech Joint Laboratory (Precision Motion Systems), Department of Electrical and Computer Engineering. My sincere thanks to the Lee Foundation for the awards of bursaries throughout my Ph.D studies.

I shall extend my thanks to all my friends and colleagues at the Mechatronics & Automation Lab, for their companionship and made my graduate experience more enjoyable. Our friendship is truly precious and priceless.

Finally, I would like to express my deepest love and gratitude to my family members especially to my parents. Thanks for providing me with much needed mental supports, sharing my ups and downs throughout this challenging but enriching journey.

Contents

Summary

This thesis focuses on the development of technologies for condition monitoring (CM) targeted for industrial and manufacturing, and healthcare, all pulled by real and significant industrial and healthcare needs. Three collaborations with industrial partners and healthcare practitioners resulted in the development of a configurable, generic, distributed and scalable wireless CM system prototypes. The prototypes leverage on an appropriate synergy of constituent technologies in embedded systems, wireless network, sensing and instrumentation, and their different applications share a unified design architecture which allows these technologies to be integrated where appropriate. Apart from a unified platform, these works are based on analogy of sound and vibrations generated, be they from industrial machine or humans under monitor. The thesis may thus be regarded as a collation of results enabling an advance in technology frontiers to allow novel industrial and healthcare CM applications, building on high power and cost efficiency, embedded and wireless CM platforms.

The first work focuses on the research of sensors placement on a precision machine for CM. The idea behind this chapter is based on the requirement from Singapore Institute of Manufacturing and Technology (SIMTech) to realize an optimal sensors placement methodology for inferring accurate vibration profiles of a critical point. Moving mechanical parts in a machine will inevitably generate vibration profiles reflecting its operating conditions. Vibration profile analysis is a useful tool for CM to avoid loss of performance and unwanted machine down-time.

The second work highlights the need to develop a new method of CM for precision machine by analyzing generated sound. This idea is pulled from the discussions with Makino regarding the common approaches used by experienced service engineers for impending machine fault detection. By manually sensing the vibration with hand, and listening to the sound generated from a machine, an engineer is able to determine if the machine is healthy and operating normally, and any abnormal vibration and sound can represent an impending machine failure. The current method is very subjective based on the accumulated experience of the engineer, and the mental models are difficult to be imparted to a new engineer. Thus, a new CM method is proposed by using the proposed CM system prototype.

The third work details the deployment of the CM system prototype reconfigured for healthcare based CM (e-HealthCM). This chapter is pulled by an aging demography in Singapore and consequent of collaboration/discussions with Southwest CDC (Community Development Council), Ministry of Health and Family Welfare, Housing Development Board, the LionsBefrienders and other welfare communities. The e-HealthCM system is tailored for use by senior citizens to allow them to age in grace in their own homes as there is an increasing trend in the number of senior citizens staying by themselves. In an increasing number of unfortunate situations, senior citizens lost their lives in their own apartments from accidental falls without anyone knowing. e-HealthCM system monitors a senior citizen's home for accidental fall activity and to automatically request for assistance when a fall is detected.

The works resulted in six papers being written.

List of Tables

List of Figures

Chapter 1

Introduction

Embedded system, wireless communication, and sensors have been the key building blocks [1] that fuel many innovative monitoring solutions in different areas that include but not limited to medical, manufacturing, engineering and logistics. The fusion of embedded system with wireless communication technology and sensors can form powerful condition monitoring (CM) solutions that are both distributed and scalable [2]. The pervasive nature of such a wireless network ensures a distributed topology with a high degree of scalability.

Each wireless sensor node can be an autonomous embedded controller controlling one or more sensors, and communicates with other similar wireless node and central station via a defined wireless network infrastructure [3] [4]. Such a platform can be deployed in different wide area (or pervasive) monitoring applications for health CM such as high technology manufacturing facilities or in a hospital setting where patients' vital signs or physiological parameters are wirelessly monitored and information relayed to a central monitoring nursing station or in the homes of senior citizens where their motion activities are monitored for unwanted falls/accidents that may lead to injuries or deaths. The potential of such a system is unlimited. When the next wave of wireless and embedded technologies emerge, the next revision of the system will be more powerful with added functionalities, smaller in term of physical size, better power utilization, and lower in cost. There are several common choices of wireless infrastructures identified as suitable for implementations with an embedded system and sensors for pervasive monitoring purposes. These are: (a) ZIGBEE wireless Personal Access Network (PAN), (b) Wi-Fi network, and (c) GSM Wireless Network. The choice of an embedded system is usually defined by the type of a micro-controller unit (MCU) used as the core processing element. MCU adoption is widely dependent on the system requirements and performance of the embedded system itself, ranging from extremely low power 8-bit MCU with limited processing and memory capacities to the 32-bit based high-end MCU with rich built-in peripherals, high processing and memory capacities. The choice of sensors are dependent on the monitoring requirements.

A Wireless sensors network (WSN) can generally be described as a distributed embedded system with sensors and wireless connectivity that form a network of wireless nodes. The wireless nodes cooperatively sense and control the environment, enabling interaction among persons or computers and the surrounding environment [5]. WSNs usually include sensor nodes, gateways and clients. A large number of sensor nodes, deployed randomly inside of or near the monitoring area (sensor field), form networks through self-organization. Sensor nodes monitor the collected data to transmit along to other sensor nodes by hopping. During the process of transmission, monitored data may be handled by multiple nodes to get to gateway node after multi-hop routing, and finally reach the remote management node through the internet or satellite. It is the user who configures and manages the WSN with the management node, publish monitoring missions and collection of the monitored data.

WSN based CM systems [6] are very well established in industrial and manufacturing sectors where networked of miniature wireless sensors are attached to machines replacing their aged or faulty wired counterparts, providing higher precision and advanced CM features with minimal disruption or modification to the original machines. The same systems also found its applications in civil and structural engineering for structural health CM, and in healthcare and smart homes automations.

Internet-of-Things (IoT) refers to uniquely identifiable objects and their virtual representations in an Internet-like structure [7]. These objects can be anything from large buildings, industrial plants, planes, cars, machines, any kind of goods, specific parts of a larger system to human beings, animals and plants. The IoT is one such all-inclusive technological framework that enable these objects to collect and exchange data and the framework is far superior than the WSN, and not limited to sensors alone. The IoT allows objects to be sensed and controlled remotely across existing network infrastructure, creating opportunities for more direct integration of the physical world into computer-based systems, and resulting in improved efficiency, accuracy and economic benefits. The ability to network embedded devices with limited resources means that IoT finds applications in nearly every field. Such systems can be put in charge of collecting information in settings ranging from natural ecosystems to buildings, factories and healthcare [8]. WSN does not have the many advanced features of IoT, but the small, rugged, inexpensive and low powered WSN sensors will bring the IoT to even the smallest objects installed in any kind of environment at reasonable costs. Integration of these objects into IoT will be a major evolution of WSNs. In fact, one of the most important elements in the IoT paradigm is the WSN. The benefits of connecting both WSN and other IoT elements go beyond the remote access applications, as heterogeneous information systems are able to collaborate and provide common services [9].

1.1 Embedded System and Sensors

Embedded system plays a crucial role in building an electronic device with a certain level of computational intelligence. Embedded systems and sensors technology create portable devices with sensing and computing capabilities. Each embedded system device has a MCU as its core processing element where control logics, algorithms and communications are implemented [10]. Modern MCU has sufficient processing and memory resources to implement the most complex algorithms.

Figure 1.1 depicts a typical block diagram of an embedded system with sensor and communication system. Embedded system designed for sensor based condition monitoring is physically small and compact, relatively inexpensive, and with some set of sensors attached. These multiple "sensor nodes" are deployed in-situ, physically placed in the environment near the objects they are monitoring. The nodes are networked, allowing them to communicate and cooperate with each other to monitor the environment. These defined characteristics: embedded controller, attached sensor(s), and the ability to communicate, define the field of simple networking and differentiate it from the traditional centralized sensing systems [11] [12]. A cluster of these devices is useful for automated information gathering and distributed micro-sensing in many civil, military and industrial applications. Sensor networks use power aware computation and communication, low-energy signaling and networking, clustering and routing [13].

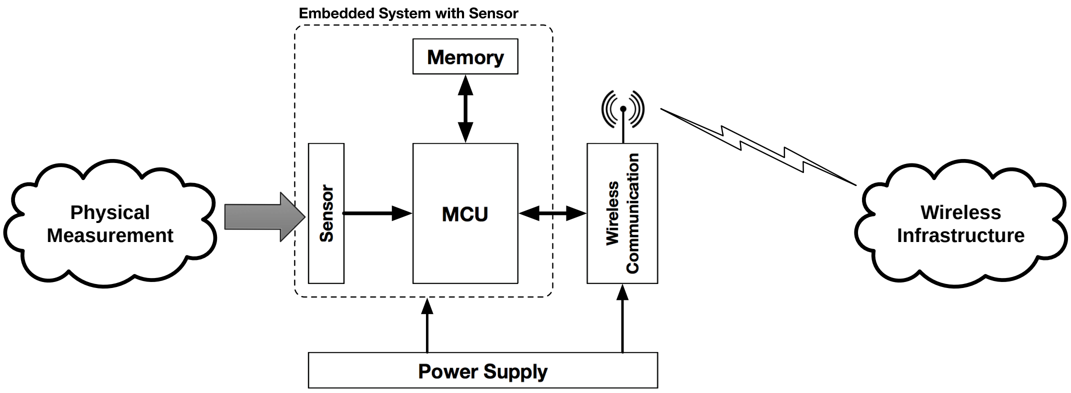

Figure 1.1: Block Diagram of Embedded System with Sensor and Communication.

Sensing technology has also kept pace with advancements of MCU, especially with the proliferation of Microelectromechanical system (MEMS) based sensors. Many such sensors have been incorporated into existing sensor node platforms. Despite their diversity, the principle of operation behind most of these MEMS sensors are the same. They all rely on environmental factors inducing changes in the electrical properties of appropriately chosen materials [14] [15]. The sensors incorporate sensitive circuitry to detect changes in these electrical properties, and are calibrated to correctly measure the corresponding environmental phenomenon. For example, a temperature sensor relies on changes in the resistivity of certain materials with temperature. The choice of material ranges from metals to semiconductors and is dictated by the required sensing range and sensitivity [15]. Similarly, a light sensor uses photoconductive materials whose electrical characteristics vary with the amount of light falling on them [16]. Finally, accelerometers measure the voltage induced by structural deformations of piezoelectric materials; these deformations are caused by vibration/acceleration [17].

1.2 Wireless Infrastructure

1.2.1 ZIGBEE Wireless PAN and WSN

ZIGBEE wireless PAN is one of the widely used low bandwidth and low power wireless communication infrastructure that implements a local area mesh-based wireless topology for WSN and other types of wireless systems. ZIGBEE's best quality is its low power consumption rate and long battery life (A fresh battery can typically lasts for months before a change in battery is required) [18]. It is one of the most established implementation in terms of link reliability and cost, and is one of the popular industry wireless mesh networking standard for connecting sensors, instrumentation and control systems [19]. ZIGBEE's low power consumption, built-in security method and ratified specifications make it very suitable to be used for sensor based condition/health monitoring [20]. ZIGBEE follows IEEE 802.15.4 specification, and is very robust and reliable even in a noisy radio frequency (RF) environment with no data packet lost or dropped [21]. ZIGBEE PAN is used to form a mesh type of inter-connecting sensors topology for pervasive monitoring.

Figure 1.2 depicts a typical ZIGBEE based WSN setup for CM. The setup consists of a ZIGBEE Coordinator module that forms and maintains a PAN, routers to extend the PAN and end devices as wireless sensors modules that are physically attached to the targets (e.g., machine) to be monitored. The Coordinator and Routers form a reliable mesh wireless PAN, and only the Coordinator connects to the Backend Server. Each end device connects to the nearest available Router or Coordinator. Data from each end device is either transmitted directly to the Coordinator or to the Coordinator via the Routers. The Coordinator transmits each sensor data to the Backend Server for processing [18] [19]. Each sensor is a wireless node and the PAN that is robust and scalable as new nodes can be easily added, and defective nodes removed/replaced [22].

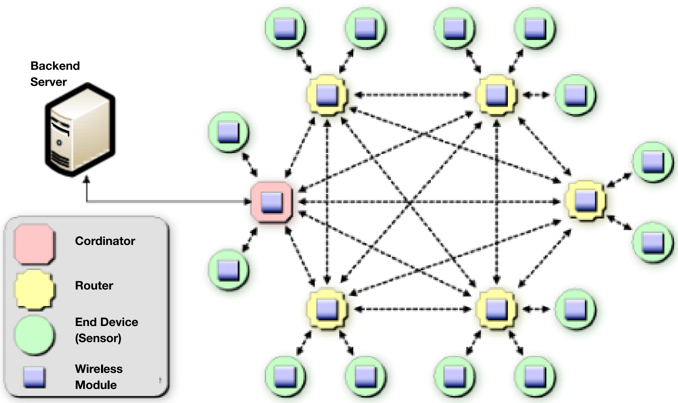

Figure 1.2: WSN Implementation Using ZIGBEE.

In a typical factory-floor scenario, wireless data communication performance is challenged by the presence of metallic machinery, which can reduce the signal strength of the wireless communication channel, create packet-losses within the data exchange, and require more robust protocol such as the IEEE 802.15.4 [23]. Despite these challenges with wireless communication in a factory, there are many potential advantages that can result from deploying WSNs. The individual nodes can be mounted on various parts of a machine tool and monitored for early fault detection and analysis. The small size and autonomy of the individual wireless nodes enables their placement in locations that are usually difficult to access. In addition, it is also possible, with minimal changes to the machine configuration, to retrofit sensors onto machinery after it has been installed. The sensor nodes not only monitor their own output but also collaborate with neighboring nodes to determine the health of the overall machines and provide early warnings of potential failure.

1.2.2 Wi-Fi and IoT

Wi-Fi is a local area network (LAN) infrastructure that provides wireless network access within an average range 30 to 100 meters [24] without repeaters. Wi-Fi is a star network where there's one central hub and all nodes or devices connect to it. This star topology makes it easy to add or remove devices without affecting the rest of the network [25]. Although faster than ZIGBEE, Wi-Fi traditionally is not a power-efficient network. Wi-Fi based devices will usually last only about 10 - 12 operating hours [26], which is one of the main reason for being less popular than ZIGBEE for WSN implementation. However, with constant technology improvements and with the strong emergence of the IoT initiative and developments, Wi-Fi is again becoming the communication technology of choice for WSN [27] [28]. A new kind of WSN, named Wi-Fi based WSN, came into reality [27] [29–32]. Wi-Fi based WSN is the combination of Wi-Fi wireless mesh network and WSNs, and it has both the features of traditional Wi-Fi network, network-centered, and WSN, data-centered [33].

Wi-Fi has attracted increasing attention in the IoT industry because Wi-Fi has the features of high bandwidth and rate, large-scale data collection and high cost-effective. But the power consumption of Wi-Fi based terminal is usually much higher than those low power based technologies like ZIGBEE, Bluetooth and etc. However, in recent years, some industry players have developed power efficient Wi-Fi chipset for sensors [34]. Studies [28] [35] have shown that these low power Wi-Fi chipset provides significant improvement on energy consumption and can be used for IoT sensors [36] [37]. Low power Wi-Fi sensors have the advantages of easy integration with an existing network infrastructure and built-in IP-based protocols, deployment without gateway. By taking advantage of existing infrastructure where most organizations already have a Wi-Fi infrastructure covering extensive areas of real estate. Adding more clients and applications is already a day-to-day activity, and given that IoT-based applications often involve infrequent transmissions and/or limited amounts of data, the additional load is unlikely to be much of a concern in most cases. Also note that many enterprize IoT applications will simply be new applications running on smart phones and similar devices that are already connected to the Wi-Fi network. Wi-Fi offers major advantages in capacity, coverage and ease of use. Low-cost, low power, and small-form-factor implementations, including a wide variety of ready-to-go Wi-Fi modules are the attractions of using Wi-Fi [38] [39]. As such, with continuous technological advancements, IoT may one day supersede the WSN.

1.2.3 GSM Cellular Wireless Network

The GSM cellular wireless network is a mobile phone based communication network that is established for wireless voice and data communication [40]. The GSM network technology has the highest penetration in both developed and developing countries [41] [42]. Most developing countries are well equipped with basic mobile phone based communication. With the availability of the basic infrastructures, it is structurally viable to deploy sensors to remote areas for monitoring purposes, with applications ranging from machine CM in manufacturing to human health monitoring in rural areas. By itself, GSM network is a matured technology, with multiple networks spanning across very wide areas defined by GSM base stations. The immediate advantage of adopting GSM network is in term of network coverage and cost savings, as network infrastructure investment is not required [43].

The GSM network used in sensor based monitoring application is usually in the form of a mobile ad-hoc/pervasive network [44]. A mobile sensor module (MSM) consists of an embedded system with an appropriate sensor attached to a GSM communication module (e.g., GSM modem, smartphone, and etc.). This MSM is by itself a self-contained autonomous module with pre-programmed intelligence that functions independently, performing its pre-programmed monitoring task and transmits result to a remote server via the GSM network. For wide geographical area remote monitoring applications, MSM is sufficient and is cost effective by making use of the existing GSM network infrastructure. Here, Wi-Fi and ZIGBEE are not suitable as they have limited wireless communication range and are suited only for local area coverage [45] [46].

Using multiple MSMs for local area monitoring will be an economical disadvantage when compared to utilizing ZIGBEE or Wi-Fi based wireless sensors. Each MSM incurs network utilization cost for utilizing the GSM network, and ZIGBEE or Wi-Fi based sensor does not incur such costs. Thus, MSM is only good for wide area based remote monitoring.

GSM network can still be deployed as part of a local area monitoring solution, but only functions as a backend communication link to a server located at a remote location. In this setup, ZIGBEE or Wi-Fi local area wireless are used for the wireless sensors nodes, and the data from all the sensors are collated and transmitted via the GSM network to a server located at a remote location. A known pitfall of the GSM network is in the area of power efficiency. GSM network is not power efficient and fares worse than the traditional Wi-Fi [47] [48], and a MSM consumes high amount of electrical power, and is not suitable for battery powered long term unattended monitoring operation [49–51]. Figure 1.3 depicts a summary where GSM network is being benchmarked with other wireless networks infrastructures in terms of power consumption, cost, complexity and data rate. It clearly indicates the GSM network is suitable to be used for pervasive monitoring in a wide geographical area network, which is the only advantage as compared to others. It fares poorly in other attributes.

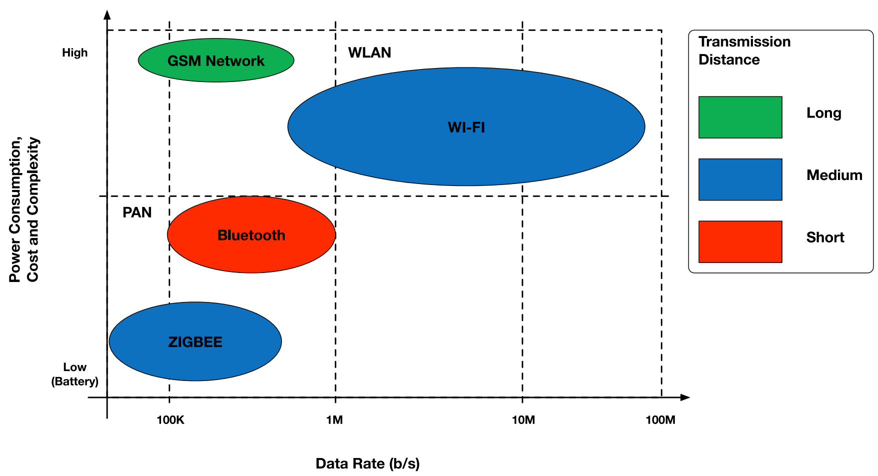

Figure 1.3: Summary of Wireless Networks' Power Consumptions, Costs, Complexities and Data Rates.

1.3 Motivation

1.3.1 Condition Monitoring for Industrial and Manufacturing

CM is a process where a target functional/operating parameter is measured from an attached sensor and being processed and analyzed. Every industrial and manufacturing system faces the problem of equipment amortization that introduces maintenance cost into the equation. Moreover, there is a need for structural and equipment CM techniques that could provide a global picture on subject condition and accurately predict equipment failures and therefore improve component and equipment reliability and performance. Furthermore, structural monitoring system detects system damages before the actual failures and minimizes the time that production line spends out of service, and thus increases the overall profit. Without CM system, it is necessary to schedule regular system checks and preventively replace production equipment, which can also include the risk of sending maintenance workers into hazardous environments.

CM can be implemented using existing WSNs or IoT frameworks, as both have the necessary resources to do so. Traditionally, CM is implemented using the WSN framework, and there are readily available and proven industrial solutions. WSN based CM has been widely deployed in areas like manufacturing, agriculture, logistic, civil engineering and in healthcare [52] [53]. In the industrial and manufacturing sectors, machine health condition is important as it affects yield and quality of the finished product produced by the machine itself. Engineers rely on CM and predictive maintenance techniques to ensure critical equipment such as generators, pumps, compressors, and motors operate more efficiently and last longer. Sensors commonly deployed for CM are: (a) accelerometer for object vibration measurement, (b) acoustic sensor for measuring object acoustic emission, (c) proximity sensor for measuring displacement, (d) tachometer for rotational speed, and (e) temperature sensor for measuring object surface temperature. In many cases, operational characteristics of a machine can be characterized by the outputs from these sensors, and a healthy machine will have a known set of characteristics (or signatures). Any deviations of these characteristics can be a sign of an impending machine fault or failure, and a maintenance for preventable machine failure can be performed [54].

In industrial and manufacturing monitoring, predictive maintenance and CM methodologies are used to enable day-to-day machinery monitoring and automation of data collection. Predictive maintenance analyzes sensors data using analytical models to estimate the condition of a component, machine, or process; whereas CM is an alarm-based methodology to monitor states of a machine. In fact, CM often supplement predictive maintenance by acting as an early warning system. Predictive maintenance [55] applications benefit from automation of the traditional manual process for collecting machine condition data and more frequent sampling, while CM applications benefit from more sensing points [56] [57]. Specific example applications of CM systems include motor analysis and machine tool performance monitoring. WSN-based CM systems can be readily used for small electric motors [58], and as a wire replacement for traditional motor vibration monitoring sensors [59]. In addition, WSNs enable new in-situ motor analysis opportunities previously not possible with wired sensors, including agent-based steady-state motor analysis [60] and onboard oil analysis [61]. Applications for machine tool monitoring include, temperature based CM sensors for end-mill inserts [62], and vibration-based CM for tool breakage [63].

Noise and vibration signals from machine contain vital information about the internal process and can provide valuable information about a machine running condition [64] [65]. Noise signals are measured in proximity to the external surface of the machine while vibration signals are measured on the surface of the machine. When a machine is in good condition, the generated noise and vibration frequency spectra will have certain characteristic shape. As faults begin to develop, the spectra change. But in most cases, these desired signals are mixed with other undesirable signals. Hence, analyses of these frequency spectra require some specialized signal processing methods to relate the spectra to the actual cause of faults in a machinery [66] [67].

In particular, vibrations of machine tools cause tool wear and tear, resulting from dynamic loading, structural element flexibility, cutting conditions, and spindle characteristics. These are often characterized by stability lobes describing regions of safe machining with respect to chatter and surface finish [68]. WSNs enable new opportunities not possible with wired sensors such as multi-sensor data fusion methods [69] to estimate tool wear using vibration monitoring of the spindle and workpiece. In addition, wireless sensing of current, voltage, and acoustic emission signals are also possible [70]. Figure 1.4 depicts a typical setup of WSN based CM where a ZIGBEE PAN is used extensively. Each end device is a wireless sensor attached to machines for CM purposes. The PAN is established by a coordinator and extended by the routers. Sensors use the PAN to transmit data to the Gateway Controller that pre-processes and collate the data before finally sending it to the Server for further data processing. The

Server sends out statuses and alerts to the receiving parties locally and remotely via a wired/wireless network.

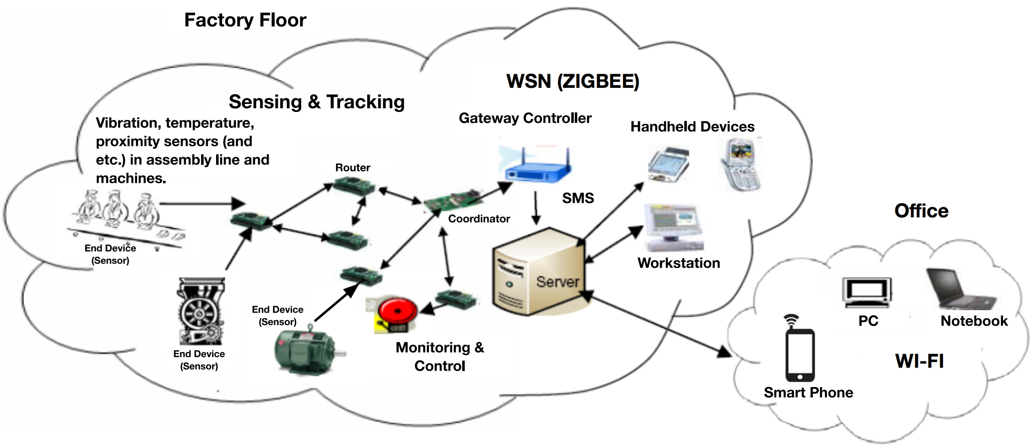

Figure 1.4: WSN for CM on a Factory Floor based on ZIGBEE PAN.

In another similar factory setting, Wright *et al* [57] propose the use of accelerometer based monitoring of machine vibrations and tackle the problem of predictive maintenance and CM of factory machinery in general. They demonstrate a linear relationship between surface finish, tool wear and machine vibrations thus proving the usability of proposed system in equipment monitoring. Krishnamurthy *et al* [71] focus on preventive equipment maintenance in which vibration signatures are gathered to predict equipment failure. They analyze the application of vibration analysis for equipment health monitoring in a central utility support building at a semiconductor fabrication plant that houses machinery to produce pure water, handle gases and process waste water for fabrication lines. Furthermore, authors deploy the same sensor network on an oil tanker in order to monitor the onboard machinery. In the end, they discuss design guidelines for an ideal platform and industrial applications, a study of the impact of the platform on the architecture, the comparison of two aforementioned deployments and a demonstration of application return on investment.

Various CM methods for unmanned manufacturing systems employing machining processes have been proposed and evaluated in the past, but evidence of these methods being adopted at the downstream is obscure. The main reason, as aforementioned, is the complexity behind the large-scale process which is affected by multiple factors and the constraints of machine to allow the retrofitting of multiple sensing and integrating them along with the control and intelligence into a single functional unit. Generally, published methods can be categorized into two main groups: (1) Direct method, which requires the machine tool to be removed from the machine, or the machine operations to be suspended in order to physically evaluate machine status such as the volumetric loss of the tool. Thus, this method is not suitable for continuous and real-time operations. (2) Indirect method leverages on the measurement of the machining variables such as force, vibration, acoustic emission and power dissipation during the machining process to compare them against normal operational signatures. The indirect method, while favorable from a practical perspective, is rather sensitive to machining parameters such as material variations and tool conditions, and a robust model is often necessary at the core of the approach. For continuous and real-time applications, the indirect approach has been the focus of various research works and they are mainly based on the algorithm of signal processing, sensor fusion and neural network [72–80].

The indirect method of machine CM relies significantly on the sensory system deployed to monitor the machine conditions. The important factors determining the effectiveness of such a scheme are: (1) Sensor placement methodologies, and

(2) Sensor selection and fusion to combine the multitude of sensory information available via intelligent signal processing algorithms to yield a machine condition indicator. Unless a good physical understanding of the machine is available, the selection of good sensor locations is mainly driven by engineering judgement and iterated with the data collected. Furthermore, it is rare that a specific location is optimal for detecting all types of disturbances, so that it is important to know the conditions under which a location is superior to another, in terms of yielding the appropriate information for machine CM. In order to obtain a comprehensive monitoring coverage with limited number of sensors, one of the important issues that must be considered is the evaluation of the relative effectiveness of various locations [81–94].

Extensive research works have been conducted in these areas, with various techniques developed to evaluate and quantify the performance. Salama *et al* [81] proposed using modal kinetic energy (MKE) as a mean of ranking the importance of candidate sensor locations. There has been several variants of this scheme based on the average kinetic energy and weighted average kinetic energy proposed by Chung and Moore [82]. Li *et al* [83] [84] studied the relation between the effective independent (EI) method and the MKE method. Kammer [85] proposed an iterative method using the EI method, based on the maximization of the determinant of the Fisher Information Matrix (FIM), to give a ranking to the sensor locations. FIM has been extensively used because it can be built from a finite element model of the machine structure or from the results of an experiment model [86–88]. Other performance indices that can be applied to sensor location evaluation are Error Covariance Matrix [90] [91], Information Entropy [92], Hankel Singular Values [93], and Controllability and Observability Gramian [94].

1.3.2 Condition Monitoring for Structural Health

Apart from industrial and manufacturing, CM is also widely used for monitoring of structural health. Advances in structural engineering depend upon the availability of many detailed data sets that record the response of different structures to ambient vibration (e.g., earthquakes, wind, passing vehicles, and etc.) or forced excitation delivered by large special-purpose shakers. Currently, structural engineers use wired or single-hop wireless data acquisition systems to acquire such data sets [95]. These systems consist of a device that collects and stores vibration measurements from a small number of sensors. However, power and wiring constraints imposed by these systems can increase the cost of acquiring these data sets, impose significant setup delays, and limit the number and location of sensors. WSNs can help address these issues, since they are easily deployable and configurable for this purpose. WSNs are used for structural monitoring (e.g., vibration monitoring) on buildings [95], wind turbines [96], coal mines [97], tunnels [98] and bridges [99] [100].

1.3.3 Condition Monitoring for Healthcare

In healthcare, CM of the human body vital and physiological parameters such as heart rate, respiratory rate, blood pressure, blood oxygen saturation, temperature and muscle activity, is analogous to the industrial based CM. The parameters can provide condition indicators of human health status (similar to machine health condition) and have tremendous diagnostic value. Healthcare

CM devices are not new and have been around for awhile, and they have seen deployments in various segments of healthcare. Sensors embedded in a variety of medical instruments for use at hospitals, clinics, and homes provide patients and their healthcare providers insight into physiological and physical health states that are critical to the detection, diagnosis, treatment, and management of ailments. Much of modern medicine would simply not be possible nor be cost effective without sensors such as thermometers, blood pressure monitors, glucose monitors, Electrocardiography (ECG), Photoplethysmogram (PPG), Electroencephalography (EEG), and various forms of imaging sensors.

Sensors beyond those that directly measure health states have also found use in the healthcare practice. For example, motion activity sensing technologies are being used in homes of senior citizens to assist in fall detections and preventions, and help maximize senior citizens' independence. For a senior citizen, experiencing a fall unobserved can be dangerous. The obvious possibility of initial injury may be further aggravated by the possible consequences if timely treatment is not obtained. For example, many elderly can suffer accidental falls due to weakness or dizziness, or due to their diminished self-care and self-protective ability. Since they tend to be fragile, these accidents may possibly have serious consequences if aids are not given in time. Statistics have shown that the majority of serious consequences are not the direct result of falling, but due to a delay in assistance and treatment. Post-fall consequences can be greatly reduced if relief personnel can be alerted in time [101].

Healthcare CM systems have the useful potentials to mitigate problematic patients access issues. Compared to patients in urban areas, patients in rural areas travel further to see trained healthcare professionals and have worse outcomes for common medical conditions such as diabetes, hypertension and heart failures [102]. Wearable wireless sensors and reliable remote healthcare CM systems have the potential to extend the reach of healthcare professionals in urban areas to rural areas and minimize these disparities [103].

CM Sensors to monitor vital signs (e.g., temperature, heart rate and respiratory rate) can be deployed, for instance when monitoring patients with congestive heart failure or patients with pulmonary disease undergoing clinical intervention [104] [103]. The major goal will be to achieve early detection of potential heart conditions by analyzing heartbeats and rhythms of the patients. Eliza *et al* [105] demonstrated a low power wearable electro-cardiogram (ECG) monitoring system for multiple-patient remote monitoring. To detect ECG, systems and methods relying upon wearable sensors have been proposed and evaluated. Each patient was required to wear an electronic wearable device featuring a miniature ECG sensor with wireless communication interface. Patients' ECG signals were monitored within the comfort of their own homes and transmitted to a centralized remote monitoring server where the data were analyzed. Healthcare professionals and caregivers would be notified in the event when abnormal heartbeats and rhythms were detected on any of the patients. This remote monitoring application will result in timely deployments of much needed medical interventions.

The earliest health CM solution relies on the GSM Cellular Wireless Network to transmit health data to remote servers. MobiHealth [106] is one of the early health CM projects that integrates all the wearable sensor devices such as mobile phones and watches that a person carries around during the day. The sensors continuously measure and transmit physiological data together with the audio and video recordings to health service providers in order to provide fast and reliable remote assistance in case of emergencies. MobiHealth is important in being one of the early studies proposing the convergence of different network systems to enable personalized and mobile healthcare.

WSN and IoT are the two modern frameworks that provide health CM solutions. WSN framework being adopted for health CM solution is never a problem given the vast accumulated experience gained from various industrial CM deployments. The IoT being a newer framework with better and more advanced capabilities than the WSN [107], taps on the rich WSNs experience especially for its miniature and low power wireless sensors [108]. Key technology players [109–112] have fused the advantage of WSN low power sensors and reliable communications with the robust Internet Protocol (IP) based addressing, scalable and open architecture of IoT, resulting in a hybrid IoT/WSN system suitable for healthcare [109] [110] that has the advantage of both the WSN and IoT frameworks.

A number of IoT/WSN enabled devices are available to patients and healthcare providers to monitor diabetes, heart conditions, and other ailments. The devices monitor vital signs and physiological parameters, adherence data, and consumer health data [112]. Zhou *et al* [113] proposed a three layer network structure for a pervasive medical supervision system based on WSN. The first layer is the medical sensor layer providing information such as the oximetry, the heart rate/pulse and the blood pressure. The medical sensors form a star schema network with a gateway node elected by either a self-organizing protocol or manual configuration. The second layer provides reliable transmission. If the patient is at home, the physiological data is transferred to one of the nearest wireless nodes that are emplaced in the house. These nodes not only relay the data to the PC with an Internet connection in a multi-hop manner but also provide contextual data such as temperature, and the patients video/picture in emergency situations. When the patient is outside, the relay mission is accomplished by a mobile phone or a PDA device. The third layer of the system is responsible for the aggregation of physiological data in a remote medical center for analysis and providing feedback data back to the patient through a mobile phone, a PDA or web services. Dohr *et al* [114] presented Keep In Touch (KIT), an IoT based Ambient Assisted Living (AAL) system that encompassed technical systems to support senior citizens and people with special needs in their daily routines to allow an independent and safe lifestyle as long as possible. The main goal was to maintain and foster the autonomy of those people and to increase safety in their lifestyle and in their home environment. The monitoring of chronic illnesses (health), on-demand provision with fresh food (safety), alarming systems (security), reminder services (peace of mind) and enabling people-to-people communication for instance with relatives (social contact) without recognizing the technology behind it are just a few mentionable applications of AAL through the IoT. Ray [115] demonstrated H^3IoT - Home Health Hub IoT for monitoring health of senior citizens at home, to cater with the needs of livelihood in a handy and easy to use manner. H^3IoT model comprises the dependency and interconnectivity of bio-sensors, communication channels, MCU, gateway, internet, and applications. The health condition of senior citizens residing at home can easily be monitored by their relatives, doctors, nearby hospitals, and caregivers staying at remote location.

There are several benefits achieved with these health CM systems. To begin with, remote monitoring capability is the main benefit of pervasive healthcare systems. With remote monitoring, the identification of emergency conditions in at risk patients will become easier and the people with different degrees of cognitive and physical disabilities will be better enabled to have a more independent and easy life.

1.4 Problem Formulation

In the prior art reviews conducted, majority of the researchers were focusing on developing CM technologies based on GSM, WSN or IoT, or a fusion of frameworks. Each development is application centric, and only caters to a specific purpose. Most of the implementations are distributed, and not all are scalable. Non-scalability results in a hardware implementation where any future upgrade is not possible or very difficult. In the reviews, CM is used very extensively in industrial and manufacturing sectors, and solutions are readily available from key industrial players. In the healthcare sector, traditional health CM conducted in hospital environment is matured [116]. However, health CM with GSM, WSN or IoT away from hospital is still very much in active research and developments, with only very limited systems ever made it to the consumer market. By studying both approach to implementing CM and the types of hardware developed, there is no synergy between each developed systems apart from the common types of wireless communication protocols used.

1.5 Thesis Contributions and Organization

This thesis contains the results of an industrial-track Ph.D research in collaboration with SIMTech which are focused on the development of technologies for condition monitoring based on a wireless, distributed and scalable platform, all pulled by real and significant needs, and is structured over six chapters. Chapter 2 involves the formulation of a common hardware system framework for CM based on a wireless, distributed and scalable platform. It spans across the development for a generic CM system hardware prototype featured in this thesis. The CM system prototype shares requirements in scalability, form factor, power consumption and cost as it is designed with uptake efficacy as an end objective. The prototype leverages on an appropriate synergy of constituent technologies in low power embedded systems, wireless communications networks with ZIGBEE, Wi-Fi and GSM, sensing (monitoring) and instrumentation. The prototype shares a unified design architecture which allows these technologies to be integrated where appropriate. The thesis may thus be regarded as a collation of results enabling an advance in technology frontiers to allow novel CM applications, building on high power and cost efficiency, embedded and wireless sensing (monitoring) platforms.

Chapter 3 extends the common CM framework proposed in Chapter 2 to suit industrial based CM applications where a detailed CM method for industrial application is defined and verified on a precision cutting machine. The chapter also focuses on the research related to sensors placement on a precision cutting machine, for CM at critical locations. The idea behind this chapter is pulled from the requirement from SIMTech to realize an optimal sensors placement methodology for inferring accurate vibration profiles of the defined critical point. These sensors are placed at sensitive measurement locations away from the critical point. Moving mechanical parts in a machine will inevitably generate vibration profiles reflecting its operating conditions. Vibration profile analysis is a useful tool for real-time condition monitoring to avoid loss of performance and unwanted machine down-time. In this chapter, an approach is proposed and validated for sensor placement, selection and fusion for machine CM. The main idea is to use a minimal series of sensors mounted at key locations of a machine to measure and infer the actual vibration spectrum at a critical point where it is not suitable to mount a sensor. The sensors locations which are subsequently used for vibration inference are identified based on sensitivity calibration at these locations moderated with normalized Fisher Information associated with the measurement quality of the sensor at that location. Each of the identified sensor placement location is associated with one or more sensitive frequencies for which it ranks top in terms of the moderated sensitivities calibrated. A set of Radial Basis Function, each of them associated with a range of sensitive frequencies, is used to infer the vibration at the critical point for that frequency. The overall vibration spectrum of the critical point is then fused from these components. A comprehensive set of experimental results for validation of the proposed approach is provided in the chapter.

Chapter 4 highlights the need to develop a new method of CM for precision machine by analyzing sound and vibration generated by the machine itself.

This idea is pulled from the discussions with Makino regarding the common approaches or methods used by experienced service engineers for impending machine fault diagnostics. By manually sensing the vibration with hand, and listening to the sound generated from a machine, a service engineer is able to determine if the particular machine under his care is healthy and operating normally, any abnormal vibration and sound can represent an impending machine failure, hence warrants a preventive maintenance. The current method is effective and is very subjective based on the accumulated experience of the service engineer in that particular machine, and the experience is difficult to be handed over to the new engineer. Thus, a new objective method is proposed by using the CM system prototype designed in Chapter 2. The CM system prototype aims to replace the hand and ear of a service engineer. Wireless sensor nodes are deployed in various locations on the machine to sense machine vibration and sound signals. The signals are pre-processed before being relayed to a central base station node, and finally being processed by a backend application software. The software contains a machine learning algorithm to learn the condition of the machine, and to predict its health condition. End user will be notified if the health condition warrants a preventive maintenance. This chapter introduces a novel method of pre-processing and classifying sound signals by using the concept of Mel Frequency Cepstral Coefficients (MFCC) which mimics a typical human ear listening to machine sound. The same method is also used on vibration signals. The deployment of the CM system on a machine to be monitored and the associated machine learning algorithm are thoroughly discussed in this chapter, together with benchmarks against other similar systems.

Chapter 5 details the deployment of the CM system prototype reconfigured for healthcare based CM (e-HealthCM), and specifically highlights the capability of the CM system prototype in adapting to different industrial and healthcare requirements. This chapter is pulled by an ageing demography in Singapore and consequent of collaboration/discussions with Southwest CDC (Community Development Council), Ministry of Health and Family Welfare, Housing Development Board (HDB), LionsBefrienders, and other welfare communities. The e-HealthCM system is tailored specifically for use by senior citizens to allow them to age in grace in their own homes as there is an increasing trend in the number of senior citizens staying by themselves in small apartments. In an increasing number of unfortunate situations, senior citizens lost their lives in their own apartments from accidental falls without anyone knowing or due to help arriving too late. e-HealthCM system monitors a senior citizen's home for accidental fall activity, and to automatically request for assistance when a valid fall is detected. e-HealthCM system consists of an e-HealthCM Base Station (e-BS) where the fall detection algorithm resides, wireless e-HealthCM Sound Sensor Module (e-SS) for CM of potential fall based on detected sound, and e-HealthCM Wearable Module (e-WM) that monitors motion activity. e-WM is also a low cost digital hearing-aid for senior citizen with hearing difficulty. Having established the fact that using only e-WM motion activity monitoring feature to detect a valid fall is insufficient and prone to false fall detection, due to the unpredictable nature of human movements [117–119], e-SS modules installed at various spots within the senior citizen's home are used to verify if a valid fall has occurred by measuring the localized sound pressure level and the sound signature for potential occurrence of fall. The prototypes of e-HealthCM have been tested in homes of several senior citizens and functionality tests were successfully concluded.

The thesis concludes with Chapter 6 listing a summary of the main contributions of the works presented and possible future works.

Chapter 2

Common Framework for condition monitoring based on a wireless, distributed and scalable platform

2.1 Introduction

In Chapter 1, the various technological components that constitute the building blocks of a wireless, distributed and scalable condition monitoring system were thoroughly reviewed. Huge potential remains to be explored for the area of industrial or healthcare based condition monitoring (CM). In a consumer driven economy [120] structure, each manufactured consumer product is competitively priced and pricing is a major influencing factor, apart from the product's quality. In order for a product to be competitively priced with an acceptable profit margin, manufacturing cost must be kept as low as possible which leaves minimal margin for machinery fault, as production must be minimally interrupted at all cost. Any manufacturing machine fault incurs repair as well as opportunity costs [121] [122]. Thus, the most common practice to reduce an occurrence of machine fault is to perform periodic preventive maintenance (PM) on the machine itself [123] [124]. Even though PM is executed for minimizing the occurrence of machine fault, but from time to time, machine fault still happens. This problem may be attributed to certain un-diagnosed machine health condition that PM failed to address. By incorporating CM protocol to the existing machine, the occurrence of machine fault can be further minimized [124] [125]. This is possible, as a typical CM system monitors the machine's health parameters in real-time, and any parameter deviations from normal can be dealt with immediately, ranging from performing PM at a much earlier stage, or change the machine's operating parameters to suite the detected health condition. As such, with CM, a machine will always be ensured to perform at an optimal level [125].

CM also plays an important role in the area of healthcare [126] [127]. 87% of the 195 countries in the world are developing ones, and together, they represent a huge 84% of the total global population [128]. Conversely, the healthcare spending of these countries only constitutes 11% of the total healthcare spending of the world, primarily due to the lagging economies, poverty and the very low doctor-to-patient ratios. Despite lagging in general healthcare, many of these developing countries are well equipped with basic mobile phone based communication and Internet access largely due to the successful penetration of telecommunication technologies. In 2015, statistics show that 68% of the world's total number of

Internet users resides in developing countries [129]. With the availability of the basic infrastructures, it is structurally viable to deploy healthcare based CM technology in developing countries to help bridge the gaps of quality healthcare to the population at large and bring forth the following benefits [128]:

1. Cost savings: Healthcare based CM devices can be deployed to homes of patients or senior citizens, and they are remotely monitored from a central location. Healthcare professional only visits when needs arise. The optimization of manpower resources results in better cost control.

2. Easy accessibility: patients and senior citizens can have basic healthcare services deliver to the doorsteps of their own homes, and do not require the need to travel often in order to seek for medical advices as their health related parameters can be remotely monitored.

3. Quality of service: optimize the distribution of limited healthcare resources to the mass population at large.

This chapter details the creation of a common hardware framework for the proposed CM system. Two CM scenarios for industrial and healthcare segments are explored by developing prototype hardware CM systems based on the proposed framework. The CM system for industrial and manufacturing segment is mainly for monitoring of machine for operational and health parameters. As reviewed in Chapter 1, different machines have different health and operational parameters to be monitored. Thus, in order to properly simulate a real-life manufacturing based CM scenario, a precision rotational cutting machine is adopted where its operating sound and vibration are monitored as part of the machine health parameters. The prototype CM system consists of wireless embedded controller modules with attached sound and vibration sensors. Each module is strategically positioned at various location on the machine for CM purposes. The captured CM data from each module is transmitted to a central base station for further processing to determine the machine's actual health condition.

The healthcare based CM system for the healthcare segment is designed to monitor health vital signs and physiological parameters of a senior citizen within a home or controlled environment. There are many cases where home alone senior citizens encounter health related emergencies without the knowledge of the caregivers or with help arriving too late [130] [131]. The purpose of the healthcare based CM is to render the much needed assistance to the elderly in a timely manner when an emergency is detected from the install CM sensors. In this thesis, a custom healthcare based CM system called e-HealthCM is designed based on the defined common framework. The purpose of e-HealthCM is to perform health CM of the motion activities of the elderly living in their own homes, and to report any detected or suspect fall incidents to caregivers so that help can be rendered in a timely manner.

The industrial and healthcare based CM systems handle and solve unique non-overlapped issues related to industrial and healthcare problems with different types of sensing technologies, and are technically challenging to have a common framework representing all three. However, a common framework is still possible as the core technologies that form the basic (core) building blocks remain largely the same. This chapter focuses directly on the various building blocks that form the common hardware framework through appropriate selection of existing technologies. The framework presented in this chapter will be used in subsequent works, as explained in the next few chapters.

2.2 Proposed Common Framework

The proposed framework consists of two distinct elements: (a) Data Acquisition and Pre-processing (DAP) element, and (b) Data Processing and Alert (DPA) element. Both elements contains the common core building blocks that are listed as follows:

1. Microcontroller unit (MCU): The MCU is the most important computational element within the proposed framework. A 32-bit MCU with internal hardware capable of performing basic digital signal processing (DSP) algorithms is required. The MCU is tasked to implement custom monitoring firmware and algorithms for CM systems to support both industrial and healthcare applications, and is capable of performing in various power saving mode by ways of controlling its operating frequency and on-chip peripherals. The MCU contains a rich set of built-in communications interfaces (I2C, SPI, Serial, etc.) and high resolution Analog to Digital Converter (ADC) to support interfacing with various CM sensors. The MCU also contains a built-in Real-Time Clock (RTC) for date and time stamping of measured CM data, and sufficient non-volatile and volatile memories for implementation of firmware and algorithm.

   For the proposed framework, Microchip PIC32 based [132] 32-bit MCU is used. Microchip based MCU is chosen for its built-in signal processing hardware support. The MCU contains rich sets of internal peripherals and require minimal external support IC chips, thus suitable for wearable devices.

2. Non-volatile Memory: A Micro-SD card [133] based non-volatile memory module is included to store offline calibration data for attached CM sensors, and for offline localized data logging of captured CM data. For the proposed framework, a commercially available 8GB Micro-SD card is more than sufficient to be used for data storage.

3. Wireless star network: Wi-Fi based wireless network with star topology for reliable and moderate to high bandwidth wireless data communication among various sensor modules [134] [135]. The network must have the ability to perform self-discovery, self-healing and self-routing when new devices are added and faulty devices are removed, and sustains a reliable end to end communication channel with a moderate to high data rate of $115,200$bps to 11Mbps. The built-in Wi-Fi compliant network also ensures IoT based application compatibility. For the proposed framework, low power and low cost RN171 Wi-Fi module from Microchip [136] is used. The module communicates via a standard RS232 serial interface [137] with the host MCU for data transfer.

4. Vibration/Inertial Measurement Unit (DAP element only): Single axis high vibration tolerance ($\geq 50g$) analog MEMs accelerometer is used for industrial vibration measurement, where the accelerometer is directly mounted onto the selected critical vibration point of a machine. Digital tri-axial MEMs accelerometer ($\leq 16g$) is used for the purpose of human motion and fall activity detection in healthcare monitoring. Analog Devices ADXL001 [138] single axis accelerometer with large measurement bandwidth (4kHz)

is used for industrial machine vibration measurement where it is capable of measuring continuous machine generated vibration of $\geq 50g$. Analog Devices ADXL345 [139] tri-axial accelerometer is used for detecting human motion activity in three-axes degree of freedoms [101], and is commonly included in most wearable devices for the purpose of human motion activity monitoring and fall detection [101] [140].

5. Broadband communication endpoint (DPA element only): broadband communication is identified as one of the core building block. There is a requirement where captured data is transmitted to a remote server for processing by using the existing broadband communication infrastructure. The GSM mobile network and the Internet are the two types of broadband communications infrastructure that are the most commonly used. The two endpoints selected for broadband communication are: (a) GSM modem for sending data via the GSM network, and (b) Internet Access Point for sending data via the Internet.

6. User Interface and Alert (DPA element only): Graphical user interface for displaying real-time status of CM in progress, and to display health alert (if any). The user interface is important as it is the only platform for human machine interactions.

7. Power Supply: Regulated power supply is an important core building block that ensures the accurate measurement of CM sensor, reliable data processing and communications for all the core building blocks listed. Depending on the target application, the input to the power supply can be from an AC wall adaptor or from a battery.

Not all of the listed core building blocks are to be used concurrently. Each of the system designed contains some but not all of the building blocks. Figure 2.1 and 2.2 depict high level functional block diagrams for DAP, and DPA elements respectively. Each CM system will have one or more DAP and only one DPA, making it a truly distributed and scalable system. Figure 2.3 depicts a scenario where a precision milling machining center is fitted with a CM system for machine health CM monitoring. The parameter of interest for each precision cutting machine is the tool condition, and any serious tool wear will affect the machine's output quality. The machining center consists of N number of milling machines being fitted with N number DAP based modules. Each DAP monitors the machine vibration and infers the vibration at the cutting tool-tip. Each DAP's vibration data is transferred to the DPA station located at the maintenance engineer's desk. Tool-tips conditions are continuously monitored and any unacceptable deterioration is reported.

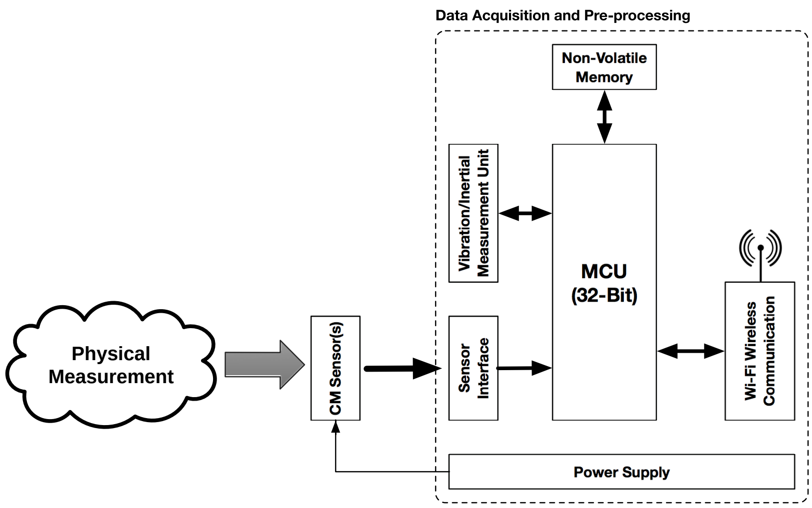

Figure 2.1: Data Acquisition and Pre-processing Element Functional Block Diagram.

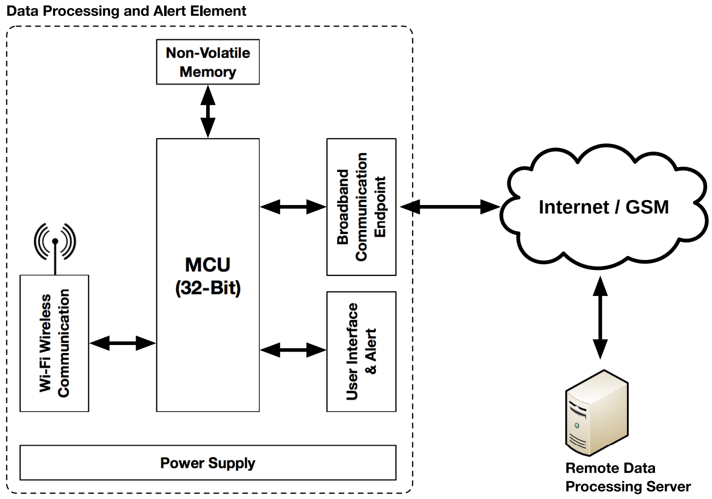

Figure 2.2: Data Processing and Alert Element Functional Block Diagram.

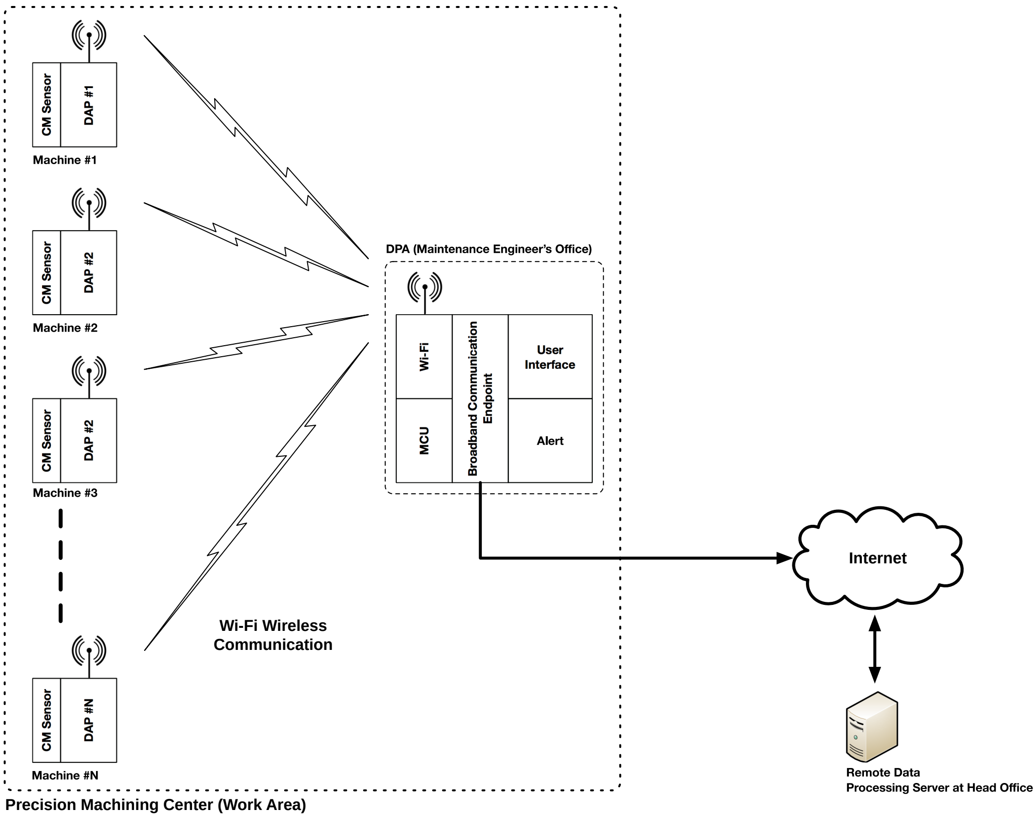

Figure 2.3: CM System Implemented in a Precision Machining Center.

The e-HealthCM system consists of: (a) a DPA based e-HealthCM Base Station (e-BS) that provides the alert and notification function and broadband communication function, (b) wireless DAP based e-HealthCM Sound Sensor Modules (e-SS) for CM of potential human fall based on detected sound and, (c) DAP based e-HealthCM Wearable Module (e-WM) that monitors human motion activities for inertial based fall occurrence. e-WM is also a low cost digital hearing-aid for senior citizen with hearing difficulty. Using only the e-WM motion activity monitoring feature to detect a human fall is insufficient and prone to false fall detection due to the unpredictable nature of human movements [117–119]. e-SS modules installed at various strategic spots within the senior citizen's home are used to verify if a valid human fall has occurred. Any detected inertial based fall activity by the e-WM is broadcasted to all the installed e-SS via Wi-Fi. Each e-SS when received the fall activity information from the e-WM checks the occurrence of a fall by measuring the sound pressure level (SPL) of its surrounding. A fuzzy logic algorithm in the e-SS determines if a valid fall has occurred. If a confirmed fall is detected, the effected e-SS notifies the e-BS via Wi-Fi and the designated caregivers will be alerted by using the GSM mobile network. Figure 2.4 depicts a typical e-HealthCM installation within an elderly person's apartment. There are 11 e-SS modules (#T01 - #T11) installed to cover the whole apartment, and 1 e-BS (#B01) that connects to the GSM mobile network. The resident elderly person wears an e-WM (#W01)that monitors motion activity.

2.3 System Architecture Overview

Conceptual representations of a CM hardware framework for local and remote monitoring are depicted in Figure 2.3 and 2.4 respectively. The figures represent CM systems that implements CM methodologies with the help of sensing technology and established communication networks. The components within

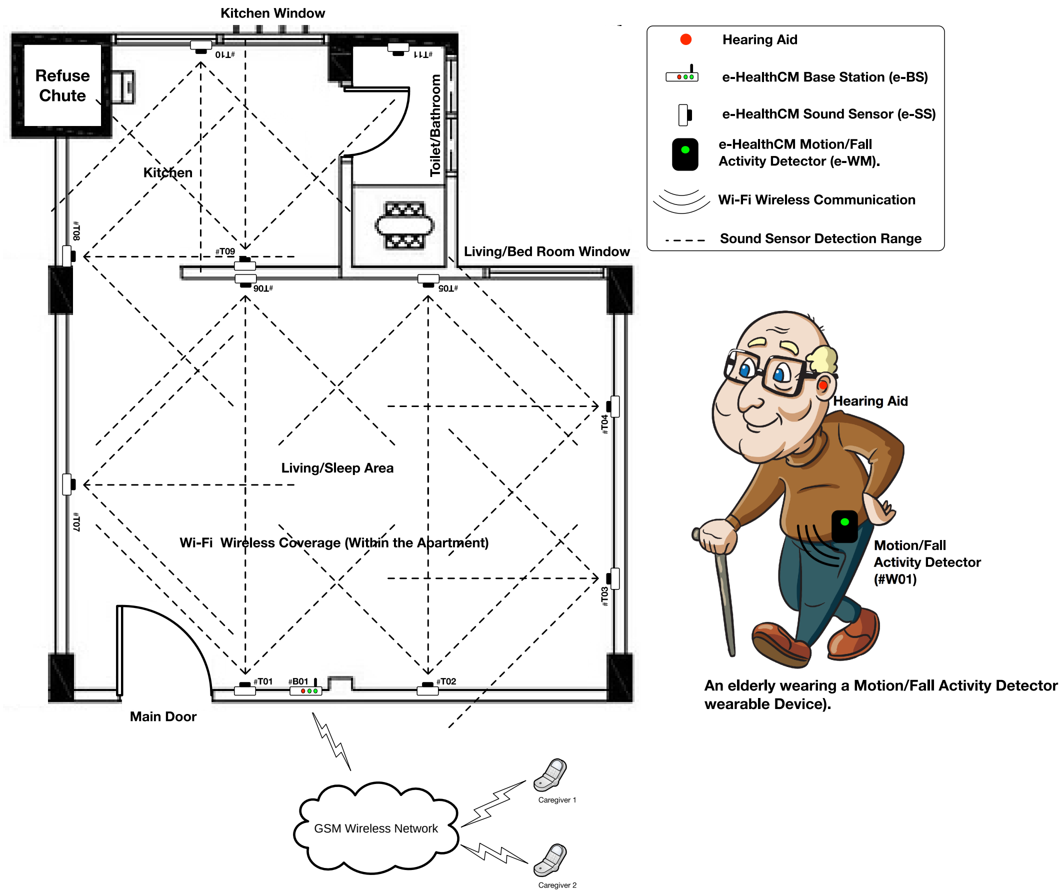

Figure 2.4: Healthcare based e-HealthCM System Implemented in an apartment for the elderly.

the framework are built from all the core building blocks defined earlier. Each of the DAP and DPA are based on the functional blocks depicted in Figure 2.1 and Figure 2.2 respectively.

CM sensor is used to gather measurement data for machine health in industrial deployment, and physiological and motion data in healthcare that enables senior citizen's status monitoring. Sensors are deployed according to the application of interest. In healthcare based CM, sensors to monitor vital signs (e.g., heart rate, respiratory rate, and core body temperature) are deployed, for instance, when monitoring patients with congestive heart disease or senior citizens with pulmonary disease that require or undergoing long term treatments.

Wireless communication is relied upon to transmit acquired or pre-processed CM data to a base station for further processing, and finally indicates the health condition. CM data can also be transmitted to a remote server via the Internet or GSM communication networks, this method is most commonly deployed in healthcare, wherein health related data is transmitted to a remote server for analyses by healthcare professionals and be notified in case of a medical intervention has to be made.

The CM system employs a series of autonomous embedded systems that are connected together via a Wi-Fi wireless communication network. Each individual component is considered a smart device incorporating its own MCU. The hardware requirement for setting up a CM system depends on the targeted application and the type of CM (sensors) required. This thesis focuses on two types of CM hardware implementations, and the hardware setups will be discussed in great details in Chapter 4 and 5 respectively.

2.4 Summary

In this chapter, a common and flexible framework for implementing CM system for industrial and healthcare applications is proposed and discussed. The important core components that form the common building blocks have been properly identified and discussed on its intended use for building practical CM systems. The hardware construction for the two prototype CM systems are based on the proposed common framework, and will be further discussed in Chapter 4 and 5. This framework presented here will be used in this thesis to implement further works and develop solutions toward practical CM systems.

Chapter 3

Sensor Placement, Selection and Fusion for Real-time Condition Monitoring of Precision Machines

3.1 Introduction

An established practice of detecting extraneous disturbances relies on human sensory [141] response to their occurrences, in which an experienced technical personnel observes the machine operational characteristics such as those in the form of the sound and vibration generated. If abnormality is observed, a certain degree of correction can be performed via manual adjustment of machine parameters such as machining speed and force to restore some operational order. However, such a method is heavily dependent on the experience of the technical personnel and the acquired skills are typically in the form of mental models which are difficult to be documented and imparted to a new personnel, not to mention replicating the skills set onto an automation system. This phenomenon is due mainly to the complex nature of the monitoring process involved multiple factors. Thus, an objective and systematic diagnostic approach is highly desirable which can perform beyond the level of current practice and amenable to continuous and online implementation.

In this chapter, a method towards sensor placement, sensory set selection and fusion for continuous and real-time monitoring of machine conditions is proposed and implemented. The approach is scalable and it employs an architecture that is modular and amenable to parallel processing of incoming data to remain viable and sustainable for real-time applications without requiring large scale retrofitting to the system. A common machine monitoring problem is adopted to serve as the background problem for illustration of the proposed method and experiments, though the method presented is applicable to other monitoring problems. The main objective under the problem posed is to use a minimal number of vibration sensors mounted at key locations of a machine to infer the actual vibration spectrum at a critical point, where direct mounting of sensors at this location is not feasible. An example of such a critical point is at the tool tip of a machining center. The quality of the end-product is very much dependent on the tool condition and hence, real-time monitoring of the vibration spectrum at the critical point is necessary to allow various control and mitigation measures to be invoked when needed. The sensor placement locations are selected on the basis of a moderated sensitivity indicator which fuses the location sensitivity to a vibration frequency at the critical point with the Fisher Information giving the measurement quality. Thus, each sensor/location is associated with a set of sensitive frequencies for which its measurement will be selected for inferencing the specific vibration frequency at the critical point. A Radial Basis Function (RBF) is used to carry out the inferencing process and the outputs of all the RBFs invoked yield the vibration spectrum of the critical point which is the basis for the CM. A comprehensive set of experimental results for verification of the proposed approach is be provided.

3.2 Method for Machine Condition Monitoring

This chapter presents a method for carrying out machine CM. A problem will be first formulated in the background for the purpose of better aligning to the proposed method and allowing a more concise illustration. The proposed CM method is also designed to be scalable towards large-scale systems (as explained in Chapter 2) and its realization is amenable towards a distributed architecture which would help to mitigate the current difficulties of realizing a full-scale CM system on large-scale machines without having to retrofit them to a proportionate scale.

3.2.1 Problem Formulation

Figure 3.1 shows a precision machining center which will serve as the system in the background for the elaboration of the proposed CM method. V_s, on the lead screw of the machine, represents a vibration source and there may be more than one present. The unwanted vibration source may arise from a loose gear, a worn lead screw or a crack bearing of the machine, as examples. The vibration source generates a vibration spectrum which propagates to the other parts of the machine. There is a critical point (L_r) on the machine at which the CM is based. There may be more than one critical points in general. In this illustration example, the critical point is shown at the tip of the tool. Monitoring of the vibration spectrum at the tool tip is important as it directly affects the quality of machined parts and the manufacturing efficiency, and that it is not possible to directly derive vibration measurements at this point since it engages the workpiece during the machining process.

The vibration spectrum at the tool tip may be adequately represented by multiple (m) discrete vibration frequencies and Y_r denotes the vibration spectrum there (a_{rj} is the amplitude of frequency ω_j where $j : 1 \rightarrow m$). Whereas, Y_n denotes the vibration spectrum measured at the sensor placement sites, they are given by:

$$Y_r = \{(a_{r1}, \omega_1), (a_{r2}, \omega_2), \cdots, (a_{rm}, \omega_m)\} \tag{3.1}$$

$$Y_n = \{(a_{n1}, \omega_1), (a_{n2}, \omega_2), \cdots, (a_{nm}, \omega_m)\} \tag{3.2}$$

The key objective to be addressed is to infer Y_r from a selected set of n sensors carefully placed at locations L_1, L_2, ..., L_n and the measurements are fused in an optimal manner, given the data available, to yield Y_r.

3.2.2 Preparation and Calibration

Prior to continuous real-time monitoring, offline preparation and calibration of key characteristics of the machine and sensors are needed.

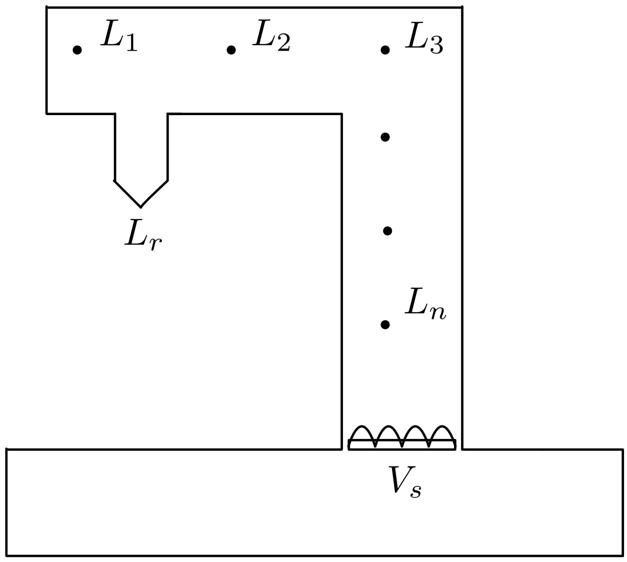

Figure 3.1: Conceptual diagram of a machining center.

3.2.2.1 Sensitivity

The relationship between the vibration at the critical point L_r and those at the sensor sites $L_1, L_2, ..., L_n$ is related to the machine structure (mechanical and geometrical) and the nature of the vibration sources. One factor determining the placement of sensors and selection of measurements from them is the sensitivity s_{ij} which governs how a small vibration at the critical point L_r at a frequency ω_j can be picked at location L_i.

$$s_{ij} = \frac{a_{ij}}{a_{rj}} \Bigg| \begin{array}{l} i : 1 \rightarrow n \\ \\ j : 1 \rightarrow m \end{array} \tag{3.3}$$

where a_{ij} and a_{rj} are respectively the amplitudes of the vibrations at frequency ω_j at L_i and L_r.

If a good mechanical model is available, the sensitivities can be obtained from Finite Element Analysis (FEA) simulation by exciting the critical point

L_r with a small vibration amplitude and measuring the vibration amplitude at location L_i. Otherwise, this calibration process can be directly carried out with an offline experiment on the machine directly. By repeating the step without bias over m discrete frequencies, a sensitivity table can be calibrated which is represented in a matrix form in Eqn.(3.4). The m frequencies should correspond to the frequency spectrum of interest to the CM.

$$S = \begin{bmatrix} s_{11} & s_{21} & \cdots & s_{n1} \\ s_{12} & s_{22} & \cdots & s_{n2} \\ \vdots & \vdots & \cdots & \vdots \\ s_{1m} & s_{2m} & \cdots & s_{nm} \end{bmatrix} \tag{3.4}$$

A sensor placement location should manifest a high sensitivity relative to other locations for at least one frequency of interest. Each row s_{ij} shows the sensitivity at all locations with respect to the frequency ω_j. This table is useful for determining the final placement of sensors. If the sensitivities along a particular column i of matrix S are identically lower than the other corresponding columns, it implies that the location L_i is a poor location and the sensor to be placed there is redundant or it is better placed in an alternate location.

3.2.2.2 Normalized Fisher Information

Accelerometers and piezoelectric transducers are commonly used for vibration measurement. Each of these sensors has its own characteristics in term of response time, bandwidth, resolution, and robustness to environmental factors. The locations for sensor placement may pose accessibility constraints too limiting on the type of sensors that can be placed there. Furthermore, specific to the machine structure, the vibration at certain locations may be less smooth and exhibit more excessive and patchy movements about the nominal vibration level than other locations. Thus, the measurement signals can manifest different degrees of quality related to both machine and sensor characteristics. Relying solely on sensitivities for sensor placement and selection runs the risk of allowing less reliable signals to pass through to the selection process without penalty. An indicator of the quality of the measurement specific to L_i as well as the sensor mounted there would be an important factor to consider in sensor placement and selection. One such possible indicator is the Fisher Information (FI) which is based on information theory of maximum likelihood estimation to serve as an indicator of the quality of a measurement [142]. It is defined as:

$$f_{ij} = \frac{1}{\sigma_{ij}^2}, \tag{3.5}$$

where σ_{ij}^2 denotes the variance of the measurement from location L_i for a vibration frequency ω_j.

However, a modification of this index is proposed for the proposed CM application since the vibration amplitude at the locations are not identical. A larger vibration amplitude will incur a bigger variance and thus a smaller FI compared to a smaller vibration amplitude. For relative comparisons, the variance from the normalized value is better interpreted relative to the vibration amplitude.

Define normalized Fisher Information (NFI) as:

$$\tilde{f}_{ij} = \frac{a_{ij}}{\sigma_{ij}^2} = a_{ij} f_{ij}, \tag{3.6}$$

where a_{ij} is the nominal amplitude measurement at that location.

Similarly, a NFI table in the matrix form is constructed as given in Eqn.(3.7). The NFI can be calibrated at the same time when the sensitivities are being calibrated. With an excitation vibration applied at the critical location (or a neighboring location), the measurements at the various locations can be processed for their respective NFIs. The NFI table is similarly useful to sieve out undesirable sensor placement locations or sensors when the indices are very small, indicating poor measurement qualities at these locations. Unlike sensitivities, the NFIs are dependent on sensor characteristics too. So, they may continue to be calibrated in real-time during operations after the initial calibration to pick up deterioration in sensor qualities over time.

$$\tilde{F} = \begin{bmatrix} \tilde{f}_{11} & \tilde{f}_{21} & \cdots & \tilde{f}_{n1} \\ \tilde{f}_{12} & \tilde{f}_{22} & \cdots & \tilde{f}_{n2} \\ \vdots & \vdots & \cdots & \vdots \\ \tilde{f}_{1m} & \tilde{f}_{2m} & \cdots & \tilde{f}_{nm} \end{bmatrix} \tag{3.7}$$

3.2.2.3 Moderated Sensitivity

The placement and selection of sensors are proposed to be based on both sensitivities and NFIs with a fused indicator by using the NFI to moderate the sensitivity at each location. This is reasonable since sensitivity with respect to the true vibration at the tip will be degraded if it is computed with a low quality measurement of the vibration signal at the location.

A scaling factor to moderate the calibrated sensitivities is defined as:

$$k_{ij} = \alpha + (1 - \alpha)[\frac{\tilde{f}_{ij} - \min \tilde{f}_{ij}}{\max \tilde{f}_{ij} - \min \tilde{f}_{ij}}] \tag{3.8}$$

where $\tilde{f}_{ij}$ is the NFI of a sensor location L_i for given frequency ω_j, $\max \tilde{f}_{ij}$ and $\min \tilde{f}_{ij}$ are respectively refer to the highest and the lowest NFI among all sensor locations L_i given the same frequency ω_j. $0 < \alpha < 1$ is a user-defined parameter to moderate the original sensitivity by up to $100(1 - \alpha)\%$. As per any cost function formulation, it is to be fixed based on the relative weigh-off between the two factors of sensitivity and measurement quality. Empirically, a default of $\alpha = 0.8$ is recommended so that a maximum of 20% moderation of the sensitivity is done on the location with the lowest quality measurement.

The Moderated Sensitivity (MS) $\tilde{s}_{ij}$ is defined as multiplication of the scaling factor with the corresponding sensitivity:

$$\tilde{s}_{ij} = k_{ij} \times s_{ij} \tag{3.9}$$

The Moderated Sensitivity Table (MST) is given in the matrix in Eqn. (3.10).

$$\tilde{S} = \begin{bmatrix} \tilde{s}_{11} & \tilde{s}_{21} & \cdots & \tilde{s}_{n1} \\ \tilde{s}_{12} & \tilde{s}_{22} & \cdots & \tilde{s}_{n2} \\ \vdots & \vdots & \cdots & \vdots \\ \tilde{s}_{1m} & \tilde{s}_{2m} & \cdots & \tilde{s}_{nm} \end{bmatrix} \tag{3.10}$$

Note that unlike the original sensitivity table which is fixed upon the initial calibration, this MST will take into consideration the measurement quality which may degrade over time. Thus, there can be periodic update to the table so that it reflects the latest set of parameters for determining sensor placement and selection.

3.2.3 Condition Monitoring Implementation

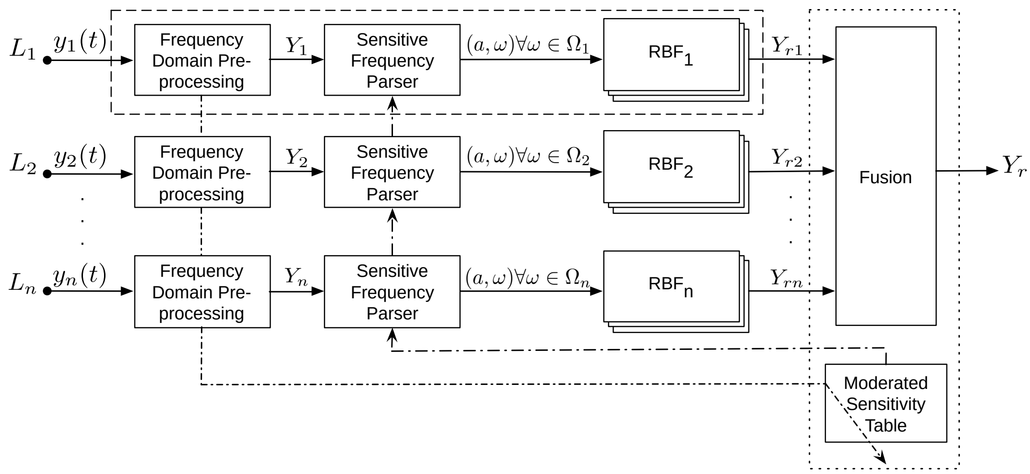

Figure 3.2: Functional block diagram of the proposed method for machine CM.

Figure 3.2 shows the functional block diagram of the method to be deployed for continuous real-time machine CM following the calibration of the machine as elaborated in the earlier sections to yield the MST. The method proposes to accept as inputs from the time-domain measurements $y_1(t), y_2(t), ..., y_n(t)$ from the sensors at the n locations $(L_1, L_2, ..., L_n)$ and it will provide an output Y_r which infers the vibration spectrum at the critical location L_r. In what follows, each of the modules under the block diagram will be elaborated.

3.2.3.1 Frequency Domain Pre-Processing (FDP)

This FDP module will take in the time domain information and output the discrete frequency spectrum Y, giving the amplitude a and frequency ω of each of the frequencies detected. A Discrete Fourier Transform (DFT) is carried out on a collated sequence of a predetermined number of input samples. So, the update is done periodically when that number of samples becomes available. The NFIs at each site can be updated with the data collated and these can then be used to refresh the MST.

3.2.3.2 Sensitive Frequency Parser (SFP)

Each sensor placement site L_i would be associated with a set of one or more frequencies (herein referred to as sensitive frequency set $\Omega_1, \Omega_2, ..., \Omega_n$) for which the MS would be highest relative to the other sites. The SFP will then sieve out these frequencies belonging to these sets from the spectrum provided by the FDP module which will subsequently be passed on to the RBF Inference module (RBF-I) to infer the vibration at these frequencies at the critical location (L_r). A simpler realization may be to only sieve out frequencies exceeding a minimal amplitude threshold or the largest amplitude among them to limit the number of RBF-I which will be subsequently invoked and thus the computational intensity. In this way, only the frequencies for which the sensor at that location is best able to pick up would be processed, and parallel and concurrent processing becomes possible.

3.2.3.3 RBF Inference (RBF-I)

The RBF-I module is used to infer the vibration spectrum at the critical location from the vibration spectrum detected at the sensor sites. RBF neural network has its foundation in the conventional approximation theory, is chosen to infer and approximate the vibration spectrum at the critical location because it is well known as a universal approximator, i.e., any continuous function can be approximated over a compact set to any degree of accuracy. The RBF network with its simpler structure, has equivalent capabilities as the well-known Multilayer Perceptron (MLP) network, but with a much faster training speed, and thus it has become a popular alternative to the MLP. RBF has the following features: (1) it is a parametric model, the output is directly computed based on the input. (2) it has smoother error modeling as it adopts non-linear interpolation for intermediate points which are not calibrated, and also (3) it has better expansion ability as it can be recursively refined based on additional conditions and factors of the training data [143–146].

Derived from function approximation theory, the RBF network is a feed-forward network. They form mappings from an input vector to an output vector. RBF is a real valued function where the output only depends on the distance from the origin or center point μ to its input $x \in \mathbb{R}^n$. The following equation describes the RBF:

$$\varphi(x-\mu) = \varphi(||x-\mu||) \tag{3.11}$$

A typical RBF networks have three layers: an input layer, a hidden layer with RBF activation function, and a linear output layer. Gaussian function is commonly used as RBF activation function as the property of universal approximation by linear superstition of Gaussian basis functions has been proved [144].

$$\varphi(x-\mu) = exp(-\frac{||x-\mu||^2}{2b^2}) \tag{3.12}$$

where x is the input, μ is the coordinate value of the center point of the Gaussian function, and $b > 0$ is the width value of the Gaussian function.

The ultimate goal is to infer the vibration at the critical point from the selected sensor location. Without loss of generality, Y_r and Y_n in Eqn.(3.1) and (3.2) consist of their respective frequency components in time-domain representation, where each respective component has frequency tolerance of ± 20 rad/s due to the effects of the bandpass filters implemented in the FDP module, and can be expressed as:

$$Y_r = a_{r1}(t) + a_{r2}(t) + \cdots + a_{rm}(t) \tag{3.13}$$

$$Y_n = a_{n1}(t) + a_{n2}(t) + \cdots + a_{nm}(t) \tag{3.14}$$

The RBF network can be written as:

$$\hat{a}_{rj}(t) = \sum_{p=1}^{P} w_p \varphi_p(||a_{ij}(t) - \mu_p||) \tag{3.15}$$

where $i : 1 \to n$ and $j : 1 \to m$. $\hat{a}_{rj}(t)$ is the inferred vibration magnitude at the tool tip, P is the size of the input, w_p is the weight value, φ_p is the Gaussian function which $\varphi_p(||a_{ij}(t) - \mu_p||) = exp(-\frac{||a_{ij}(t)-\mu_p||^2}{2b_p^2})$, $a_{ij}(t)$ is the vibration magnitude at the sensor location L_i for a given frequency ω_j, μ_p is the basis center of RBF, and b_p is the width of the RBF.

The squared error function, E is a common method for measuring the discrepancy between the target vibration amplitude a_{rj} (this can be measured with a vibrometer) and the RBF output $\hat{a}_{rj}$:

$$E(t) = \frac{1}{2}(a_{rj}(t) - \hat{a}_{rj}(t))^2 \tag{3.16}$$

The tuning algorithm used to obtain the function parameters of w and μ is the gradient descent method based on error backpropagation. Define the parameter set $W = (w_p, \mu_p)$, and the learning rate η, the parameters can be updated as:

$$W(t+1) = W(t) - \eta \nabla E(W(t)) \tag{3.17}$$

The discrete time of the backpropagation algorithm is given as [147]:

$$w_p(t+1) = w_p(t) + \eta_w(a_{rj}(t) - \hat{a}_{rj}(t))\varphi_p(||a_{ij} - \mu_p||) \tag{3.18}$$

$$\mu_p(t+1) = \mu_p(t) + \eta_\mu(a_{rj}(t) - \hat{a}_{rj}(t))w_p((a_{ij} - \mu_p)/b_p^2) \tag{3.19}$$

where $\eta_w > 0$ and $\eta_\mu > 0$ are the learning rate of w and μ, b_p is chosen as a constant. In order to end the iterative weights tuning process, a termination condition is formulated in terms of the backpropagated error E. Thus, the optimal weights $W^* = \{w_p^*\}$ can be obtained. In addition, it is always a trade-off between the quality of fitting and the iteration time. Since the tuning process is done offline, more emphasis may be given to deriving a better fit at the expense of incurring longer tuning time.

Upon completion of training, RBF-I module for each set of sensitive frequencies $(\Omega_1, \Omega_2, ..., \Omega_n)$ will be fully controlled by the respective SFP module. Each RBF-I module is invoked when its respective SFP yields a signal amplitude (a) associated with a frequency in its sensitive frequency set to its input. The resultant output $Y_{rj} = (a_{rj}, \omega_j)$ represents a frequency spectrum component which will be channeled into the Fusion module.

3.2.3.4 Fusion

Each RBF-I will process only one vibration frequency. The Fusion (F) module will sum up the individual inference results to yield the overall frequency spectrum Y_r at the critical location. Y_r will be the basis of the CM function which will use the latest update of Y_r to determine the next appropriate course of actions to maximize productivity and quality.

3.2.4 Scalability

One of the common deterrence to the uptake of a real-time CM system is in the retrofitting of the machine and the wiring of sensors to central monitoring system and algorithms, especially when these may cause physical restraints or downtime to the machine which may not be acceptable. The architecture of the proposed CM method, however, is amenable to realization in the form of small portable monitoring units (shown in dash box in Figure 3.2) at each location comprising of the sensor, wireless transceiver, the FDP, the SFP and the RBF-I sub-modules collectively realized as a single module. These modules can be battery powered and thus easily attached to the machine to be monitored without inducing unnecessary restraints. They communicate wirelessly with a base module which will comprise of the F module and the MST (shown in dotted box in Figure 3.2).

3.2.5 Low Frequency Monitor

The vibration sensors can pick up frequency signals during machine operations. These signals must be within each sensor's operational bandwidth. However, many useful information indicating of machine deteriorated performance can be picked up from low frequency signals generated by the machine, which may fall outside of the bandwidth of the vibration sensor. The proposed CM method allows other sensors (e.g., sound sensors) to be deployed efficiently in an integrated manner.

3.3 Case Study: Results and Discussion

A case study is conducted to validate the effectiveness of the proposed CM method. The equipment setup in this study includes: (1) three-axis precision motion system with (2) custom test fixture emulating a machine tool, (3) DC Eccentric Rotating Mass (ERM) vibration motor attached to the test fixture to serve as the vibration source, (4) accelerometers as the vibration sensors measuring the critical vibration at the tool tip and sensor placement locations, and (5) National Instrument CompactDAQ for data acquisition and signal generation. Figure 3.3 depicts the experiment setup. Figure 3.4 shows the custom fixture with the ERM motor. There is a total of 30 possible sensor placement locations on the test fixture. Each location is uniquely identified with the (x, y) coordinates. The location marked L_r at the tool tip is the critical point at which the vibration is to be closely monitored. The grey areas are the off-limit zones for possible sensor placements.

3.3.1 Data collection and calibration

As discussed in Section 3.2, offline data collection and calibration need to be done prior to the continuous real-time CM of the machine. The details of data collection and calibration are discussed in the following subsections.

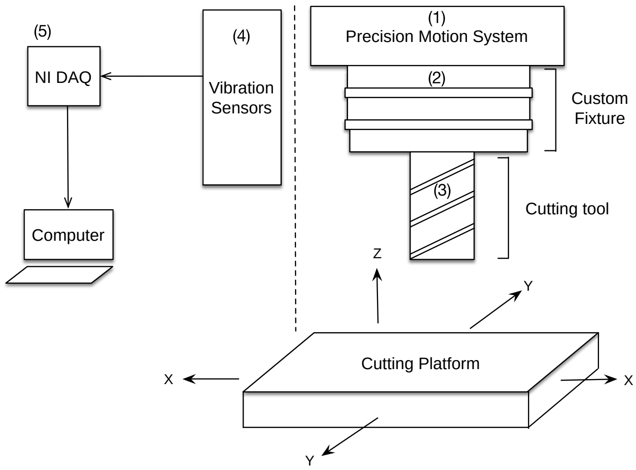

Figure 3.3: Experiment Setup.

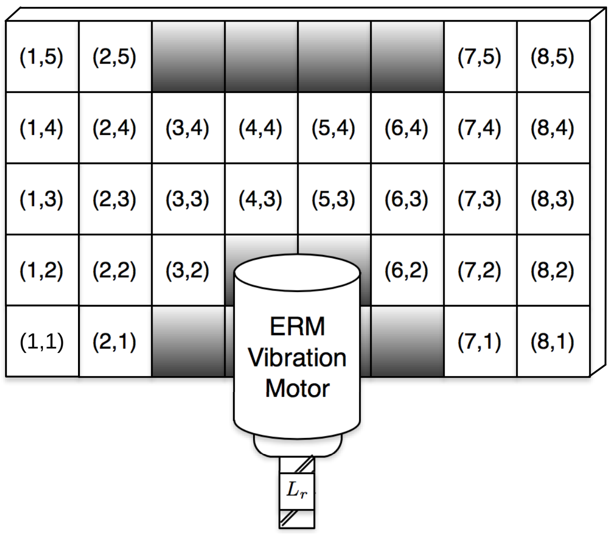

Figure 3.4: Sensor placement locations on the test fixture.

3.3.1.1 Vibration source

The DC ERM vibration motor is attached to the tool tip where L_r is based. It has a dual role; to emulate as a vibration source for the case study as well as a frequency generator during the calibration phase. The ERM is actually a DC motor with a non-symmetric mass attached to its shaft. As the ERM rotates, the centripetal force acting on the mass is asymmetric, resulting in a net centrifugal force which causes a displacement of the motor. With a high number of revolutions per minute, the motor is constantly being displaced, and it is this repeated displacement that leads to a vibration.

The ERM motor in this experiment is driven by a uni-directional motor driver. The NI DAQ's analog output generates a control signal v_{ctrl} to the motor driver, which controls the resultant frequency and vibration magnitude of the ERM motor. In this experiment, the frequencies of interest in the CM are 100Hz and 120Hz and they are generated primarily via the ERM. In this experiment, v_{ctrl} is a periodic trapezoid signal as depicted in Figure 3.5 which is controlled to increase with time until it reaches v_{max}, remains stable at v_{max} for duration of time t_{ctrl}, and finally decrease to v_{min}. The ERM motor will start to rotate at rated frequency and vibration magnitude once $v_{ctrl} = v_{max}$, rotates at decreased frequency and vibration magnitude when $v_{ctrl} < v_{max}$, and finally stalled when $v_{ctrl} = v_{min}$. This process of rotating the ERM motor at rated frequency and vibration magnitude, slowing it down, and finally stopping it, repeats periodically. The resultant I-V characteristic of the ERM motor is depicted in Figure 3.6. Operating the ERM motor at $v_{ctrl} = v_{max}$ yields an operating frequency of 120Hz. When attached to the tool tip, and due to the tool tip mechanical vibration modes characteristics, additional frequency components are invariably induced to yield a more complex vibration frequency and amplitude as depicted in Figure 3.7. By capturing the resultant vibration signals at the tool tip, and analyzing it in frequency domain, these vibration frequency components of 100Hz and 120Hz generated are accordingly contained in the vibration sources.

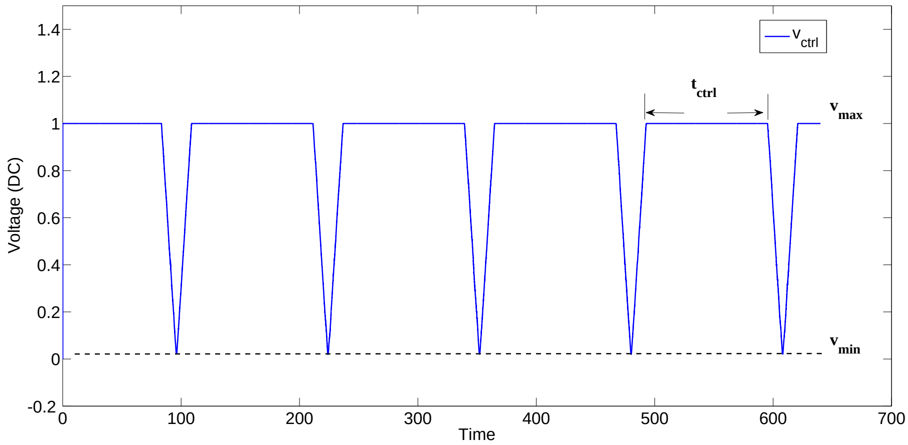

Figure 3.5: Periodic trapezoid signal (v_{ctrl}).

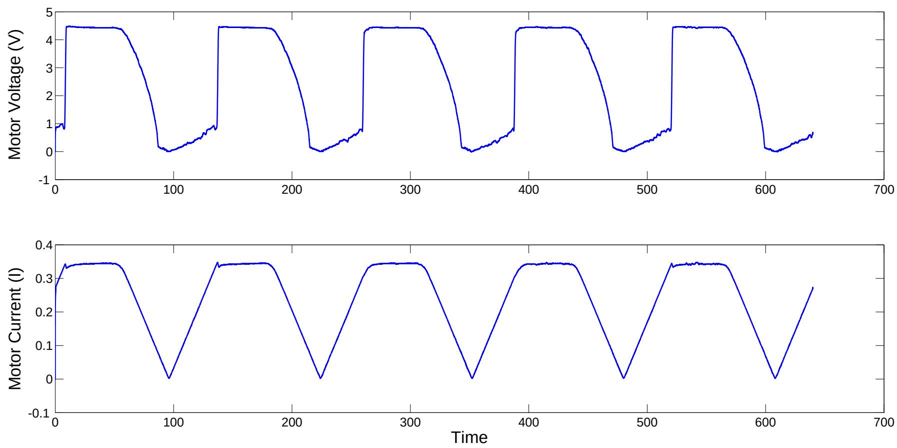

Figure 3.6: ERM vibration motor excitation characteristics.

3.3.1.2 Vibration measurements

In this experiment, identical three-axes Kistler accelerometers (model: 8690C50) are used at each of the sensor placement locations. There is a total of 30 possible sensor placement locations identifiable via their (x, y) coordinates as illustrated in Figure 3.4. A similar accelerometer is attached to the tool tip at L_r to measure the vibration at the tool tip. NI DAQ's analog input with the sampling rate of 1kHz is used to collect the time domain vibration signals from each accelerometer for further signal processing and analysis. Figure 3.7(a) and Figure 3.7(b)

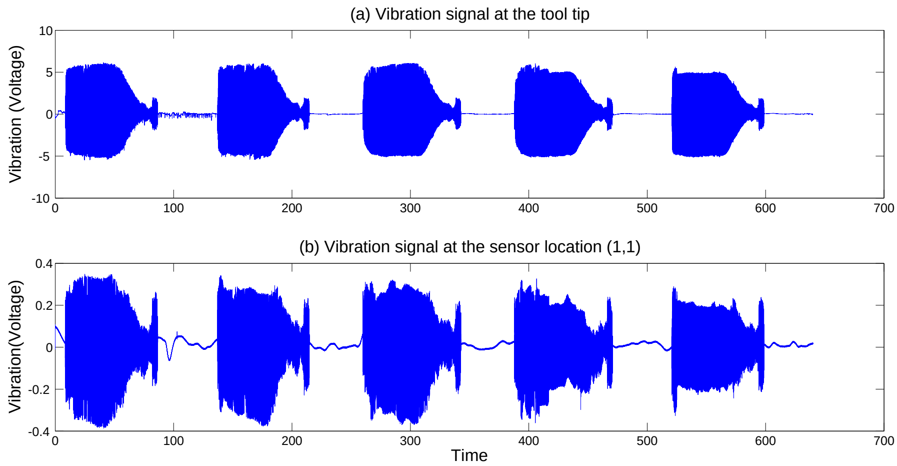

Figure 3.7: Vibration signals for x-axis.

provide an example of x-axis vibration data sampled from critical location L_r and sensor location $(1, 1)$ respectively.

3.3.1.3 Frequency domain pre-processing

The collected time domain vibration signals will first be examined in the frequency domain to obtain and segregate the dominant frequency components. Fast Fourier Transform (FFT) algorithm is used for this purpose to compute the DFT of the vibration signals to yield the dominant frequency components. With the vibrations generated by the ERM as explained in the preceding section, the dominant frequencies are correspondingly 100Hz and 120Hz.

3.3.1.4 Dominant frequency components extraction

Bandpass filters are required to extract the two frequency components from the collected vibration signals. Finite Impulse Response (FIR) bandpass filter is chosen for this purpose. FIR filter is selected over Infinite Impulse Response (IIR) filter due to FIR's inherent stability and linear phase response characteristics, even though more digital signal processing resources are required for implementation. Figure 3.8 depicts the block diagram of a M-taps filter, where $y[i]$ is the discrete signal input for sample i, and $y'[i]$ is the respective filtered signal output. $h[0], h[1]...h[g]$ are the filter's coefficients obtained by performing z-transform on the filter's impulse response. Eqn.(3.20) highlights the FIR bandpass filter with M-taps.

$$y'[i] = \sum_{g=0}^{M-1} h[g].y[i-g] \tag{3.20}$$

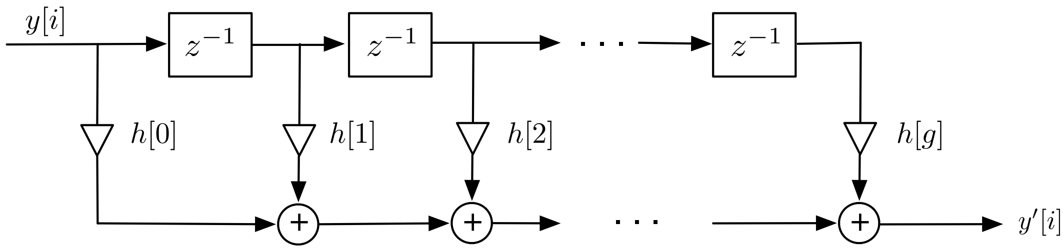

Figure 3.8: Block diagram of bandpass filter design.

In this experiment, 100-taps FIR bandpass filters are constructed for center frequencies (dominant frequency) of 100Hz and 120Hz. Collected vibration signals are processed with these filters. For illustration purpose without loss of generality, only 120Hz frequency components are shown here. Figure 3.9(a) and Figure 3.9(b) are the filtered signals from the location (1,1) and L_r at 120Hz respectively.

The resultant processed signals for each dominant frequency are processed into the instantaneous Root Mean Square (RMS) form using a sliding rectangular window centered at each point in the signal. Figure 3.10(a) and Figure 3.10(b) depict the RMS equivalents of the vibration signals for the 120Hz frequency component. They verify that the measured vibrations at these dominant

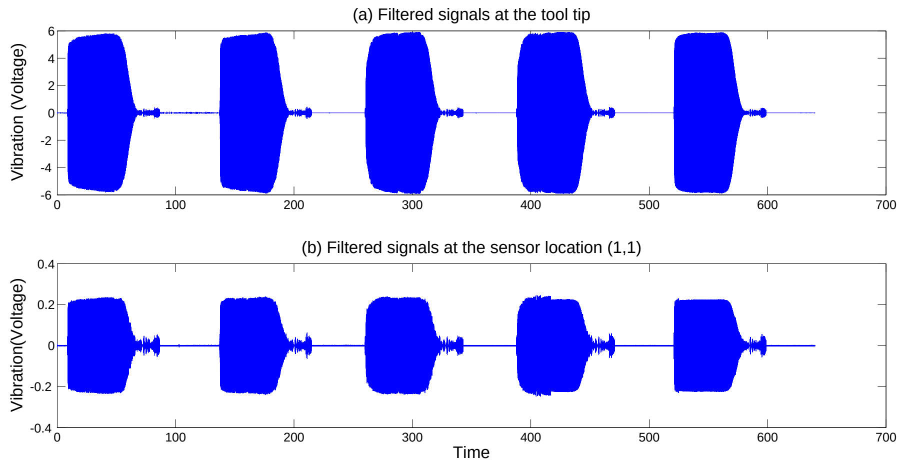

Figure 3.9: Filtered signals, 120Hz.

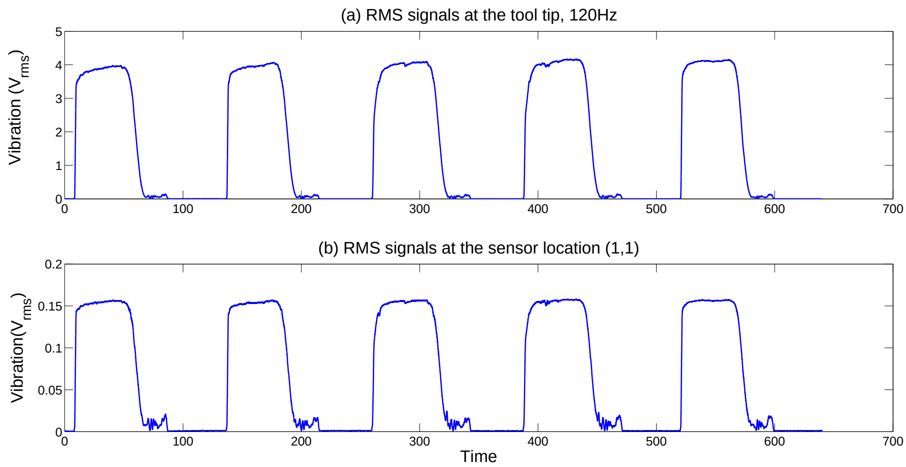

Figure 3.10: RMS signals, 120Hz.

frequencies are repeatable.

3.3.1.5 Sensitivity

The sensitivities at each sensor location for frequencies 100Hz and 120Hz, are calculated based on Eqn.(3.3) and plotted in 2D as depicted in Figure 3.11 and Figure 3.12 respectively. For illustration purpose, only the sensor x-axis measurements are shown here. The 2D sensitivity plots show that sensors placements locations $(7,1)$, $(8,1)$ are the most sensitive locations for the frequency

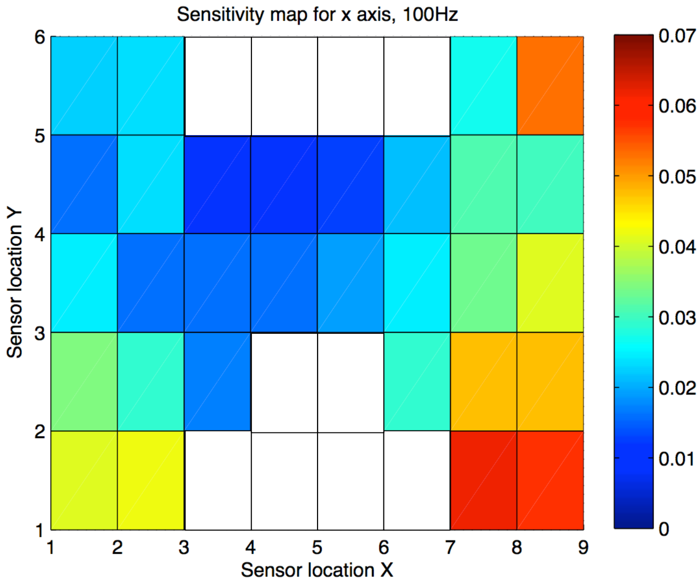

Figure 3.11: Sensitivity map for 100Hz.

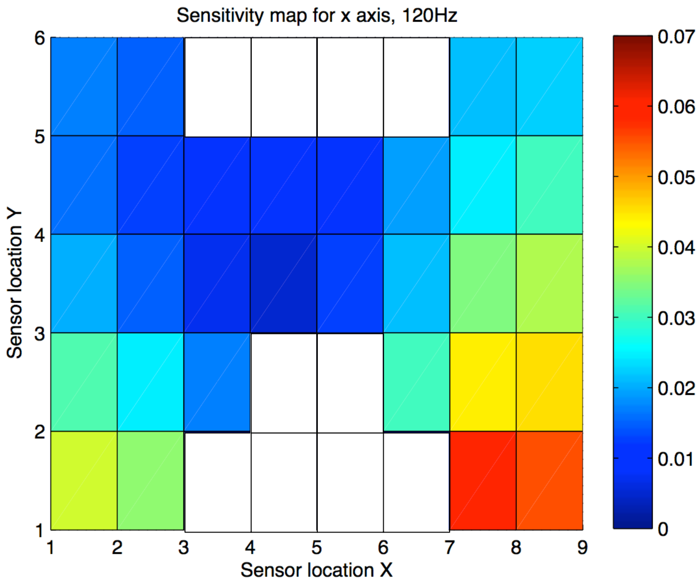

Figure 3.12: Sensitivity map for 120Hz.

100Hz, and $(7, 1)$ is most sensitive for 120Hz. Nonetheless, these are not the final sensor placement locations pending the moderation with the NFI for the respective frequencies which may churn out new locations. The unshaded areas are for the screws and vibration mounting hence no measurement at these locations.

The NFI at each sensor location, for frequencies 100Hz and 120Hz are calculated based on Eqn.(3.6) and shown graphically in Figure 3.13 and Figure 3.14 respectively. The results show that for frequency 100Hz, the NFI at sensor placement locations $(2,3)$, $(2,4)$, $(7,4)$ are relatively higher compared to the other locations. On the other hand, for frequency 120Hz, NFI at sensor locations $(1,4)$, $(2,4)$ are relatively higher compared to the others. In a sense, NFI gauges measurement quality at the various locations. Hence, a higher NFI implies relatively higher quality measurements. In this experiment, it is observed that higher values of NFI occur at locations with low sensitivities for both the 100Hz and 120Hz frequencies as shown in Figure 3.11 and Figure 3.12. Hence, there is a trade-off between sensitivity and NFI in determining the sensor locations to use. Since the same type of sensors is used, the variation of NFI at each location is mainly due to the influence from the machine's mechanical structure such as its stiffness and geometrical properties.

3.3.1.6 Normalized Fisher information and Scaling factor

The scaling factor at each sensor location, for the frequency of 100Hz and 120Hz are calculated based on Eqn.(3.8) and shown in Figure 3.15 and Figure 3.16 respectively. From the plots, it is observed that the more sensitive areas are associated with relatively low scaling factors of between 0.81 and 0.84, and certain areas of low sensitivity are associated with higher scaling factors very close to 1. This is due to large NFIs at the low sensitivity areas as compared to NFIs at the high sensitivity areas, which is consistent with the NFI plots.

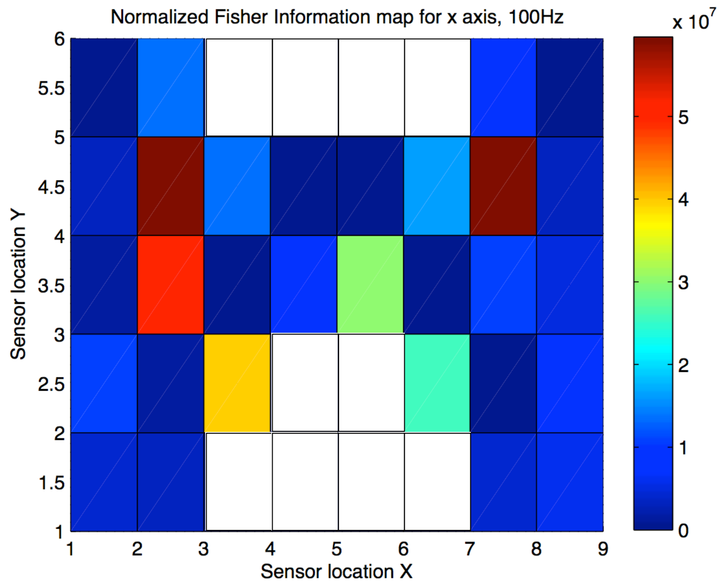

Figure 3.13: Normalized Fisher Information map, 100Hz.

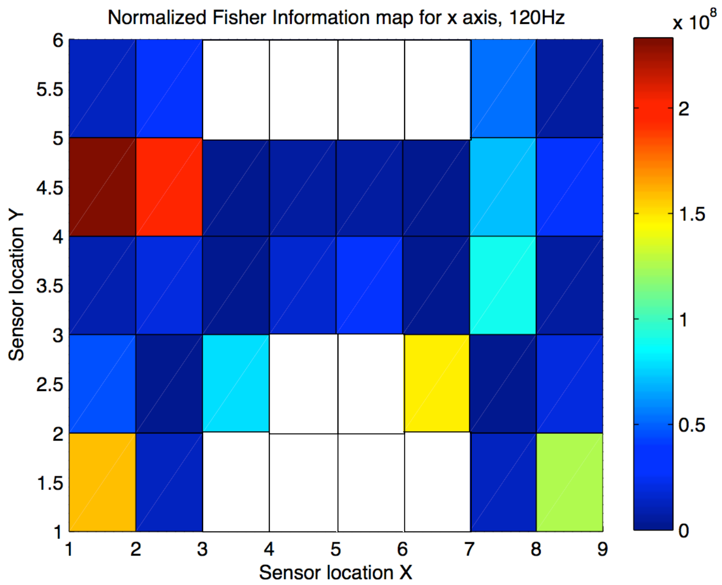

Figure 3.14: Normalized Fisher Information map, 120Hz.

3.3.1.7 Moderated Sensitivity

MS at each sensor placement location for frequencies 100Hz and 120Hz are obtained based on Eqn.(3.10) with sensitivity information from Figure 3.11 and Figure 3.12, and the scaling factors from Figure 3.15, and Figure 3.16. The

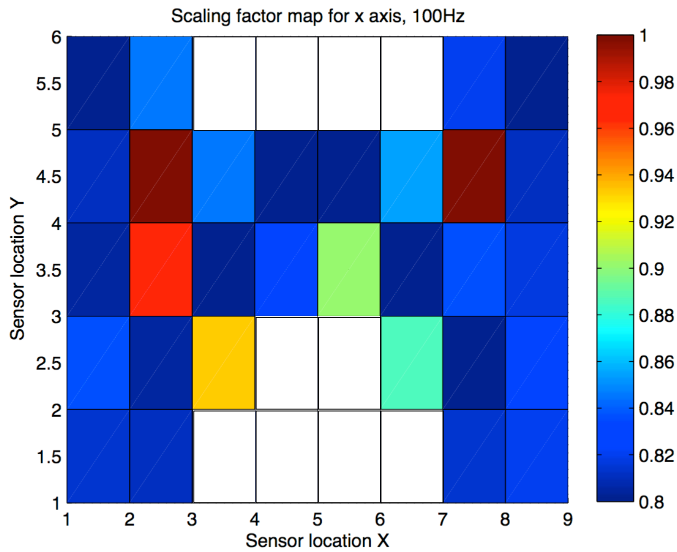

Figure 3.15: Scaling factor map, 100Hz.

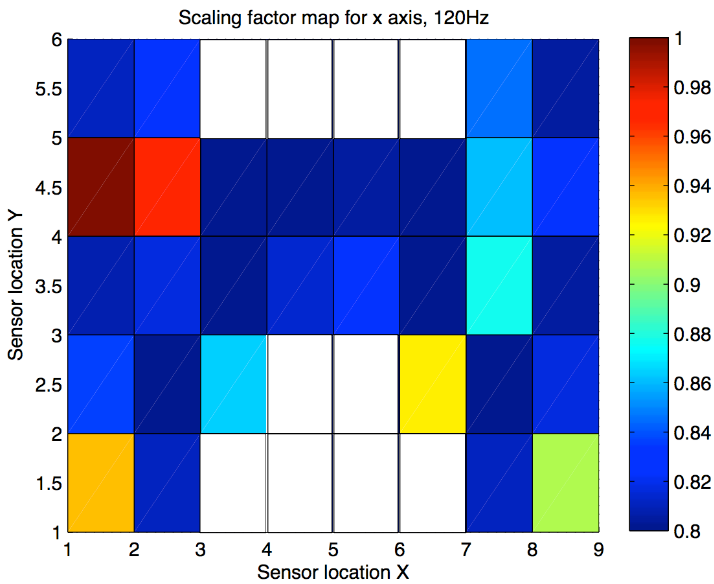

Figure 3.16: Scaling factor map, 120Hz.

MS results given in Figure 3.17 and Figure 3.18 show that $(7, 1)$ is the most sensitive location for 100Hz and $(8, 1)$ is the most sensitive location for 120Hz, hence differing from sensor locations suggested in Figure 3.11 and Figure 3.12. These two locations are the preferred sensor placement locations for the dominant frequencies based on the scaling factor effects.

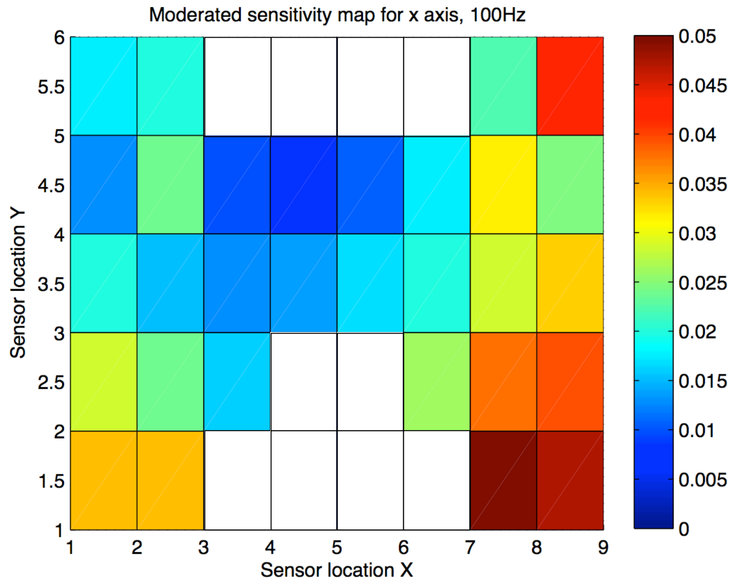

Figure 3.17: Moderated sensitivity map, 100Hz.

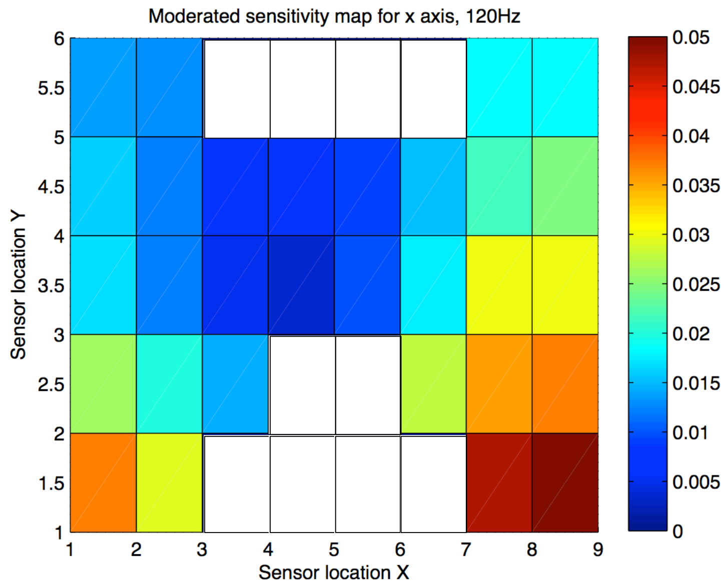

Figure 3.18: Moderated sensitivity map, 120Hz.

3.3.1.8 Radial Basis Function

Figure 3.19(a) depicts the RMS equivalent data for 100Hz at the sensor location $(7, 1)$ and reference L_r. There is a total of 12800 sample data and 50% of the sample data is used for training and the other 50% is used for verifying the trained RBF. Before RBF training is performed. Here, the RBF network is trained using 6400 samples of data. Thus, $P = 6400$ and $b = 0.05$ are selected for the RBF training. As the parameter adaptation process is done offline with pre-acquired data, a longer training time with relative small value of the Mean Squared Error (MSE) is used to obtain better fitting results. $MSE < 0.05$ is selected as the termination condition for the parameter adaptation, and the learning rate η_w and η_μ are chosen to be 0.01. The training time taken for this RBF network with 6400 sample data is a few seconds with small variations due to the convergence time. The weights w and center μ are updated according to the Eqn.(3.18) and Eqn.(3.19). As discussed in the RBF-I elaboration in Section 3.2, the parameter adaptation process will converge according to the gradient descent method based on the error backpropagation algorithm. Once the RBF training process converges to the termination condition, the trained weights w and centers μ are available to commission the RBF estimation of inference the vibration magnitude at the target location.

The results of the RBF approximation shown in Figure 3.19(b), where the solid lines represent the RBF approximation at $(7, 1)$ and the cross-line represent the desired output at reference L_r which is the measurement taken at this location. In order to verify the accuracy of the trained RBF, another 50% of the sample data that has not been used for training are fed into the trained RBF net. Figure 3.19(b) shows the RBF verification result where the RBF able to approximate the desired output accurately with a MSE of 5.8%. Figure 3.20 shows the RBF inference result of sensor location $(8, 1)$ for the frequency of 120Hz, the MSE of the RBF approximation is 2%. Here, for conciseness, only the results for location $(7, 1)$ and $(8, 1)$ are shown. The same procedures can be applied to other sensor locations for RBF inferences.

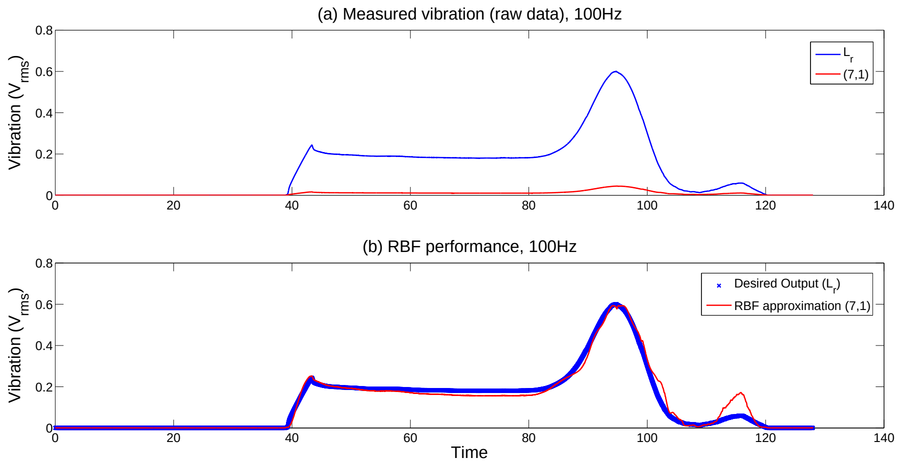

Figure 3.19: RBF Approximation for sensor location (7,1).

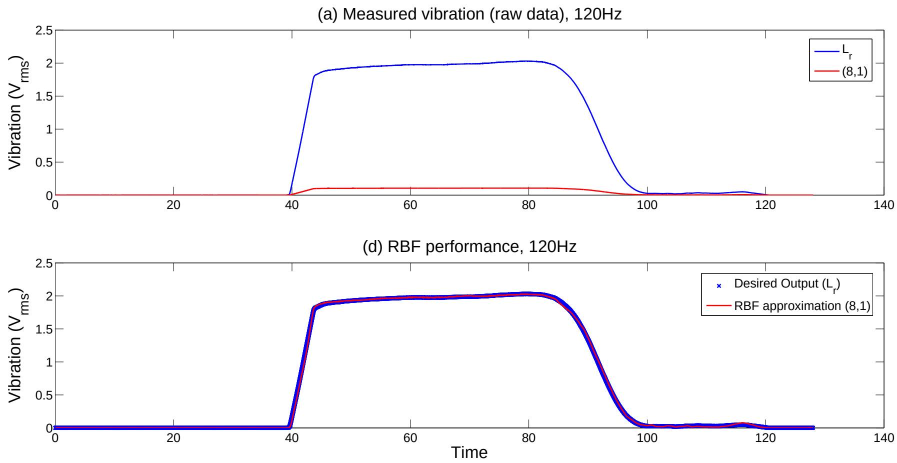

Figure 3.20: RBF Approximation for sensor location (8,1).

3.3.2 Real-time Condition Monitoring

Once the calibrations are completed and the RBF networks trained, real-time CM of the tool tip of a precision machine can be initiated. Figure 3.21 is the block diagram of the real-time CM system, and Figure 3.22 - Figure 3.24 are the modular program flows for each of the blocks of the monitoring system.

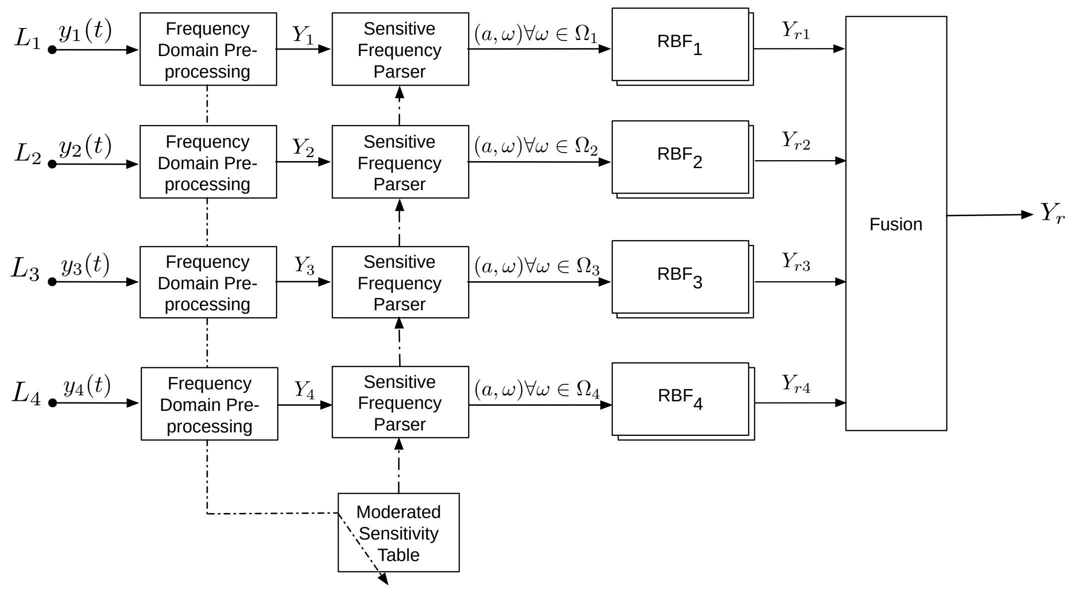

Figure 3.21: Block diagram for real-time CM.

Based on the MS results shown in Figure 3.17 and Figure 3.18, four sensor placement locations $(7,1),(7,2),(8,1)$ and $(8,2)$ are selected for real-time CM which correspond to L_1, L_2, L_3 and L_4. These four locations are selected due to their high MS values following the offline calibration done. In the event a sensor at the primary location degrades in performance, the next best ranked sensor at a secondary location will assume the primary duty. L_1, L_3 are the primary sensors, while L_2, L_4 are the secondary ones. These four sensors are concurrently measuring vibration signals $(y_1(t), y_2(t), y_3(t)$, and $y_4(t))$ respectively. The ERM motor now play its second role as a vibration source in this case study.

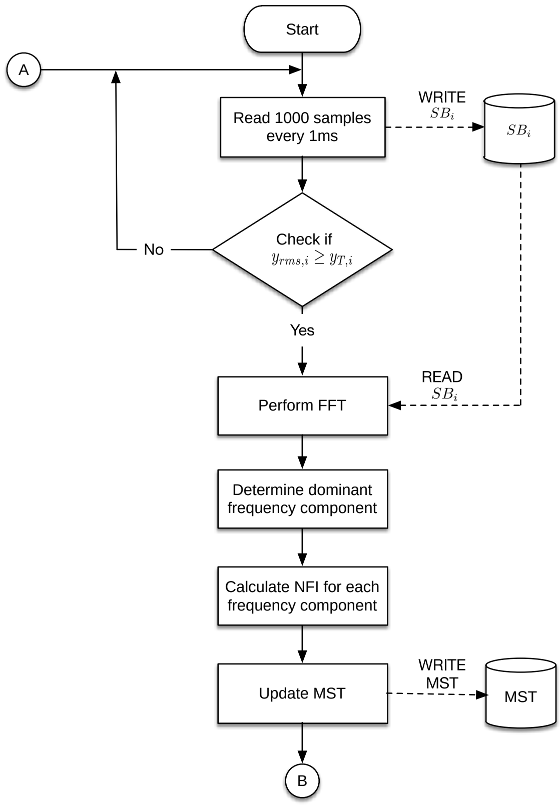

Figure 3.22: Frequency domain preprocessing (FDP) flowchart.

The sensor at each L_i, is connected to the FDP$_i$ module. Within the FDP$_i$, vibration signal $y_i(t)$ is sampled every 1ms interval, and 1000 samples are written into a Sample Buffer (SB$_i$). The RMS value of y_i is calculated and denoted as $y_{rms,i}$ which will serve to determine if the flow should continue by comparing with a small threshold $y_{T,i}$. The threshold is empirically determined and unique for each machine. For very small vibration, no further processing is needed when $y_{rms,i} < y_{T,i}$, the collected samples in SB$_i$ are discarded, and new values are collected for re-evaluation.

When $y_{rms,i} \geq$, the vibration is significant enough to warrant further processing for CM. FFT is performed on SB$_i$ to determine the dominant frequency components present. In this case study, the ERM generate vibrations mainly at

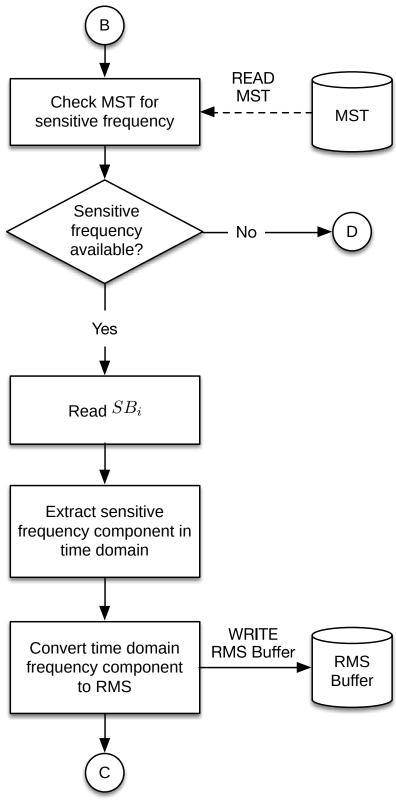

Figure 3.23: Sensitive frequency parser (SFP) flowchart.

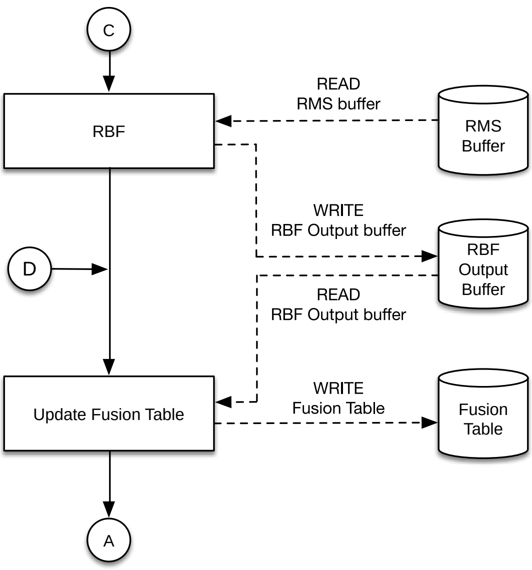

Figure 3.24: RBF and Fusion (F) module flowchart.

two frequencies of 100Hz and 120Hz and thus, these two frequencies manifest in these computations along with the respective nominal vibration amplitudes.

NFI is calculated at each of the locations L_i based on Eqn.(3.6) from the data in the SB_i. With the NFI information thus available, the scaling factor (k_i) at each L_i can be calculated. Since the sensitivity at each L_i is already known from the offline calibration process, the MS can be computed using Eqn.(3.10) and the latest value will be used to update the MST which stores the MS data of all L_i with respect to frequency ω. Figure 3.22 maps the detailed program flow of the FDP module.

Table 3.1 is a snapshot of the MST filled with offline calibration data at startup. The elements within the MST are sensitivity s_{ij}, NFI $\tilde{f}_{ij}$, scaling factor k_{ij} and MS $\tilde{s}_{ij}$. At this first instance when monitoring begins, MST, based on $\tilde{s}$ yield L_1 and L_3 as the best locations for monitoring vibrations at 120Hz and 100Hz respectively. The MST is subsequently and continuously refreshed with new data from each sensor, and new locations and sensors can be invoked accordingly. The MST is non-volatile and contains the latest parameters reflecting the optimal configuration for real-time monitoring of the machine.

Table 3.1: MST

L_i	s_{ij} $(\times 10^{-2})$		$\tilde{f}_{ij}$ $(\times 10^{6})$		k_{ij}		$\tilde{s}_{ij}$ $(\times 10^{-2})$	
	100Hz	120Hz	100Hz	120Hz	100Hz	120Hz	100Hz	120Hz
L_1	6.14	5.8	4.062	11.87	0.896	0.816	5.5	4.73
L_2	4.73	4.42	0.294	1.882	0.8	0.8	3.78	3.54
L_3	5.73	5.49	5.897	126.5	0.9427	1	5.4	5.49
L_4	4.76	4.5	8.147	20.17	1	0.8294	4.76	3.73

The output of each FDP_i is the discrete frequency spectrum Y_i which provides information of amplitude a and frequency ω of the dominant frequencies detected at L_i. Y_i is fed into the SFP_i module. The main function of SFP_i is to compare Y_i against the sensitive frequency set associated with L_i stored in the MST. If the frequency components are members of the sensitive frequency set, it means the sensor at L_i will register the highest MS for these frequencies. Thence, the SB_i will be read to retrieve the stored 1000 vibration signal samples, and the sensitive frequency components are extracted in the time-domain and processed into the RMS form. Figure 3.23 maps the detailed program flow of the SFP_i module.

Next, the signals in respective RMS formats are fed into the trained RBF-I_i module to infer the vibration at the tool tip at these frequencies. The outputs of RBF-I_i modules are Y_{r1}, Y_{r2}, Y_{r3} and Y_{r4} which are the inferred vibration spectrums at the tool tip.

The inferred vibration signals Y_{r1}, Y_{r2}, Y_{r3} and Y_{r4} are channeled into the Fusion (F) module for data collation based on its dominant frequency. The collated result buffered in the F Table is Y_r, which represents unified inference result representing different dominant frequencies. Each column of F Table represents a detected frequency component. The rows of F Table represent discrete RMS magnitudes for each frequency component. Each ascending row is a discrete RMS magnitude corresponding to time. The table is constantly updated with oldest data being overwritten in a circular manner. F Table can be utilized as an important part of a precision machine health or fault monitoring system, where it provides detailed real-time vibration data in the form of dominant frequencies components that represent detected vibration sources.

In this experiment, F Table has 2 columns: a column for 100Hz vibration component and a column for 120Hz vibration component respectively. F Table has 1000 rows for each column, capable of buffering 1000 RMS data (at 1ms interval per data) per column. The inference results are from Y_{r1} and Y_{r3}, whereas, Y_{r2} and Y_{r4} are on hot standby for failsafe purpose, and only to be invoked when both sensors related to Y_{r1} and Y_{r3} are faulty or degraded to an extent that they are favored according to the latest MST. Figure 3.24 maps the detailed flowchart of the RBF and F modules.

Figure 3.25 shows the vibration signals ($y_1(t), y_2(t), y_3(t)$, and $y_4(t)$) respectively from the sensors mounted at L_1, L_2, L_3 and L_4. In this experiment, sensors at L_1 and L_3 are the primary sensors selected for measuring vibration components at frequencies 100Hz and 120Hz respectively. Figure 3.26 shows the 100Hz vibration component at input to RBF-I$_1$, and its corresponding inferred vibration output at the tool tip, which incurs 7.2% error compared to the actual vibration measured at the tool tip. Figure 3.27 shows the 120Hz vibration component at input to RBF-I$_3$, and the corresponding inferred vibration output at the tool tip, which shows a 5.4% error compared to the actual vibration measured at the tool tip.

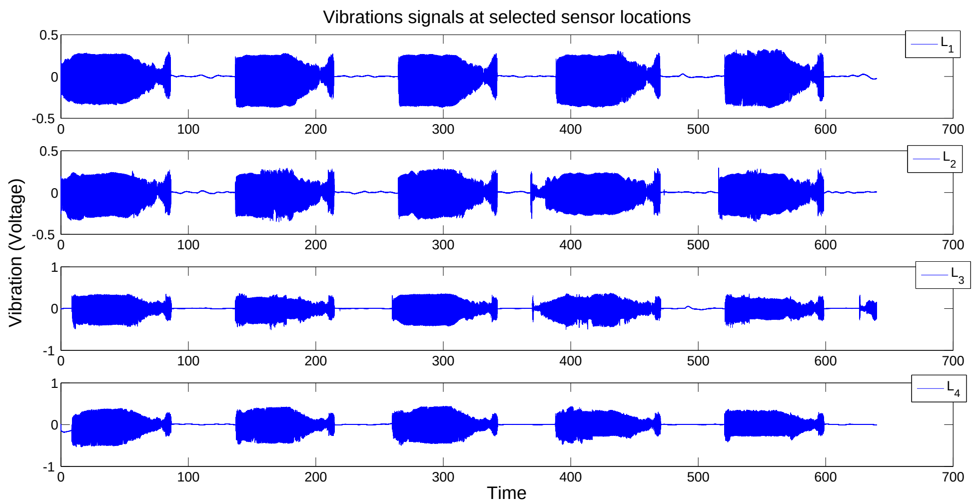

Figure 3.25: Vibrations signals at the selected sensor locations.

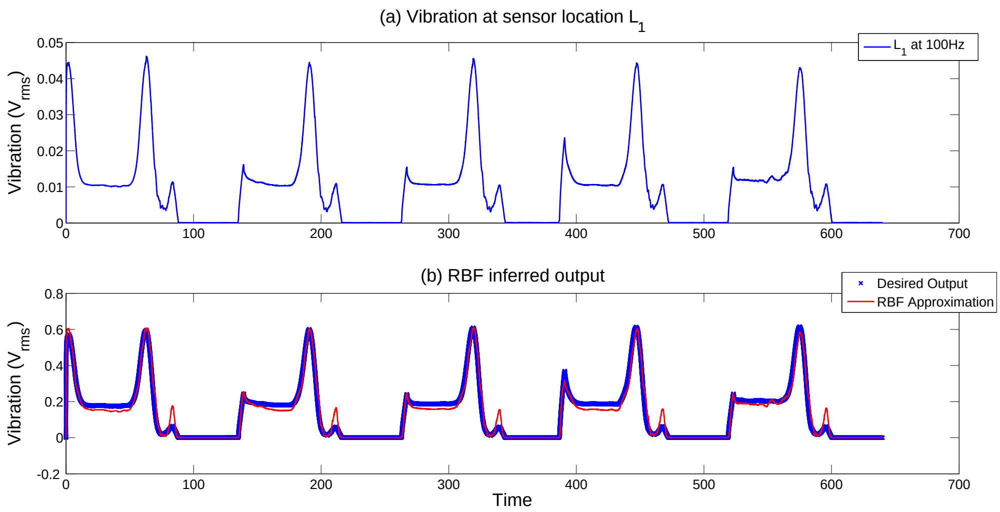

Figure 3.26: RBF inference result for L_1 (7,1),100Hz.

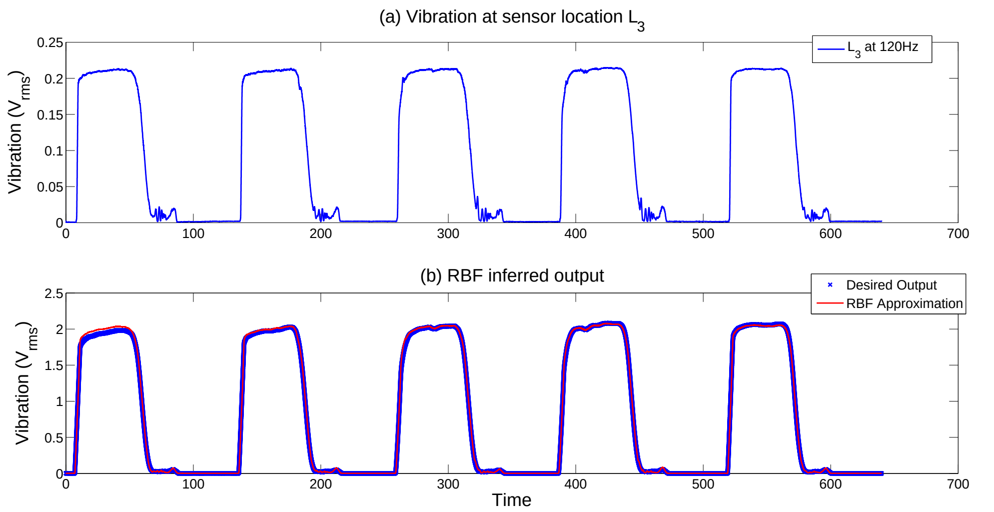

Figure 3.27: RBF inference result for L_3 (8,1),120Hz.

3.4 Discussion

This chapter has proposed and demonstrated a feasible method towards sensor placement, sensory set selection and fusion for continuous and real-time monitoring of machine conditions. The methodology is demonstrated in this chapter by using a precision cutting machine, with the objective to use an optimal (minimal) number of vibration sensors mounted at identified locations of the machine to infer the actual vibration frequencies spectrums at the cutting tool tip (critical point). Each mounted sensor is sensitive to a particular vibration frequency component and contributes to the accuracy of the inferred vibration measurement at the tool tip.

The generated vibration frequency components are dependent on the material of the workpiece and the deployed cutting tool. For a typical cutting machine, changes in measurement requirement is almost certainly related to the change in the type of material to be machined and the cutting tool. Different material when machined emits a range of vibration frequencies components [148–150] that can be used for machine CM. Thus, additional sensors can be mounted at other identified locations if there is a change in the measurement requirement of the critical point (e.g., change in workpiece material or cutting tool).

The existing system for monitoring of tool tip vibration is scalable and can be expanded when necessary in the event of changes to the workpiece material or the cutting tool. In the example, 100Hz and 120Hz frequency components are identified as the required components for accurate inference of vibration at the tool tip, with the known sensor mounting location for each frequency. The MST contains information pertaining to these two frequencies of interest based on regular updates from the FDP, and the SFP for each sensor sieves out the relevant sensitive frequency from each sensor. The trained RBF network for each sensor will infer the required frequency components at the tool tip and the inferred components are fused to form the inferred vibration at the tool tip.

In the event of a different workpiece material with different cutting tool are introduced to the existing cutting machine, there will be new sets of vibration frequencies to be inferred at the tool tip. The existing system for vibration monitoring can be easily scaled to accommodate this new requirement. Assuming a new 50Hz vibration frequency component is required for inference of the vibration at the tool tip, the new sensor location (L_{new}) sensitive to this new frequency must be determined by using the procedure prescribed in this chapter. MST is modified to include an entry for the new frequency, and the SFP of the new sensor will sieve out the 50Hz component based on the MST information. A RBF network for this new frequency must be trained to correctly infer this new frequency component at the tool tip. The final vibration at the tool tip comprises of the fusion of the inferred frequency components (50Hz, 100Hz and 120Hz).The modified vibration monitoring system can now work with different workpiece materials and different tools. Thus, new locations sensitive to new frequencies components can be easily determined and additions of new sensors will further improve the existing tool tip vibration monitoring system for use in machine CM system to cater for different workpiece materials and different cutting tools.

The existing vibration monitoring system uses only vibration sensors for its measurements. In a situation where a vibration sensor is not sensitive enough to pick up any form of low frequency vibration from the tool tip, other type of sensors may be used. One such possibility will be a directional sound sensor with active noise cancelation for measuring low level machine sound emission [151] [152]. The sound sensor is positioned to be directed towards the location of the tool tip, and the measured sound emission can be fused together with the inferred vibration signal at the tool tip to produce a tool tip sound - vibration fusion signal (or data) that will reflect the tool tip condition with greater accuracy and can be used by a machine CM system.

Inferred tool tip conditions can be used to determine (or predict) the health condition of a cutting machine. The various tool tip conditions can be classified for various machine health conditions (or levels). A machine CM system can use the tool tip conditions as its primary input. Internally, the CM system has a classifier that processes the tool tip conditions and determine (or predict) the machine's health condition. There are several known classification methods such as the well-known Support Vector Machine (SVM) or the artificial neural network (ANN) based classifiers.

3.5 Summary

An approach for sensor placement, selection and fusion for continuous machine CM has been proposed and validated in this chapter. The approach uses a minimal series of sensors mounted at key locations of a machine to measure and infer the actual vibration spectrum at a critical point where it is not suitable to mount a sensor. The selection is based on an indicator which leverages on sensitivity and the Fisher Information which is pre-calibrated over a range of frequencies. The top ranked sensors for each frequency can vary dynamically with time and the selected ones are used to infer the vibration at a critical point using a RBF network. A comprehensive case study was set up and used to validate the methodology behind the proposed machine CM method.

Chapter 4

Machine Condition Monitoring based on Acoustics

4.1 Introduction

Traditionally, monitoring, diagnosing, and operating the machines on the manufacturing floor are the important works of operators, technicians and engineers. Possible human errors that occurred during such works will give rise to serious problems with respect to the safety and reliability of the overall machines. In each machine, some of the critical components (or parts) are operating under constant stress due to production related demands. In manufacturing, monitoring of various parameters indicative of a machine's operation can be useful in determining the health of the machine, and predicting when and what type of service may soon be required for the machine. Machines of all types are subject to health condition monitoring (CM), and data about machine operation can be gathered in many different ways and reflecting a multitude of parameters.

Vibration sensor coupled with advanced signal processing techniques have been developed to detect vibration signal resulted from machine fault and tool wear but with varying degree of accuracy because the method requires a high Signal to Noise Ratio (SNR), and the fault signal must be significantly larger than the background vibration (noise). An alternative to identify machine fault is to measure sound emission from the machine. Sound signal analysis is performed in the time and frequency domains to acquire insights into the nature of the sound patterns under different operating conditions. Techniques such as the Fourier Transform (FT), the Continuous Wavelet Transform (CWT), and the Wigner-Ville distribution (WVD) are the several commonly used signal processing techniques for sound signal analyzes in different signal domains [153] [154]. For sound analysis, the SNR is important, and with properly directed microphones and advanced audio signal filtering and pre-processing, the SNR can easily be increased. However, the result of an analyzed sound signal is of varying degree of accuracy because of the sensitivity of the microphones in easily picking up unwanted environmental sound signals.

In contrast to vibration signals, sound signals from a machine can be measured at distances sufficiently far from a vibrating machine surface with the help of microphones [155] [156]. This allows the sound signal to be measured for machine working at a condition (extreme temperature and humidity) which is not suitable for vibration measuring sensors such as proximity transducers or accelerometers. In certain situation, it is advantageous to use a single sound sensor to obtain superimposed sound signals from more than one machine elements and to collectively process the signals to determine the health of the different machine elements which otherwise may not be possible with the vibration signals. Unfortunately, at the same time, the sound sensor can very easily pick up sound signals from other unwanted sources.

In some cases, the basic human sense of listening is also utilized as a form of manual CM to determine machine health condition. For a properly trained and experienced service engineer who has been handling a specific machine for a long time, finding potential machine faults with this method is not an issue and albeit rather subjective [157]. The service engineer listens for sounds made by the machine in order to identify machine faults indicators as early as possible. In all, the method is relying on accumulated experience of working with a certain machine, and is accurate only after a long period of machine handling. This method is well known and very established.

4.2 Problem Formulation

In order to further understand the requirement of a real-life machine CM, a visit to Makino Computer Numerical Control (CNC) precision machining center was arranged. Makino provides precision machining services, and trains their engineers in monitoring and maintaining their range of precision machining equipments. For an experienced and well-trained service engineer, and by carefully listening to the emitted sound when a machine is in operation, he will be able to gauge the machine's operating condition. Any unfamiliar sound may warrants an investigation into its cause, as it may represents a fault or an impending fault. This is the easiest and most commonly used direct analysis method utilizing human listening skill and relevant domain knowledge for machine CM. The method is effective and accurate if executed properly.

By using human sensory and judgement skills in machine CM implies that the person in-charge of performing the machine CM must be highly skilled with sufficient domain knowledge on the operation of the machine to be monitored [157] [158]. A person in-charge of the machine health inspection may miss out on important sound signatures or tell-tale signs of the impending machine faults, if during the inspection process, he is distracted or not in full concentration, thus affecting the consistency of diagnostic results. In another scenario, if the experienced person suddenly leaves his job, it will take valuable amount of time to retrain a new person taking over the machine, and the new person may not be as proficient as the one who left. Issues surface when any of the trained personnel leaves the designated job (e.g., resignation), and Makino has to go through the tedious process of training for a new replacement. Such a scenario frequently happens, and over the years Makino has attempted to automate the machine CM methods with the standard approach discussed earlier, but with mixed levels of accuracies.

Consider a car engine as an example of a rotating machine that is in operation. A car engine can be considered as a complex mechanical structure with many internal vibration sources that contribute to an overall machine vibration. The engine, when running produces noise that is related to its rotating speed. Thus, a car driver (machine operator) gets accustomed to the engine sound in a normal driving condition. When the car gets older, the engine parts start to wear and faults may soon develop inside the engine. These faults can be recognized by the driver when he suddenly hears a strange unfamiliar noise among the familiar car noise. A fault with a low contribution to the spectrum may be masked by high-energetic frequencies from other engine components (e.g., water pump, air-conditioning compressor, or a functioning gearbox). When a noticeable fault develops, a clearly distinguishable sound component at some unfamiliar audible frequency can emerge. Thus, one of the well-known way to diagnose the problem is to let the engine runs and listen carefully to the engine sound. The driver becomes aware of the type of fault by relating it to the type of unconventional sound (or engine noise) produced by the engine. This scenario highlights a well-known method of machine fault diagnostic and CM by listening and analyzing sound emissions from a running machine, detecting and diagnosing faults in an early stage [157], which is feasible since faults will manifest themselves as pure tones or strange machine sounds in the overall machine vibration. This approach will require fault versus machine sound signature relational database for each new machine, since each machine may vibrate in its own specific manner.

Sound analysis is a method of using sound signal information (e.g., waveform, spectral and phase) to aid in the diagnosis of a machine health condition [159] [160]. When a machine cannot be taken out of service for detailed inspection, the efforts of diagnosing the machine condition can be challenging. The efforts require an understanding of the machinery behavior, operating conditions, and diagnostic techniques. In this analysis, the health condition of the machine based on collected data can be analyzed. This allows the changes within the machine to be determined precisely, and appropriate corrective action can be initiated. Although there are several methods of CM, sound analysis is chosen for several reasons: (a) It is easy to be implemented and is reliable, (b) Different defects produce different sound patterns (signatures) and can relate to a specific mechanical component defect (e.g., bearing), and (c) Sound monitoring is relatively inexpensive. The assessment of machine's condition varies from machine to machine. The successful operation of a machine relies on the performance of each machine component, and requires a detailed understanding of the behavior of these elements and their interaction.

This chapter introduces a novel approach towards machine CM. The approach closely mimics the human ear listening process, and attempts to learn the machine operating conditions via the detected sound signatures. With proper machine learning, this approach will be able to distinguish the machine operating conditions in an autonomous manner without human intervention, and minimize the need of highly skilled personnel to monitor the machine condition.

In a machining center, each CNC precision vertical milling machine (rotating machine) has a vertical cutting tool that is based on the same cutting method of a manual control milling machine. Thus, a milling machine which is simpler in the overall structure than a CNC machine is used extensively for the purpose of illustrating the sound based machine CM. A typical milling machine consists of a rotating driving element (e.g., an electric motor) driving a precision work tool element (e.g., cutter) through a series of mechanical couplings (gears, belts, etc.). Mechanical bearings are used to reduce mechanical frictions at all the rotating shafts. In order to ensure an optimal operating condition for the machine, and to produce quality end products, all the elements discussed must be of good working condition. For this class of machine, the most commonly encountered mechanical defects are attributed to the mechanical bearings wear, where each bearing is subjected to extensive mechanical wear and tear, and due to the work tool element wear. Bearing and work tool failures are the foremost causes of rotating machine breakdown. The failures can be catastrophic and usually result in costly machine downtime. This chapter concentrates on the method of machine CM via machine sound analysis in order to identify bearings and cutting element wears.

4.3 Hardware Design

The CM hardware designed for Makino is based on the modular components framework defined in Chapter 2 with (a) CM Data Acquisition and Pre-Processing (CM-DAP) module, and (b) CM Data Processing and Alert (CM-DPA) module. Figure 4.1 depicts a scenario of a small scale precision machining center where its milling machine is fitted with the proposed CM system. In this setup, the CM system monitors the crucial bearings and cutting tool health conditions. As such, sound sensors are directed to the appropriate locations reflecting the bearings and the cutting tool. Two sets of CM-DAP modules (CM-DAP-1 and CM-DAP-2) are deployed on the milling machine. CM data collected from each CM-DAP is wirelessly transferred to a CM-DPA module connected to a host computer for real-time display of monitoring results.

Figure 4.2 and 4.3 depict the functional block diagrams of the CM-DAP and CM-DPA modules. Both modules are designed based on the common hardware framework defined in Chapter 2. In Figure 4.2, the CM-DAP consists of a Sensor Interface, Non-Volatile Memory, Microcontroller Unit (MCU), Wi-Fi Wireless Communication and Power Supply sub-blocks. A pair of external uni-directional

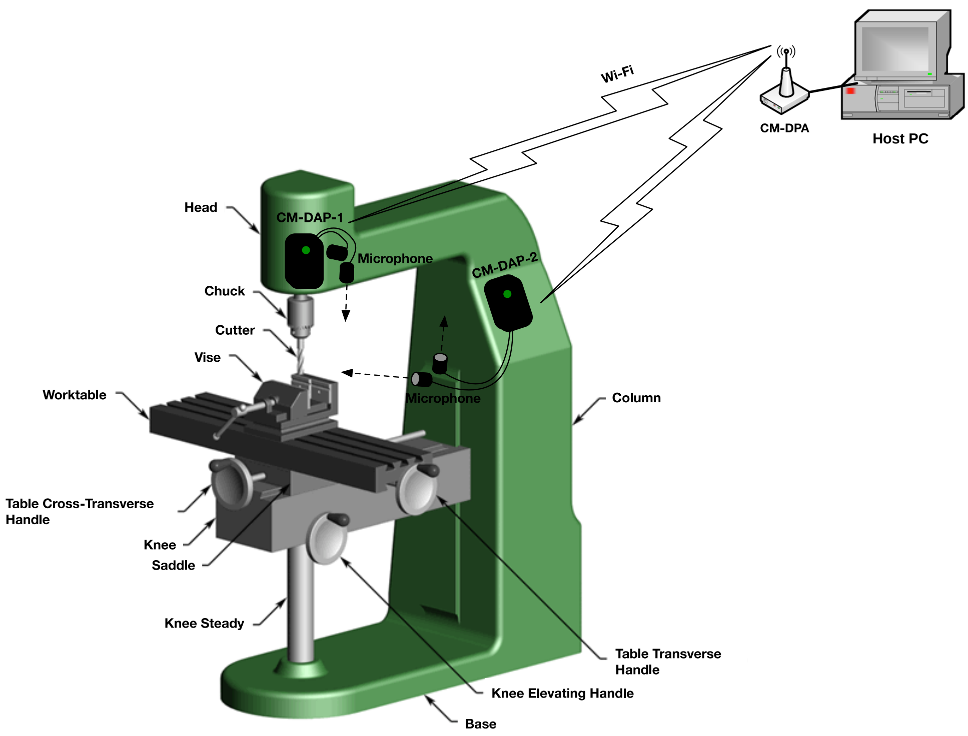

Figure 4.1: Precision Machining Center with Proposed Condition Monitoring Solution.

microphones (sound sensors) are connected to the Sensor Interface that provides the necessary biasing and signal conditioning. Sound signal is sampled and pre-processed by the digital signal filtering and pre-processing algorithm in the MCU, and the pre-processed sound data is transmitted wirelessly to the CM-DPA module via the Wi-Fi Wireless Communication, for further processing. Signal filtering and pre-processing coefficients are stored in the Non-Volatile Memory. Power Supply provides regulated and DC supply for the CM-DAP.

The CM-DPA depicted in Figure 4.3 contains Wi-Fi Wireless Communication, MCU, Non-Volatile Memory, User Interface and Alert and Power Supply sub-blocks. The Wi-Fi Wireless Communication receives sound data from the CM-DAP modules. The MCU processes the digital sound data received from the CM-DAP modules using the custom CM algorithm and coefficients stored in the Non-Volatile Memory. The User Interface and Alert interfaces to a host computer to display CM results and alerts.

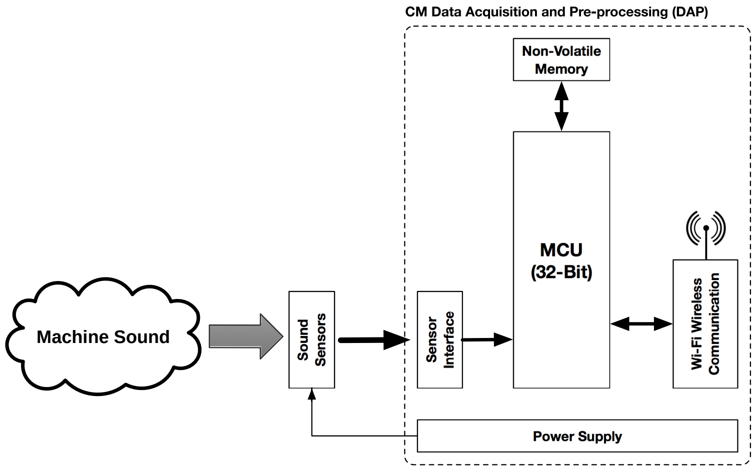

Figure 4.2: CM Data Acquisition and Pre-processing Module Functional Block Diagram.

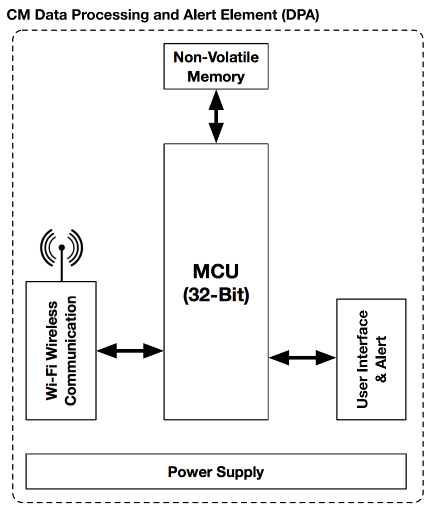

Figure 4.3: CM Data Processing and Alert Module Functional Block Diagram.

Figure 4.4 and 4.5 depict the completed hardware prototypes of the CM-DAP and CM-DPA modules respectively.

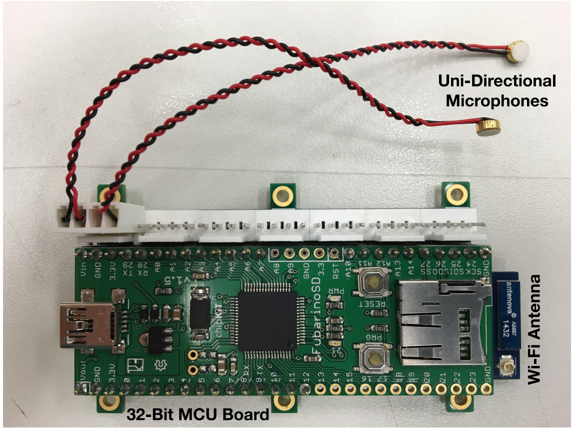

Figure 4.4: CM Data Acquisition and Pre-processing Module Hardware Prototype (with attached 2 uni-directional microphones).

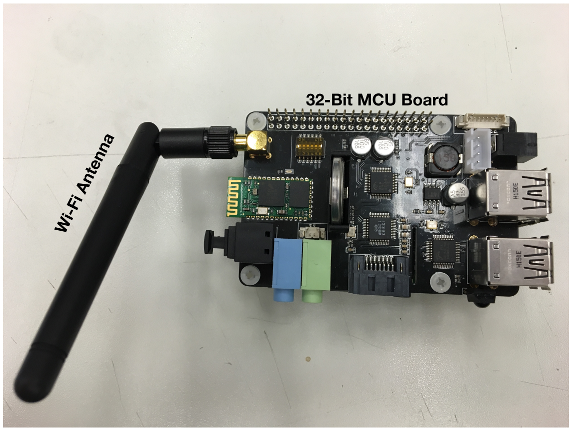

Figure 4.5: CM Data Processing and Alert Module Hardware Prototype.

4.4 Machine Sound Analysis

When a machine is in operation, machine sound can be defined as a time-varying vibration that propagates as an audible mechanical wave of pressure and displacement through the air. Machine sound analysis constitutes of two important digital signal processing algorithms: (a) Sound signal filtering and pre-processing performed by the CM-DAP hardware module and, (b) Sound feature (signature) classification performed by the CM-DPA hardware module.

4.4.1 Sound Signal Filtering and Pre-processing

This section highlights in detail the two important procedure of adaptive filtering of machine sound and the extraction of sound feature (signature). The two procedures are performed by the CM-DAP hardware module. The conceptual signal flows within CM-DAP is depicted in Figure 4.6. MIC 1 is the primary microphone to capture the machine sound signal $d(k)$, and MIC 2 is the reference microphone to capture the environmental noise (reference) signal $n_2(k)$. Both $d(k)$ and $n_2(k)$ are processed by a Least Mean Square (LMS) based adaptive filter resulted in noise suppressed $\hat{d}(k)$ output. Next, Mel Frequency Cepstral Coefficients (MFCC) features vector $\mathbf{c}$ are extracted from $\hat{d}(k)$, and transmitted wirelessly via Wi-Fi to the CM-DPA.

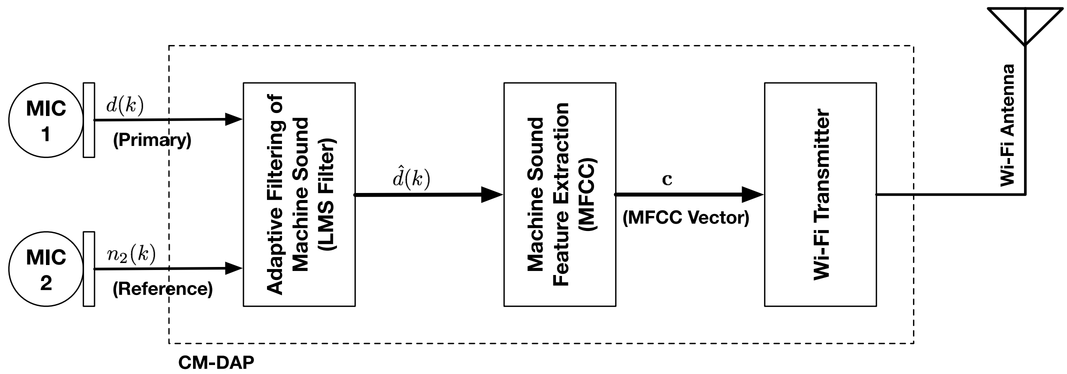

Figure 4.6: Conceptual Signal Flows within CM-DAP.

4.4.1.1 Adaptive Filtering of Machine Sound

Machine sound acquired from a running machine contains the machine specific sound signal superimposed with background environmental sound (ambient sound). The resultant sound signals are non-stationary, without any form of filtering and signal processing, the sound signal is practically unusable. Thus, the acquired machine sound is first pre-processed by a digital filter in order to minimize the ambient sound components. The filtered machine sound is then further processed to extract its machine sound signature.

Ideally, a digital filter is deployed to remove the ambient sound components, but in practice, it is impossible to do so, as the ambient sound frequency components usually overlap with the machine sound frequency components. Thus, a certain level of high ambient sound components attenuation can be achieved while maintaining minimal attenuations to the machine sound components. The digital filter based signal pre-processing stage implementation can be in the form of: (a) Finite Impulse Response (FIR) or Infinite Impulse Response (IIR) filter with fixed filter coefficients [161], or (b) A complex adaptive filter based on FIR or IIR with adaptive filter coefficients [162]. A FIR or IIR filter with fixed filter coefficients behaves like a classical analogue signal filter defined by the filter's cutoff frequency, and does not have the ability to discriminate machine sound signal from the ambient sound signal. Hence, it is not suitable for use in this chapter. On the other hand, a complex adaptive filter with adaptive filter coefficients has the capability to adaptively attenuate most of the ambient sound signal components if and objective function to determine the filter coefficients is properly defined.

Figure 4.7 depicts a simplified block diagram of an adaptive filter functional block based on the LMS algorithm. The filter has two signals inputs and is used to attenuate ambient sound components while retaining the majority of the machine sound components [163] [164]. The block diagram consists of two signals input vectors $\mathbf{d}(k)$ and $\mathbf{n_2}(k)$ representing the primary (desired) signal and the background noise (reference) signal respectively. $\mathbf{d}(k) = \mathbf{x}(k) + \mathbf{n_1}(k)$ consists of ideal desired signal vector $\mathbf{x}(k)$ being contaminated with noise vector $\mathbf{n_1}(k)$. It is further established that $\mathbf{n_1}(k)$ and $\mathbf{n_2}(k)$ noise signals are correlated, and for simplicity, both $\mathbf{n_1}(k)$ and $\mathbf{n_2}(k)$ are not correlated with $\mathbf{x}(k)$.

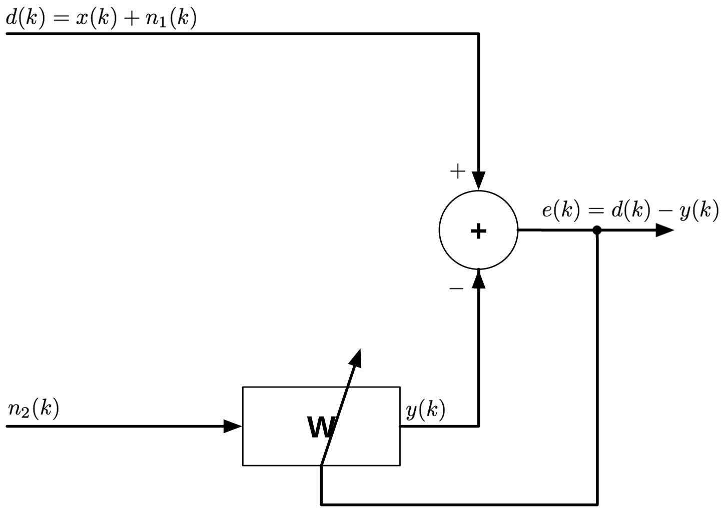

Figure 4.7: Two Input Signals Adaptive Filter Block Diagram.

The error signal vector is $\mathbf{e}(k) = \mathbf{d}(k) - \mathbf{y}(k)$, where $\mathbf{y}(k)$ is the estimated noise signal output vector filtered from noise signal input vector $\mathbf{n_2}(k) = [n_2(k), n_2(k-1), ..., n_2(k-N)]^T$ using an adaptive filter W. The adaptive filter W is based on a transversal FIR filter structure (or tapped-delay line) with tunable adaptive filter coefficients vector $\mathbf{w}(k) = [w_0(k), w_1(k), ..., w_N(k)]^T$, where N represents the filter length (or order). Thus, filter W output of $y(k)$ can be represented with a standard equation for FIR filter with tunable coefficients in Equation 4.1 [164].

$$\mathbf{y}(k) = \mathbf{w^T}(k) \cdot \mathbf{n_2}(k) \tag{4.1}$$

For consistency, the error signal vector $\mathbf{e}(k) = \mathbf{d}(k) - \mathbf{y}(k)$ is rewritten as

Equation 4.2 which reflects the ideal desired signal vector $\mathbf{x}(k)$ being contaminated with noise signal $\mathbf{n_1}(k)$, and subtracting the estimated (or filtered) noise $\mathbf{y}(k)$. Thus, $\hat{\mathbf{d}}(k) = \mathbf{e}(k)$ is the estimated desired signal with $\mathbf{n_1}(k)$ suppressed.

$$\mathbf{e}(k) = \mathbf{x}(k) + \mathbf{n_1}(k) - \mathbf{y}(k) = \hat{\mathbf{d}}(k) \tag{4.2}$$

One of the most widely used objective function ($\xi(k)$) in adaptive filtering to achieve optimal $\hat{\mathbf{d}}(k)$ is via the Mean-Squared Error (MSE) approach [164], where:

$$\xi(k) = E\{\mathbf{e^2}(k)\} = E\{\mathbf{d^2}(k) - 2\mathbf{d}(k)\mathbf{y}(k) + \mathbf{y^2}(k)\} \tag{4.3}$$

By assuming $x(k)$ is uncorrelated to $n_1(k)$ and $n_2(k)$, Equation 4.3 is further simplified into:

$$\xi(k) = E\{\mathbf{x}^2(k)\} + E\{[\mathbf{n_1}(k) - \mathbf{w^T} \cdot \mathbf{n_2}(k)]^2\} \tag{4.4}$$

Equation 4.4 depicts that if the adaptive filter having $\mathbf{n_2}(k)$ as the reference input signal (background noise), is able to accurately predict the noise signal $\mathbf{n_1}(k)$, the minimum MSE is depicted in Equation 4.5. Thus, the error signal $\mathbf{e}(k)$ is equal to the estimated desired signal $\hat{\mathbf{d}}(k) \approx \mathbf{x}(k)$ with $\mathbf{n_1}(k)$ suppressed.

$$\xi_{min}(k) = E\{\mathbf{x}^2(k)\} \tag{4.5}$$

A gradient based LMS adaptive algorithm [164] depicted in Equation 4.6 is used to achieve ξ_{min}, where μ is the convergence factor, and is defined to be in the range of $0 < \mu < \frac{1}{\lambda_{max}}$ to guarantee convergence, where λ_{max} is the largest eigenvalue of a correlation matrix $E\{\mathbf{n_2}(k) \cdot \mathbf{n_2}^\mathbf{T}(k)\}$.

$$\mathbf{w}(k+1) = \mathbf{w}(k) + 2\mu e(k) \cdot \mathbf{n_2}(k) \tag{4.6}$$

Figure 4.8 depicts the functional block diagram realization of the LMS algorithm for a transversal (delay line) input $\mathbf{n_2}(k)$. Typically, one iteration of the LMS requires $N+2$ multiplications for the filter coefficient updating and $N+1$ multiplications for the error $e(k)$ generation.

The adaptive LMS algorithm is continuously updating $\mathbf{w}$ for $k \geq 0$. A brief summary of the LMS algorithm updating procedure and implementation in a MCU:

- Step 0: Initialize: $\mathbf{n_2}(0) = \mathbf{w}(0) = [0,\ 0,\ ...,\ 0]$ or known initial values.
- Step 1: For $k \geq 0$, continue to Step 2.
- Step 2: Evaluate: $e(k) = d(k) - \mathbf{n_2}^\mathbf{T}(k)\mathbf{w}(k)$, continue to Step 3.
- Step 3: Evaluate: $\mathbf{w}(k+1) = \mathbf{w}(k) + 2\mu e(k) \cdot \mathbf{n_2}(k)$, continue to Step 4.
- Step 4: $k = k + 1$
- Step 5: Go to Step 1.

4.4.1.2 Machine Sound Feature Extraction

In this section, a method that closely mimics a human ear in listening and extracting sound feature of a running machine is proposed, with the objective of achieving accuracy, repeatability and consistency of identifying sound features related to various machine operating conditions. In human voice identification, there are various well-known methods of feature extractions that are accurate and used for the purpose of speaker identification. One of them is the MFCC

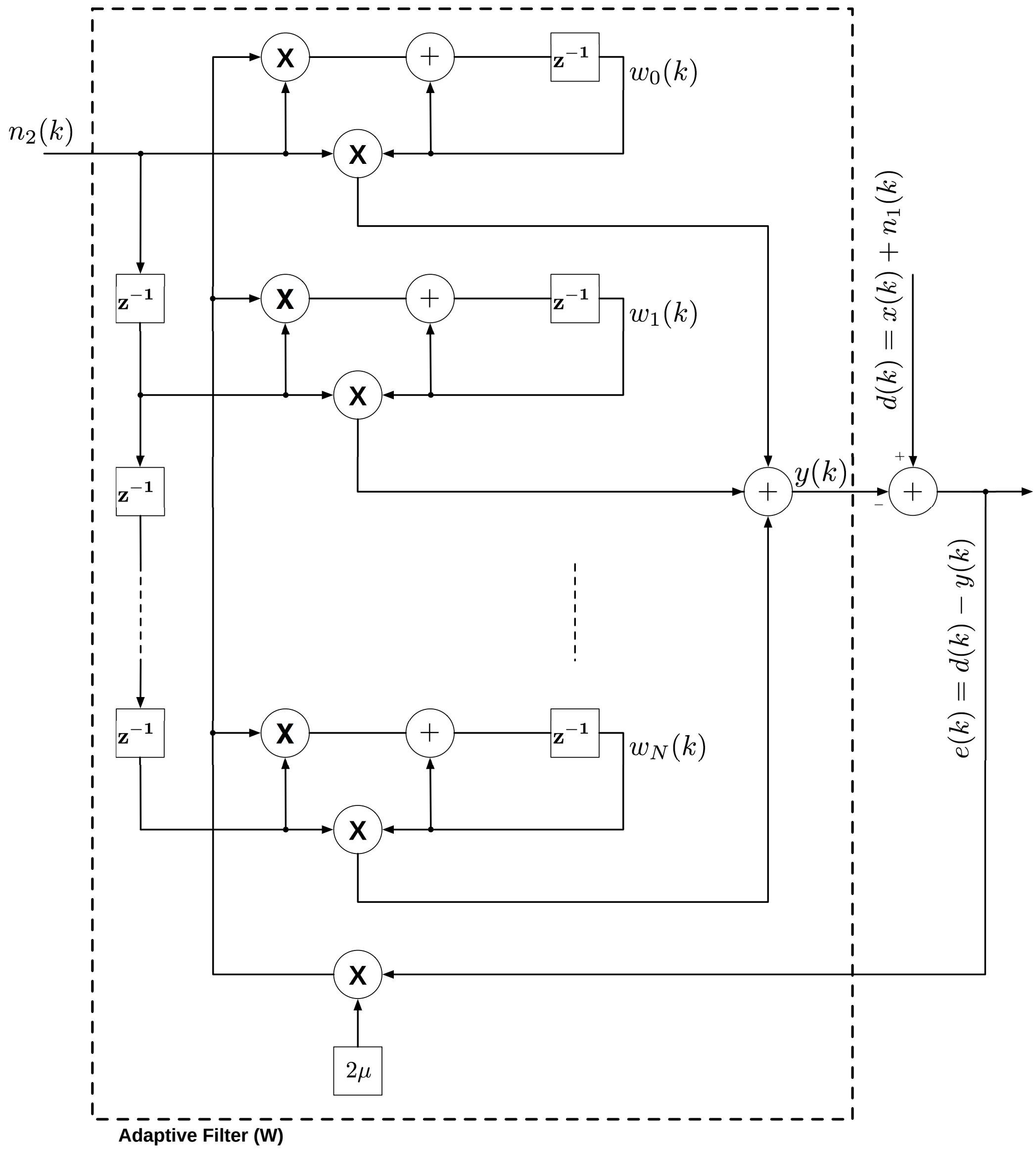

Figure 4.8: Two Input Signals LMS Adaptive Filter Block Diagram.

parameterization method [165] [166]. A Mel is a psychoacoustic unit of measure for the perceived pitch of a tone, rather than the physical frequency. The correlation of the Mel frequency to the physical frequency is not linear, as the human auditory system is a nonlinear system. Figure 4.9 depicts the non-linear relationship mapping of Mel frequency to the physical frequency. The physical frequency is determined to be in the range of 0 to 8kHz, which is sufficient to observe the sound signal emission of a machine in operation. This nonlinear scale is important as it mimics the human listening process [167]. MFCC features vector are extracted using a standard Mel scale and a linear scale, where different filters sets (number of filters and frequency range) are applied [168] [169].

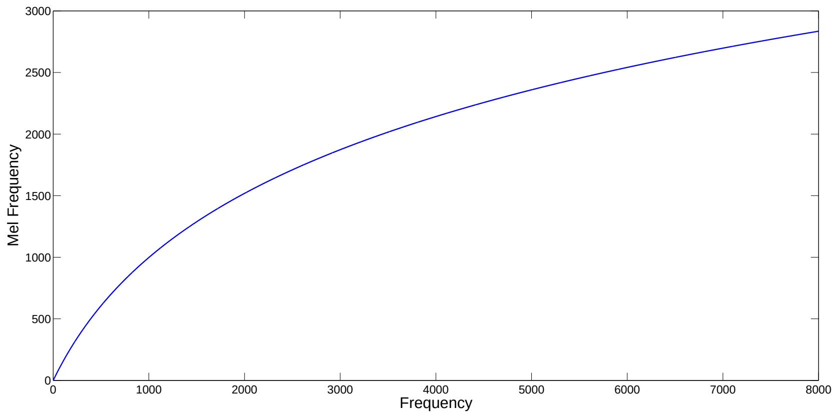

Figure 4.9: Non-linear relationship mapping of Mel frequency to the physical frequency.

$\hat{d}$ is the filtered machine sound output from the adaptive filter with its noise component n_1 suppressed (from previous sub-section). The next step is to extract the sound feature that can uniquely identify the types of machine sounds associated with different machine operating conditions. To calculate the MFCC features vector, $\hat{d}$ is divided into an evenly short time windows of size N_f. Discrete Fourier Transformation (DFT) [170] of each time window for $\hat{d}$ with length N_f resulted in $D(k_f)$ frequency components, is determined with Equation 4.7, with $n = 0, 1, ..., N_f - 1$ representing discrete time signal sample up to $N_f - 1$, $k_f = 0, 1, ..., N_f - 1$, where k_f corresponds to the frequency $f(k_f) = \frac{k_f \cdot f_s}{N_f}$, f_s is the sampling frequency (in Hz) and $w_h(n) = 0.54 - 0.46cos(\frac{2\pi n}{N_f - 1})$ is a discrete Hamming windowing function [171] [172] of $N_f - 1$ length.

$$D(k_f) = \sum_{n=0}^{N_f-1} w_h(n) \cdot \hat{d}(n) \cdot \exp(\frac{-j2\pi nk_f}{N_f}) \tag{4.7}$$

For the next step, $|D(k_f)|$ is scaled in both magnitude and frequency into the Mel scale equivalent (Figure 4.9) by using Equation 4.8, where $H(f(k_f), m)$ is a Mel filter bank with characteristic defined in Equation 4.9.

$$\hat{D}(m) = ln\left(\sum_{k_f=0}^{N_f-1} |D(k_f)| \cdot H(f(k_f), m)\right) \tag{4.8}$$

$$H(f(k_f), m) = \begin{cases} 0 & for \quad f(k_f)c < f_c(m-1) \\ \frac{f(k_f)-f_c(m-1)}{f_c(m)-f_c(m-1)} & for \quad f_c(m-1) \leq f(k_f) < f_c(m) \\ \frac{f(k_f)-f_c(m+1)}{f_c(m)-f_c(m+1)} & for \quad f_c(m) \leq f(k_f) < f_c(m+1) \\ 0 & for \quad f(k_f)c \geq f_c(m+1) \end{cases} \tag{4.9}$$

The center frequencies on the Mel Scale in the Mel filter bank are computed by approximating the Mel scale with $\psi = 2595 \cdot log_{10}(\frac{f}{700}+1)$ which is a commonly used approximation [172]. ψ is not linear for all frequencies. A fixed frequency resolution in the Mel scale is determined, corresponding to a logarithmic scaling of the repetitive frequency using $\Delta\psi = (\psi_{max} - \psi_{min})/(M+1)$ where ψ_{max} is the highest frequency of the filter bank on Mel scale computed from f_{max}, ψ_{min} is the lowest frequency in the Mel scale having a corresponding f_{min}, and M is the number of filter banks. The center frequencies on the Mel Scale are given by $\psi_c(m) = m \cdot \Delta\psi$ for $m = 1, 2, ..., M$. f_c (in Hz) in Equation 4.9 can be calculated with $f_c(m) = 700 \cdot (10^{\frac{\psi_c(m)}{2595}} - 1)$ [172]. Figure 4.10 depicts the magnitude (gain) plot of the resultant Mel filter banks based on M number triangular bandpass filters.

The final step to determine the Mel Coefficients is to compute the Discrete Cosine Transform (DCT) of $\hat{D}(m)$ with Equation 4.10 for $l = 1, 2, ..., 12$ where

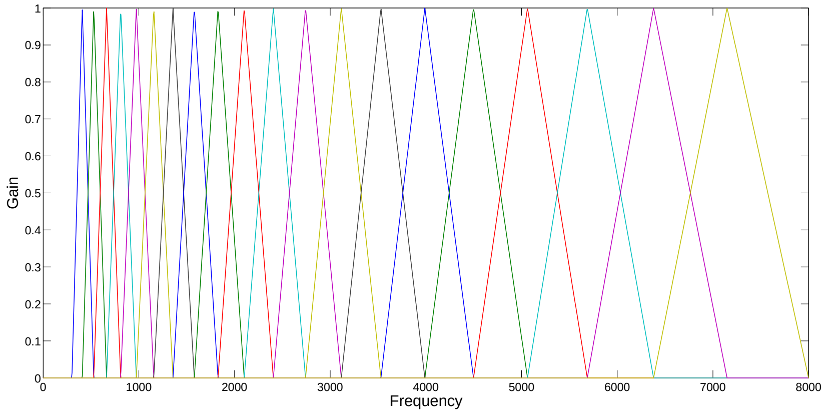

Figure 4.10: Mel filter banks.

$c(l)$ is the l^{th} MFCC. Thus, $\mathbf{c} = [c(1), c(2), ..., c(12)]^T$ represents the MFCC vector of $\hat{d}$. Traditionally each MFCC vector has a total of 12 cepstral feature coefficients that can be used to determine a machine health condition.

$$c(l) = \sum_{m=1}^{M} \hat{D}(m) \cdot cos(l \cdot \frac{\pi}{M}(m - \frac{1}{2})) \tag{4.10}$$

4.4.2 Sound Feature Classification

The extracted MFCC features of the captured machine sound have to be classified accordingly to the various types of defined machine operating conditions. In machine CM, the four basic machine operating conditions are defined as: (a) Normal, (b) Satisfactory, (c) Warning, and (d) Faulty. In CM, Normal and Satisfactory operating conditions do not warrant much attention besides the routine scheduled maintenance. The Warning operating condition warrants some attention, even though the machine is still in productive mode, there are evidences that some components are failing, and a preventive maintenance is therefore recommended. When a Faulty operating condition is detected, the machine has to be shutdown for maintenance and no longer in productive mode.

The developed CM-DPA hardware module is tasked into performing the sound feature classification process by receiving the MFCC features vector wirelessly via Wi-Fi from the CM-DAP. Figure 4.11 depicts the conceptual signal flows of the signal classification process. MFCC vector **c** received from Wi-Fi is processed via a trained Radial Basis Function (RBF) based classifier to determine the machine operating condition.

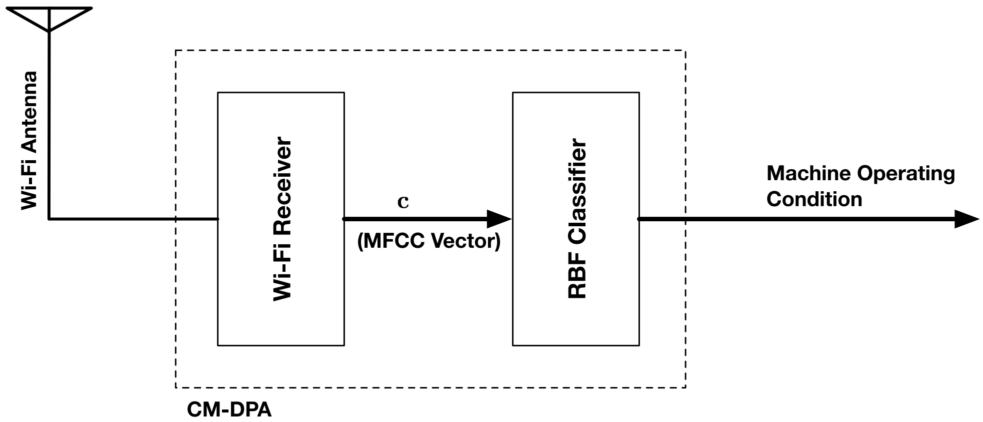

Figure 4.11: Conceptual Signal Flows within CM-DPA.

4.4.2.1 Radial Basis Function (RBF) based Classifier

There are many types of classifiers that can do the required classification task, ranging from using the Hidden Markov Model (HMM) or Support Vector Machine (SVM) classifiers, to the Artificial Neural Network (ANN) based classifiers (e.g., Radial Basis Function, Multilayer Perceptron and etc.). ANN based RBF inference procedure has been thoroughly discussed and demonstrated in Chapter 3. In this chapter, RBF network is used for the purpose of machine CM classification. The main reason of choosing RBF over the other conventional classifier such as SVM is due to the gradient-descent feature of the RBF and the multi-class classification requirement of the machine operating conditions. Figure 4.12 depicts the architecture of the RBF network based classifier. The input layer of the RBF network is the input vector $X(z)$. The extracted MFCC vector $\mathbf{c}$ received from CM-DAP forms the elements of $X(z)$, where $X(z) = [c_1(z),\ c_2(z),\ ...,\ c_{12}(z)]^T$, where $z = 0, 1, ...,\ Z$. Z is number of segmented signal frames determined from the full signal length of $\hat{d}$ divided with signal window size N_f. The hidden layer includes the parameters of RBF center C_i, and the Gaussian width σ_i of each RBF unit which represents its corresponding subclass. The output layer can be represented in Equation 4.11, where b_i represents the individual weight and ϕ_i represents the individual Gaussian activation function. i represents the index of the hidden layer (RBF unit) and I is the size of the hidden layer (RBF network).

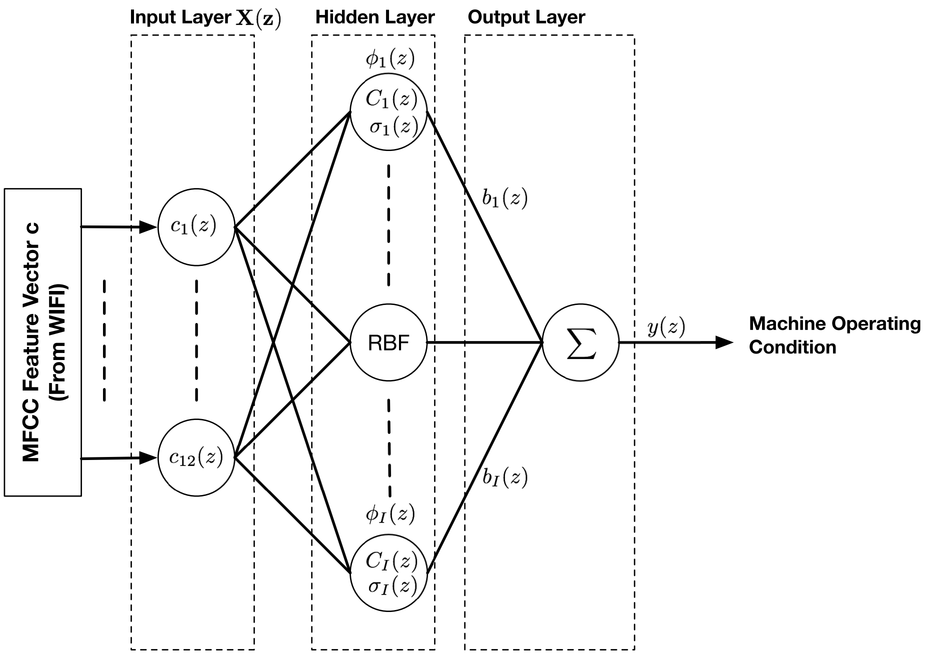

Figure 4.12: RBF based Classifier Architecture.

$$y(z) = \sum_{i=1}^{I} b_i(z)\phi_i(z) \quad i = 1,\ 2,\ ...,\ I \tag{4.11}$$

The Gaussian activation function ϕ_i is represented in Equation 4.12.

$$\phi_i(z) = \exp\left(-\frac{\|X(z) - C_i\|}{\sigma_i^2}\right) \tag{4.12}$$

The classification using RBF is based on the distance between the input and the center values of each subclass. In Equation 4.12, $\|.\|$ denotes the Euclidean norm of the input.

There is a possible scenario where some newly discovered machine sounds (discovered at later stage) are not expose to the RBF training process. Thus, there exists a possibility that the newly discovered machine sounds may cause the already trained RBF network to incorrectly classify them and generates the incorrect machine operating condition. By default, the CM-DPA handles the un-classified sounds as Faulty machine operating condition. CM-DPA has an information logging function built into its firmware to record the MFCC vectors and related information related to the Faulty machine operating condition. The recorded information will be properly reviewed and examined by some skilled personnel to ascertain that the trained RBF network has correctly classified the machine as Faulty. In the event when the newly discovered machine sounds are encountered, and it is determined that the machine is still operating within the acceptable range, the respective MFCC vectors will be used to re-train the RBF network, and the newly discovered machine sounds will be properly classified by the RBF network when the machine is back in operation. The concept of re-training of a trained RBF network is well-known and has been demonstrated by Li *et al* [173]. The re-training of the RBF network can be conducted during the scheduled machine maintenance. This feature of re-training the trained RBF network with newly discovered machine sounds is feasible as the machine aged, newly discovered machine sounds may surface during machine operations. Thus, the performance of trained RBF network will be improved in its classification accuracy.

4.4.2.2 RBF based Training Procedure

Prior to the start of RBF network training, streams of MFCC vectors calculated from the machine sounds are collected and stored. The machine sounds must be sufficiently large and must include the various examples of Normal, Satisfactory, Warning and Faulty machine operation conditions. The resultant MFCC vectors related to the relevant machine operating conditions are collected and grouped together and each group is assigned a unique identification number (0:Normal, 1:Satisfactory, 2:Warning, 3:Faulty).

70% of the data within each group are being utilized to train the RBF network, while 30% are reserved for use in the verification of the trained RBF network. The training procedure is based on the steps defined in Chapter 3. The training duration is solely dependent on the MSE of the trained output with the training data, and training will only stop when MSE condition is achieved.

The RBF by default is a good approximator, thus for this specific machine CM application, the trained RBF network output must be rounded to nearest integer if the output is in the form of a decimal. A simple Rounding-off Function is represented by Equation 4.13, where $\hat{y}(z)$ is the processed output of $y(z)$.

$$\hat{y}(z) = \begin{cases} 0 & for \quad y(z) < 0.5 \\ 1 & for \quad 0.5 \leq y(z) < 1.5 \\ 2 & for \quad 1.5 \leq y(z) < 2.5 \\ 3 & for \quad y(z) \geq 2.5 \end{cases} \tag{4.13}$$

4.5 Experiment and Verification

An experiment was conducted on a milling machine, where tool wear CM is conducted for its cutting tool. The machine was used to cut pieces of 1cm thick aluminum of 40cm in length, with a cutting rate of 0.17cm/s. A CM-DAP hardware is setup with its primary uni-directional microphone (front sound sensor) positioned at 10cm from the cutting tool and pointing in perpendicular position from the side of the cutting tool. A background (ambient) noise uni-directional microphone is positioned at the same position as the primary microphone, with its front sound sensor rotated at 90° away from sound sensor of the primary microphone. The 10cm distance is determined to be an optimal location for the primary microphone, as the location provides a sound pressure level of at least 90dBA [174] during machine operation which is safe for human ear. The sound pressure level was measured by a standard Sound Level Meter. A CM-DPA hardware is used to perform the tool CM.

Figure 4.13 depicts the machine sound resulted from the cutting process using a new cutting tool that highlights the captured sound that is un-processed (un-filtered in blue) and processed (adaptive filtered in green). The adaptive filter implements in the CM-DAP module is able to adaptively filter away the unwanted ambient noise that presents during the cutting process. The filtered machine sound represents the overall cutting process with great detail. The adaptive filter length N was empirically determined to be 61. A large filter convergence factor μ leads to faster filter output convergence but increases in instability which may resulted in uncontrolled output oscillation. Thus, $\mu = 0.01$ is empirically determined to provide the acceptable convergence time.

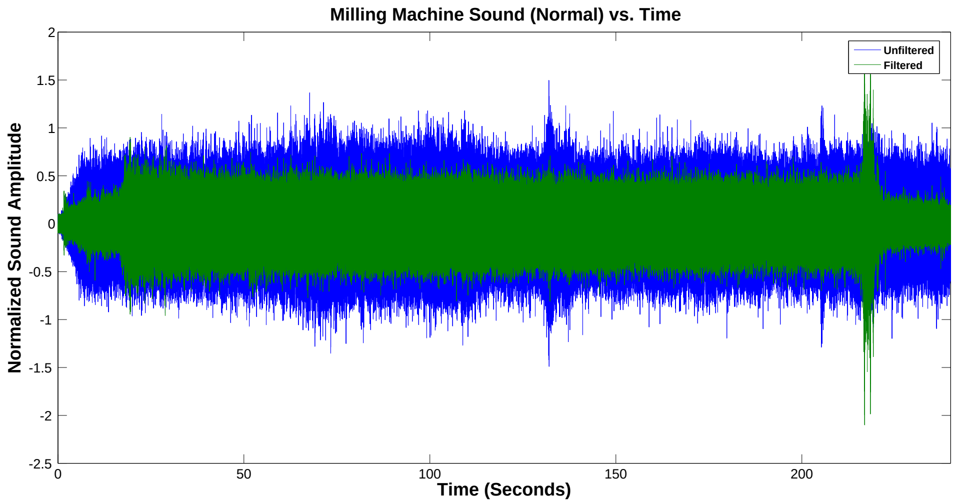

Figure 4.13: Unfiltered (Blue) and Filtered (Green) Machine Sound for a New Cutting Tool.

Various types of machine sound samples were captured representing the four types of machine operating (tool wear) conditions by using the four types of similar cutting tools with varying degrees of tool wear. “Normal” corresponds to a new and sharp tool, “Satisfactory” corresponds to a used tool still in good working condition, “Warning” corresponds to a used tool that has worn significantly but still usable, with signs of impending tool failure, and “Faulty” corresponds to blunt tool, unsuitable for use. Thus, there are four groups of machine sound data. Figure 4.14 to 4.17 depict the sound data depicting the machine sound for the four types of tool wear conditions. It can be roughly observed that the overall sound amplitude increases as tool wears.

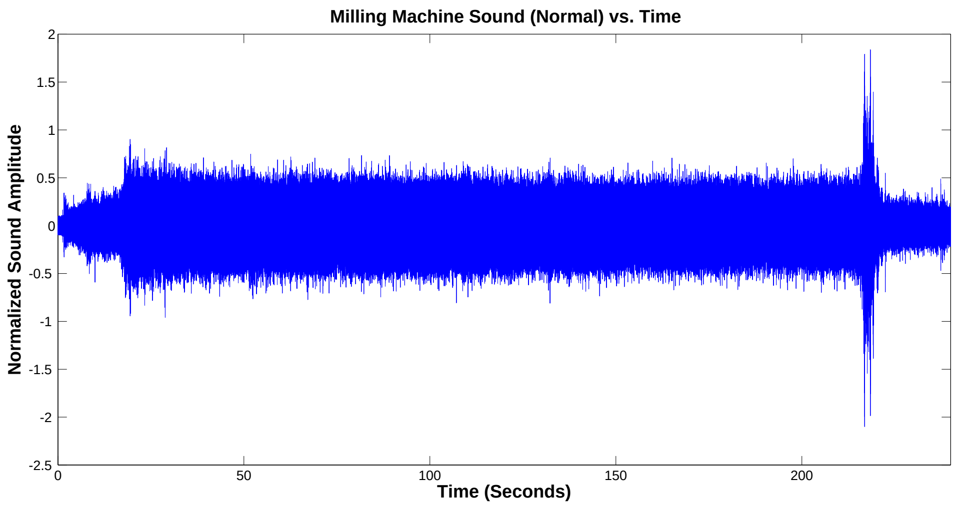

Figure 4.14: Filtered Machine Sound for a New Cutting Tool (Normal).

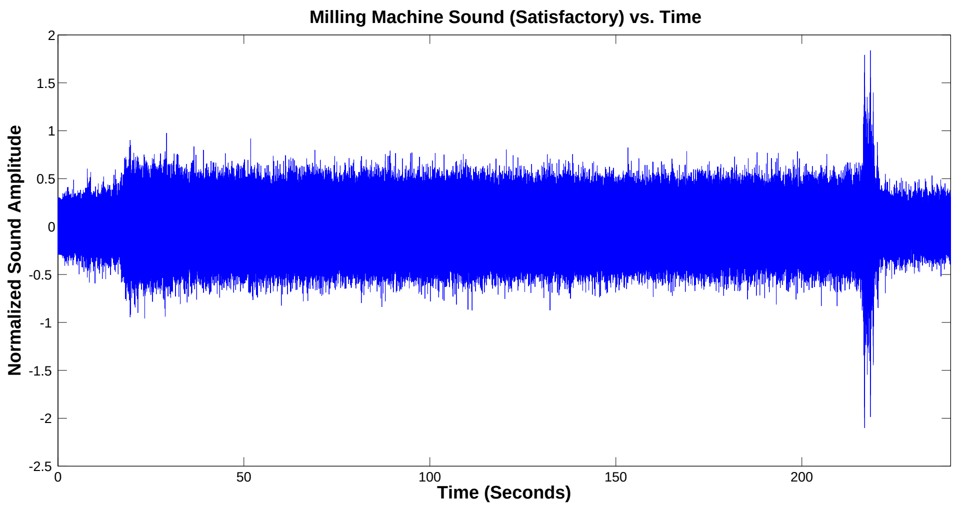

Figure 4.15: Filtered Machine Sound for a Used Cutting Tool in Good Condition (Satisfactory).

For each cutting tool, a 4 minutes sound sample was captured and processed. Sampling frequency $f_s = 16$kHz was sufficient for the experiment. For each machine operating condition, a length of $3,840,000$ raw sound data is captured for the 4 minutes duration. A small frame size of $N_f = 400$ samples is chosen, and with an overlap at every 10ms. Thus, there are $24,000$ effective sound

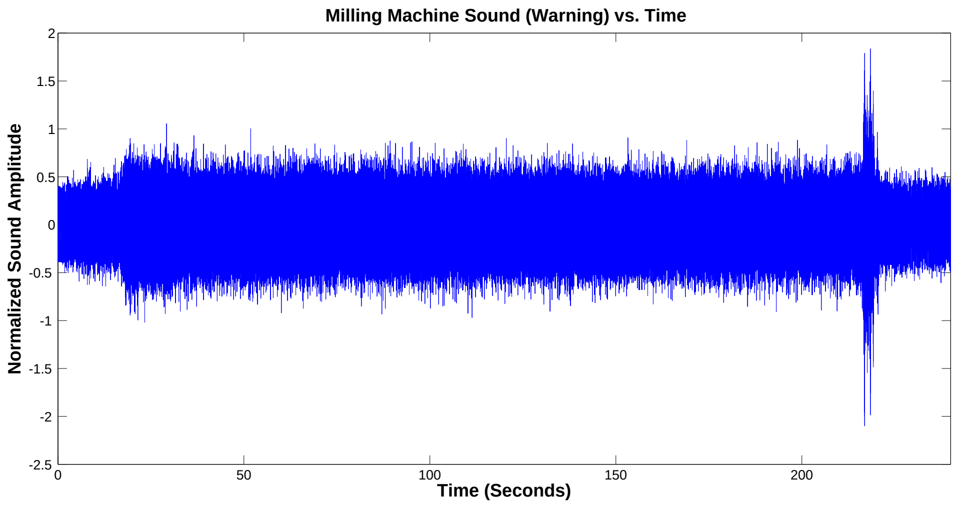

Figure 4.16: Filtered Machine Sound for a Used Cutting Tool in Usable Condition with Signs of Impending Tool Failure (Warning).

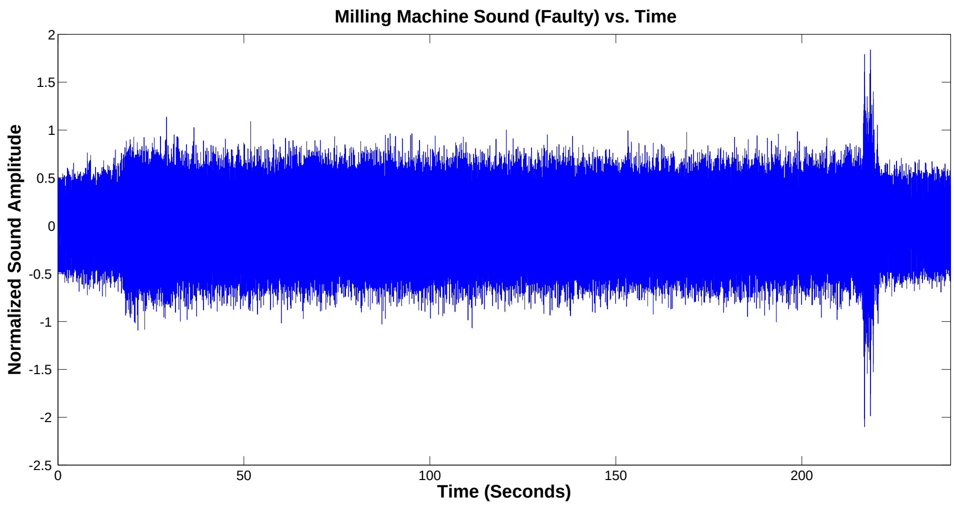

Figure 4.17: Filtered Machine Sound for a Blunt (Failed) Cutting Tool (Faulty).

frames. For a 4 minutes sound signal, it generates a total of $24,000$ MFCC vectors. The MFCC vectors are grouped according to its tool condition and each group is assigned a unique ID (defined in previous section). The MFCC vectors are transmitted wirelessly to the CM-DPA hardware module for machine learning. There are $16,800$ MFCC vectors training data set from each group are used to train the RBF network, and the remaining $7,200$ vectors verify data set are used to verify the trained RBF network.

Table 4.1 depicts MFCC vectors grouping and arrangements used for the RBF training using the training datasets and its training results. The condition to stop training is governed by the overall MSE. A large MSE results in fast convergence, but at the expense of an inaccurate output, while a small MSE causes the RBF training longer time to converge or may not converge at all. Thus, an acceptable minimum MSE of 0.05 is empirically determined with a fully converged RBF training.

Table 4.1: Machine sound MFCC training datasets arrangements and RBF training results

MFCC Vectors	Parameters/Results				
	Sound Type	ID	Target MSE	Trained MSE	Converge
$\mathbf{c}_{NT}$	Normal	0	0.05	0.02	Yes
$\mathbf{c}_{ST}$	Satisfactory	1	0.05	0.02	Yes
$\mathbf{c}_{WT}$	Warning	2	0.05	0.04	Yes
$\mathbf{c}_{FT}$	Faulty	3	0.05	0.01	Yes

The trained RBF network is verified for its CM accuracy by using the machine sound MFCC verify data set. Table 4.2 depicts the verification results of the trained RBF network. Classification errors from the verify data set occur throughout. The least error occurs during the identification of the Normal tool condition. The $\mathbf{c}_{NV}$ (Normal) verify data set results in 98% classification accuracy, with 144 misclassified as Satisfactory tool condition. The $\mathbf{c}_{SV}$ (Satisfactory) data set results in 92% classification accuracy with 576 misclassifications (112 - Normal, 464 - Warning). The $\mathbf{c}_{WV}$ (Warning) data set results in 94% classification accuracy with 432 misclassifications (233 - Satisfactory, 199 - Faulty). The $\mathbf{c}_{FV}$ (Faulty) data set results in 97% classification accuracy with 216 misclassifications (216 - Warning). The misclassifications maybe due to the changing ambient sound levels and the accuracy of the adaptive filter in filtering away those unwanted ambient signals that interfere with the actual machine sound. It should be noted that the classification accuracy of at least 92% is reasonable given the robustness of the RBF network.

Table 4.2: Machine sound MFCC verify datasets arrangements and RBF verification results

MFCC Vectors		Classification		
	Size	Correct	Wrong	% Error
$\mathbf{c}_{NV}$	7200	7056	144	2
$\mathbf{c}_{SV}$	7200	6624	576	8
$\mathbf{c}_{WV}$	7200	6768	432	6
$\mathbf{c}_{FV}$	7200	6984	216	3

4.6 Summary

This chapter has demonstrated the feasibility of using only machine generated sound for CM. CM-DAP and CM-DPA scalable hardware prototypes have been successfully developed and deployed on a precision cutting machine. The adaptive sound signal filtering algorithm has been demonstrated to be able to remove (or minimize) the unwanted ambient noise surrounding a machine in operation. The MFCC based sound feature extraction algorithm has been demonstrated to be able to extract sound features that correctly distinguish the various machine operating conditions. Lastly, the RBF based CM classifier is able to learn from the large amount of MFCC based sound feature data sets for various machine operating conditions, and has the acceptable accuracy to identify the various machine operating conditions. All the algorithms have been successfully tested and deployed to the respective hardware prototypes.

Chapter 5

e-HealthCM: A Non-Intrusive Fall Detection Monitoring for the Elderly

5.1 Introduction

Senior citizen is exposed to an ever increasing risk of fall or related accident or a sudden onset of age induced acute disease such as stroke or heart attack. Any of these incidents may lead to a loss of live if help is not rendered in a timely manner. In Singapore, there are many cases of lone senior citizens losing their lives in their own home due to accidents or disease without anyone knowing [175], and in most cases, valuable lives can be saved if help arrived in a timely manner. However, timely help arrival may not be possible as the affected elderly persons are unable to inform the designated caregivers as they may have already been rendered unconscious or immobile.

Electronics sensors and video monitoring systems implementing remote health condition monitoring (CM) solutions such as vital signs monitors, fall detectors, door monitors, bed alerts, pressure mats, smoke and heat detectors are examples of technologies that can improve senior citizens safety, security and ability to cope at home. For many senior citizens, health CM technology makes the difference between being able to live independently or having to get long-term nursing care. Many of those who use some form of health CM technology are able to reduce their dependencies on others and continue to live independently and safe from accidents or deprivation, resulting in improved health.

5.2 Problem Definition and Proposed Solution

Falls are the major cause of both fatal and non-fatal injury among people and create a hindrance in living independently. The frequency of falls increases with age and frailty level. Between 2007 and 2011, in Singapore, at least 50 elderly persons have been found dead in their own homes from causes related falls and illnesses [175]. With the rapid technological advancements, various small and non-intrusive remote health CM solutions have been proposed and developed with the objectives to solve or mitigate problems encountered by elderly people living alone, and ultimately to save lives by providing them timely assistance. Commercial product development and active academic research on fall detection have been motivated by the considerable risks of falls and the substantial increase of the elderly people population. A typical fall detection system has two major functional components: (a) the detection component, which detects falls and (b) the communication component that communicates with emergency contact after fall detection.

In Singapore, the government takes initiative in making elderly people friendly public housing for the elderly people so as to facilitate aging in place [176]. In 2013, a pilot CM project called Elderly Monitoring System (EMS) was deployed to 500 public housing flats occupied by lone elderly residents. These in-home CM and alert system monitors round the clock activity levels of each resident in a non-intrusive way, and trigger an alert to a designated caregiver in the event of anomalies [176]. With the initial success of the pilot runs, several similar health CM systems [177] [178] were also proposed and underwent trials by different competing solutions providers aimed to solve or mitigate the same set of problems defined earlier.

The various health CM solutions proposed and demonstrated by different solutions providers, in many ways are similar to the CM idea where at home elderly people are for being monitored for motion activities. In most cases, optical camera and passive infrared (PIR) motion detectors are used for such purpose. The primary triggering criteria when a registered caregiver is alerted will be based on the abnormal lacks of motion activities or from a manual trigger by an elderly person requesting for an assistance. Until now, an important monitoring criteria (or feature) is currently not automatically included in all the competing CM solutions. With the best efforts to understand the implementation of the various CM solutions, an automatic and reliable method of detecting an elderly person falling down is currently missing or not actively promoted. This feature lapse is intentional, as the various methods for reliable fall detections are currently still in active research, and the available fall detection algorithms and methods are not able to provide 100% human fall detection accuracy. A robust fall detection system is one that is able to classify the valid and invalid falls under real life conditions. If a fall event occurs and the system does not detect it, the consequences can be dramatic. However, if the system reports an excessive number of false fall alerts, caregivers may perceive it as ineffective and useless, which may lead to device rejection. There are commercially available systems that offer human fall detections, but these systems come with disclaimers stating that accuracy in detecting a valid human fall is not guaranteed. Several reviews [179–183] of the commercially available fall detection system shown that the commercially available systems are already available and deployed, but not in a widespread use. The products are mainly offered as paid services for monitoring the safety of elderly people staying by themselves, and for eldercare centers. For the wearable products, they use either accelerometers or tilt sensors to detect a valid human fall.

To date, one of the most common implementation for detecting a fall requires an elderly person to wear a portable electronics wearable device with a built-in inertial sensor in the form of a tri-axial accelerometer, a wireless communication interface, and a battery. The accelerometer continuously detects motion accelerations in the three-dimensional vector space, and by analyzing the motion acceleration behavior, human fall occurrence can be ascertained or predicted. One of the well-known and practical accelerometer based fall detection algorithm is developed by Ning Jia [101] using an Analog Devices ADXL345 digital MEMs tri-axial accelerometer [139]. The well-known algorithm detects a sequence of known motion based activities (e.g., free-fall, weightlessness, strike, motionless and long time motionless) that can be pieced together in order to approximate a valid fall. In another well-known implementation, Bourke *et al* [184] [185] on the other hand, developed a fall detection algorithm using a tri-axial accelerometer to detect fall impact and human posture. The algorithm, considered the sum of vectors of the accelerometer outputs and the detected posture to decide if a valid fall has occurred. Both algorithms are highly accurate in detecting a real human fall process. However, both algorithms are also sensitive to human motion attributed to daily movements (sitting, standing, etc.) and each human motion is person dependent. In both approaches, a change in body orientation from upright to lying that occurs immediately after a large negative acceleration indicates a fall. However, generally despite all the research dedicated to fall detection, there still isn't a 100% reliable algorithm that catches all falls with no false alarms. Hence, both algorithms also provide unwanted and false valid human fall results (false positive). In field implementations, both algorithms suffer substantial setbacks in terms of the relatively large amount of false positive fall detections.

For each elderly person, individual movement and physical reaction to the occurrence of a fall is not the same [117–119], thus it is difficult for the algorithms to cater to all forms of fall patterns, hence the incurred setbacks of false fall detections. In order to have an accurate detection, both algorithms require the elderly person to physically moves or reacts to a fall in a certain way expected by the device manufacturers, which is neither logical not practical. Thus, using only accelerometer to detect a valid fall is insufficient where good accuracy with minimum false positive is desired.

e-HealthCM is a proposed health CM solution that automatically detects and predicts an elderly person accidental fall occurrence. The basic functionality of e-HealthCM is similar to the various health CM solutions for fall detection, where it monitors a senior citizen's home for accidental fall activity, and to automatically request for assistance when a valid fall is detected. Based on the discussed shortfalls and known restrictions of an accelerometer only fall detector, the e-HealthCM improves on the overall fall detection accuracy by providing a second level of sound based fall sensing as an enhancement to the accelerometer only fall detector.

5.3 Hardware Development

e-HealthCM consists of: (a) an e-HealthCM Base Station (e-BS) where detected fall alerts and caregivers notification are being handled, (b) wireless e-HealthCM Sound Sensor Modules (e-SS) for CM of potential fall based on detected sound, and (c) wireless e-HealthCM Wearable Module (e-WM) that monitors accelerometer based motion activity. In addition, e-WM is also a low cost digital hearing-aid for aiding senior citizen with hearing difficulty to communicate effectively.

Having established the fact that using only e-WM motion activity monitoring feature to detect a valid fall is insufficient and prone to false fall detection due to the unpredictable nature of human movements [117–119], e-SS modules installed at various spots within a senior citizen's home are used to verify if a valid fall has occurred by measuring the localized sound pressure level for potential occurrence of a fall. Figures 5.1, 5.2 and 5.3 depict the respective hardware block diagrams for e-BS, e-SS and e-WM. The hardware are designed based on the framework defined in Chapter 2. Thus, there will be some level of similarity when compared to the hardware in Chapter 4.

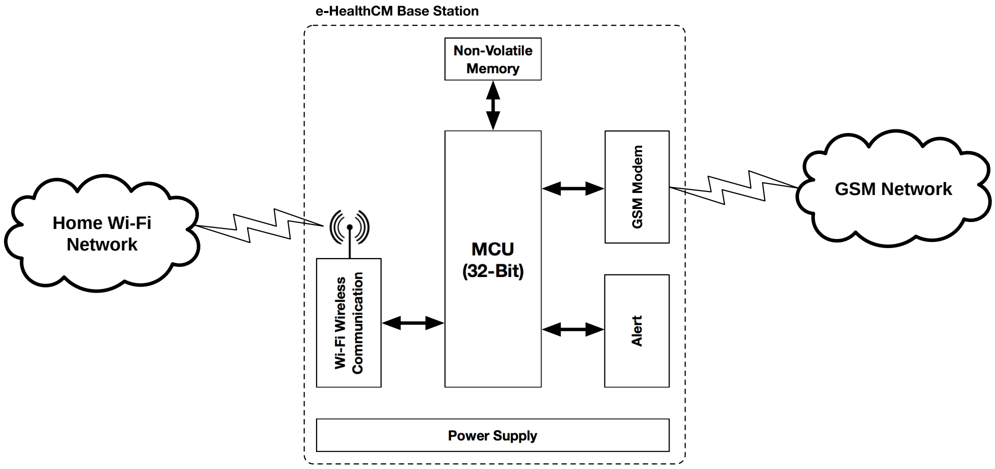

Figure 5.1: e-HealthCM Base Station Hardware Block Diagram.

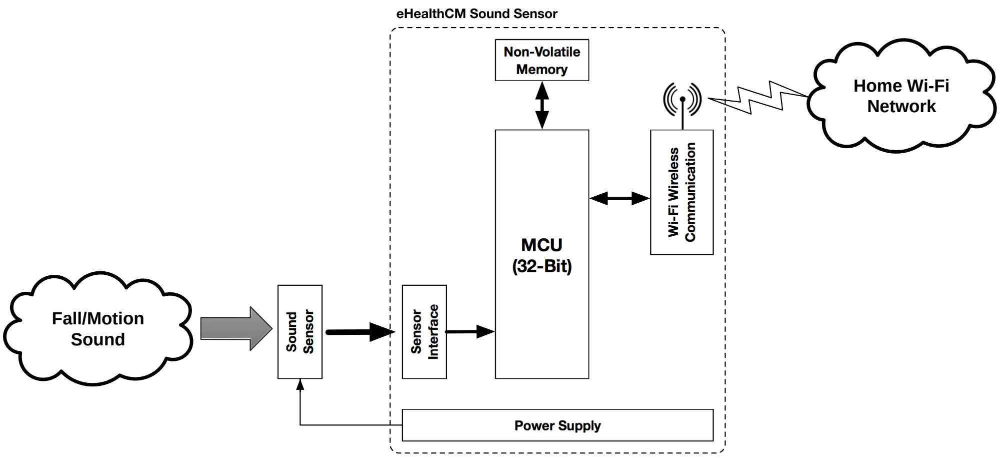

Figure 5.2: e-HealthCM Sound Sensor Hardware Block Diagram.

The e-BS module depicted in Figure 5.1 contains the various sub-blocks: (a) Wi-Fi Wireless Communication interface, (b) Microcontroller Unit (MCU), (c) Non-Volatile Memory, (d) GSM Modem, (e) Alert and (f) Power Supply. The Wi-Fi Wireless Communication interface receives Valid Fall Alert (VFA) message (or information) from the e-SS modules. The MCU processes the information,

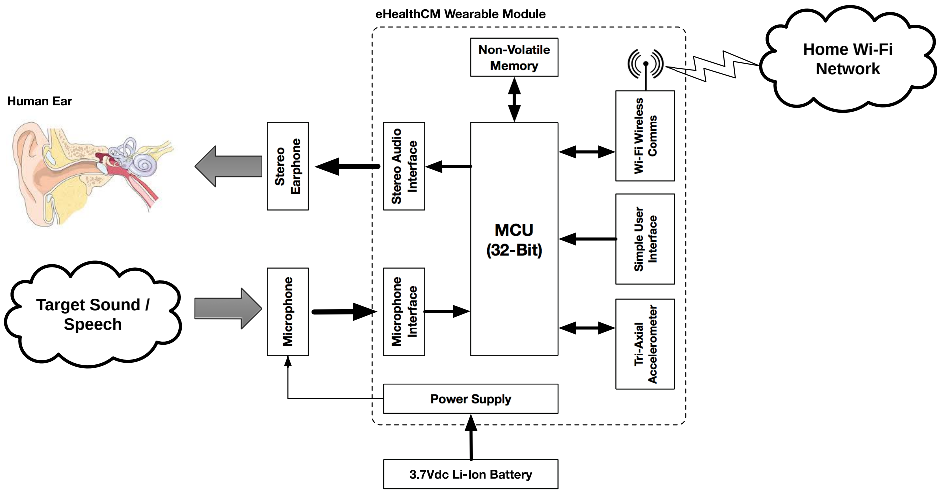

Figure 5.3: e-HealthCM Wearable Module Hardware Block Diagram.

activates the Alert function (local audible sound alert) to notify anyone in the vicinity that a fall has occurred, and notify the designated caregivers of the fall occurrence via the attached GSM Modem (using SMS message). The Non-Volatile Memory stores the caregivers contact information.

In Figure 5.2, the e-SS consists of a microphone based Sound Sensor Interface, Non-Volatile Memory, MCU, Wi-Fi Wireless Communication interface and Power Supply sub-blocks. The Sound Sensor Interface provides the necessary biasing and signal conditioning to a connected uni-directional microphone (sound sensor). The microphone has a sensitivity of -46 dB/Pa, and a detection angle of 60°. The MCU continuously samples and processes the sound signal picked up from the microphone in order to determine the current sound pressure level (SPL) [186] while waiting for an Inertial Fall Alert (IFA) Wi-Fi broadcast message from the nearby e-WM. If a valid IFA message is received, the SPL and IFA message (or information) are processed by a fuzzy logic based fall detection algorithm in order to determine if a valid fall has occurred. In the event of a valid fall, e-SS sends VFA message to the e-BS via Wi-Fi. Coefficients required for the sound pressure measurement and fuzzy logic are stored in the Non-Volatile Memory. Power Supply provides regulated and DC supply for the e-SS. Each e-SS is positioned perpendicularly on the wall surface of the senior citizen's apartment with an overlapped detection range (refer to Figure 2.4 in Chapter 2).

In Figure 5.3, the e-WM depicts a hardware block diagram of an accelerometer based fall detector with an additional functionality of a pseudo-binaural hearing aid. e-WM consists of a Stereo Audio (Driver) Interface, Microphone Interface, Non-Volatile Memory, MCU, Wi-Fi Wireless Communication, Simple User Interface, Tri-Axial Accelerometer, and Power Supply with Li-Ion Battery sub-blocks. The Stereo Audio (Driver) Interface where an external stereo earphone can be attached and a Microphone Interface with an attached onmidirectional microphone are the extra functionalities added to provide e-WM with a hearing aid capability. The hearing aid feature is enabled only if an elderly person benefits from it. Like many other accelerometer based fall detectors, e-WM relies on the built-in digital tri-axial accelerometer to sample the elderly person's motion information, and the MCU processes the information using an accelerometer based fall detection algorithm (with coefficients stored in the Non-Volatile Memory) to determine if a possible fall has occurred. If a fall is detected, e-WM broadcasts an IFA message via Wi-Fi to all the nearby e-SS modules. e-WM contains a Simple User Interface where an elderly person can manually request for assistance or to configure its various device features, and it is powered via a small 3.7 VDC Li-Ion rechargeable battery. e-WM is either worn on the waist (clipped to the belt) or attached to a lanyard and hanged around the neck. e-

WM is designed to be small and light so as to minimally invade into the daily activities of an elderly person.

The respective hardware prototypes of e-BS, e-SS and e-WM are depicted in Figure 5.4 (a), (b) and (c).

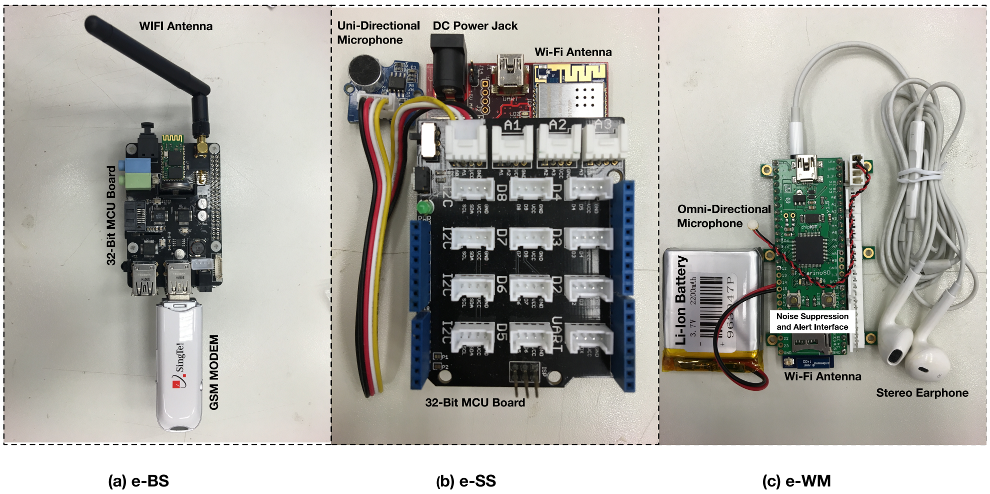

Figure 5.4: e-HealthCM Hardware Prototypes depicting (a) e-BS, (b) e-SS, and (c) e-WM.

5.4 Algorithms for Human Fall Detection

e-HealthCM is designed to automatically detect an elderly person's accidental fall occurrence. e-HealthCM implements both accelerometer based and sound based detections for possible occurrence of human fall. e-WM implements the accelerometer based fall detection algorithm, e-SS implements the fuzzy logic based fall detection algorithm that takes in IFA message and SPL information, and e-BS implements the local alert and caregivers alerts.

5.4.1 Accelerometer based Fall Detection

The inertial fall detection sensor embedded in the e-WM is the ADXL345 digital tri-axial MEMs accelerometer [139]; a small, low power accelerometer with a 13-bit high resolution measurement of ±2g, ±4g, ±8g, ±16g acceleration. The built-in free fall detection feature makes it a very suitable detector for e-HealthCM. The digital output data is formatted as a 16-bit length, and is accessible through an I2C digital interface. As part of the power saving feature, the accelerometer can signal the MCU when to wake up and when to go back to sleep again by configuring a predefined interruption threshold through the MCU firmware.

The measured accelerations in directions of x, y and z axis of the accelerometer are represented by vectors A_x, A_y and A_z, respectively. Let A_c denotes the composition of accelerations in the three directions, whose amplitude can be traditionally computed by Equation 5.1.

$$|A_c| = \sqrt{|A_x|^2 + |A_y|^2 + |A_z|^2} \tag{5.1}$$

During the algorithm development process, daily human motion activities and fall detections procedure demonstrated by Ning Jia [101] is used. This procedure has been widely known to be highly reliable in detecting a valid fall, but also known to falsely detect falls from various normal (non-fall) motion activities. A volunteer emulating an elderly tested the ADXL345 on the e-WM by hanging it around the neck and performed the following daily motion activities: (a) Walking up a flight of stairs, (b) Walking down a flight of stairs, (c) Sitting down, and (d) Standing up.

Figure 5.5 - 5.8 depict the acceleration data plots of the motion activities.

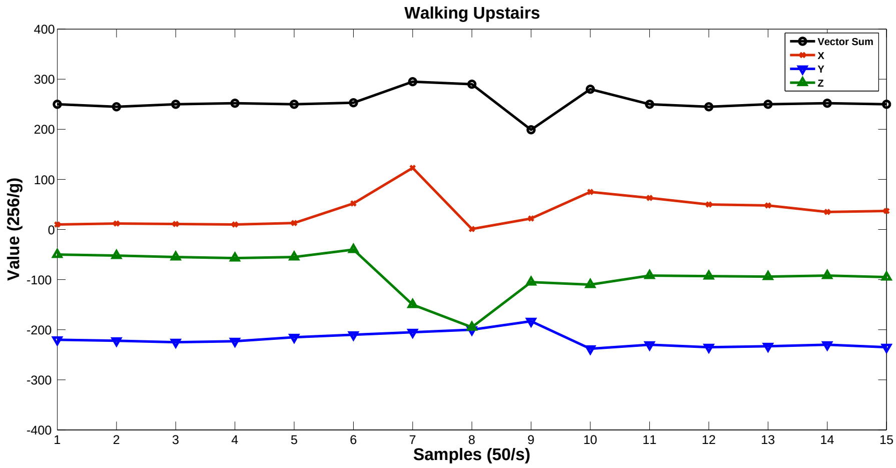

Figure 5.5: Volunteer walking up a flight of stairs.

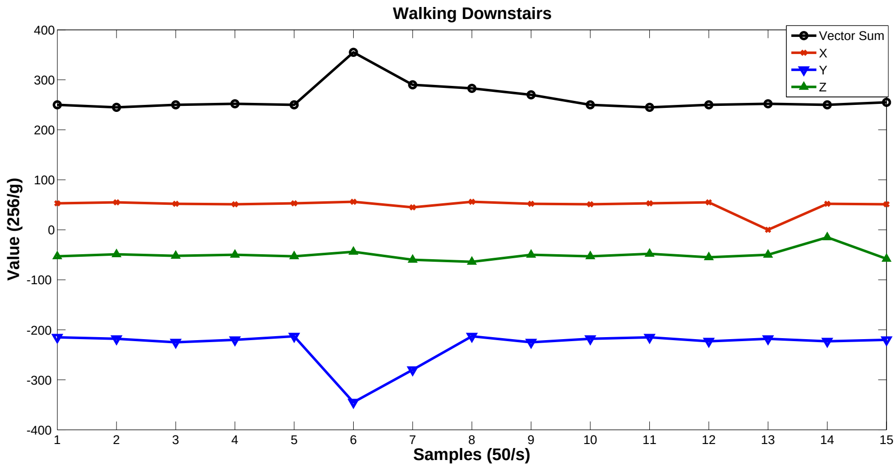

Figure 5.6: Volunteer walking down a flight of stairs.

Movement of an elderly person is comparatively slow [101], the acceleration change will not be very conspicuous during the walking motions. The most obvious acceleration change is a spike in Y (and the vector sum) at the instant of sitting down (Figure 5.7). The volunteer conducted emulated falls on a well cushioned floor (overlaid with a 1.5" thick foam rubber mat). The emulated falls mimic possible falls encountered by an elderly person based on some studies conducted [187] [188]. The accelerations during falling are completely different.

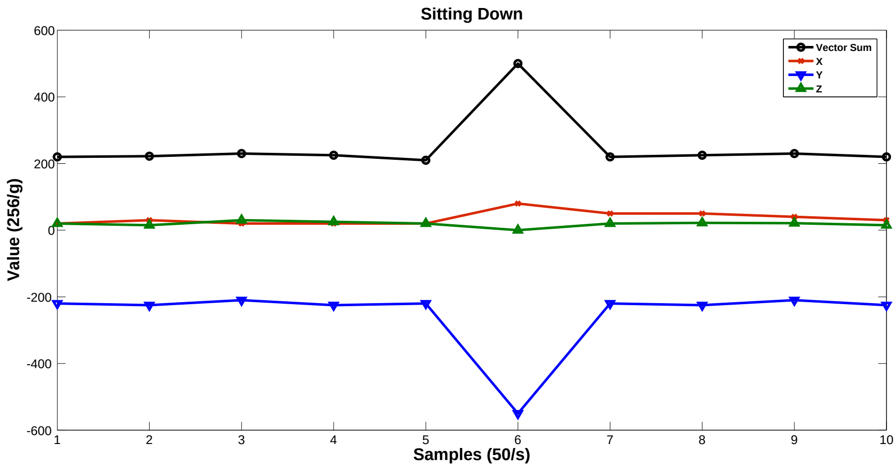

Figure 5.7: Volunteer sitting down.

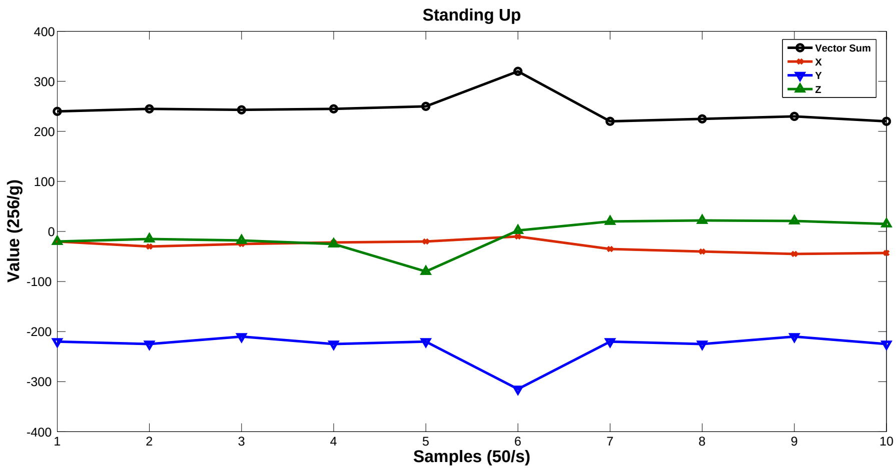

Figure 5.8: Volunteer standing up.

Figure 5.9 shows the acceleration changes during an emulated accidental fall.

By comparing Figure 5.9 with Figure 5.5 - 5.8, four critical characteristics of an emulated human falling event are observed that can be used as the major criteria for fall detection [101]. The characteristics are marked in the red boxes (Figure 5.9) and explained in detail:

1. **Weightlessness**: The weightlessness phenomenon always occurs at the start of an elderly person (volunteer) fall event. It will become more significant during free fall, and the resultant vector sum of acceleration value

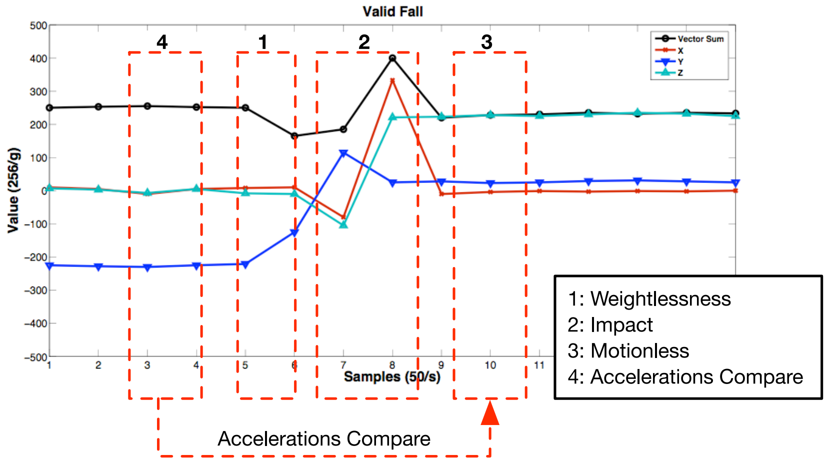

Figure 5.9: Volunteer emulates a fall.

will be towards 0g. The duration of the condition depends on the height of free fall. Even though weightlessness during an ordinary fall is not as significant as that during a free fall, the vector sum of acceleration is still substantially less than 1g (under the normal condition, it is generally greater than 1g). Thus, the first basis of fall detection is to examine the fall status that is easily done by the ADXL345 FREE_FALL interrupt.

2. **Impact**: After experiencing weightlessness, the elderly person's body will impact the ground or other objects. This represents on the acceleration curve as a large transient shock. This transient shock is detected by the ACTIVITY interrupt of ADXL345. Thus, the second basis of fall detection is to determine the ACTIVITY interrupt right after the FREE_FALL interrupt.

3. **Motionless**: The elderly person, after a fall and an impact, will remain in a motionless position for a short period (or longer period as a possible sign of unconsciousness). On the acceleration curve, this shows as an interval of

flat line, and is detected by the ADXL345 INACTIVITY interrupt. Thus, the third basis of fall detection is to determine the INACTIVITY interrupt after the ACTIVITY interrupt.

4. **Accelerations Compare (before Weightlessness and during Motionless)**: After a fall, the elderly person's body will be in a completely different orientation than before a fall, hence the static acceleration in the three axes will be different from before the fall (before Weigthlessness). In Figure 5.9, it is clear that the elderly person (volunteer) falls on the side, since the static acceleration has changed from -1g on the Y-axis to $+1$g on the Z-axis. Thus, the fourth basis to determining a valid fall is to compare the difference between an initial acceleration value (at time before Weigthlessness) and a final acceleration value (at time during Motionless). When the difference in acceleration exceeds a certain threshold, a valid fall can be ascertain.

The combination of the four characteristics realized an inertial based fall-detection algorithm that is able to generate an IFA event when a fall has occurred. The various timing parameters and the related acceleration thresholds have to be properly fine tune in order to realize an effective algorithm with minimal false fall detections. The proposed fall detection algorithm takes full advantage of the internal function registers of the ADXL345, thus minimizing the complexity of the algorithm due to minimum access the actual acceleration value (calculated using Equation 5.1). Figure 5.10 depicts the flowchart of the accelerometer based fall detection algorithm.

From the algorithm flowchart in Figure 5.10, the algorithm functions as fol-

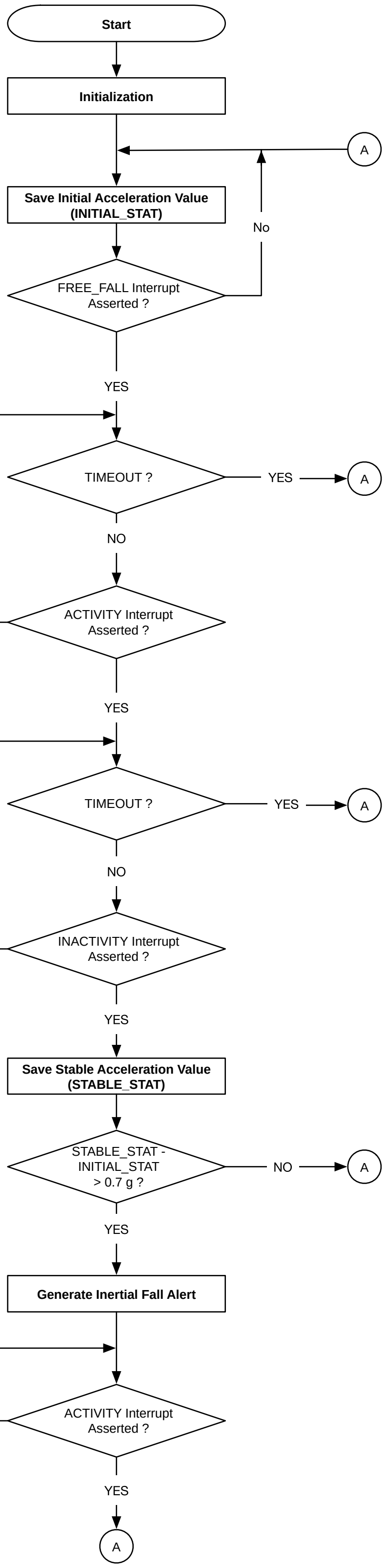

Figure 5.10: ADXL345 based Fall Detection Algorithm.

lows:

1. After an Initialization procedure, the algorithm waits for the FREE_FALL interrupt to occur (Weightlessness). Free Fall Acceleration threshold (THRESH_FF) is set empirically to 0.8g and Free Fall Acceleration Timeout (TIME_FF) is set empirically to 30ms.

2. After FREE_FALL interrupt is asserted, the algorithm waits for the ACTIVITY interrupt (Impact). Activity Acceleration threshold (THRESH_ACT) is set empirically to 2g.

3. The time interval threshold between FREE_FALL interrupt (Weightlessness) and ACTIVITY interrupt (Impact) is set empirically to 200ms. If the actual time interval between the two interrupts is greater than 200ms, the algorithm restarts as the encountered condition is not valid.

4. After the ACTIVITY interrupt is asserted, the algorithm waits for the INACTIVITY interrupt (Motionless After Impact). Inactivity Acceleration threshold (THRESH_INACT) is set empirically to 0.2g and Inactivity Acceleration Timeout (TIME_INACT) is set to 3.5 seconds.

5. The INACTIVITY interrupt (Motionless After Impact) must be asserted within 3.5 seconds after the ACTIVITY interrupt (Impact). Otherwise, it is not a valid condition and the algorithm restarts.

6. The stable acceleration value after INACTIVITY interrupt (STABLE_STAT) is compared against the initial acceleration value (INITIAL_STAT, recorded after Initialization), and if the difference exceeds the 0.7g threshold, a Valid Fall is detected, and the algorithm generates an IFA event.

7. After detecting a fall, the ACTIVITY interrupt is continuously monitored to determine if the elderly moves after a fall. The THRESH_ACT is set empirically to 0.5g, Once the elderly moves, the ACTIVITY interrupt is generated to complete the entire fall detection sequence, and the algorithm restarts.

5.4.2 Fuzzy Logic based Fall Detection

In the earlier sections, an accelerometer based fall detection algorithm is proposed and developed and the known limitations pertaining to the accelerometer based fall detector are also highlighted. In this section, a new algorithm to further improve on the fall detection accuracy is proposed with the use of fuzzy logic. This new algorithm does not replaces the accelerometer based fall detection algorithm discussed earlier, it provides an overall fall detection accuracy enhancement by introducing a sound based fall detection methodology. Each e-SS module continuously measures SPL in its vicinity, and receives IFA information broadcast via Wi-Fi if an inertial based fall has been detected. The idea is to fuse the IFA message from the e-WM with the SPL (sound) based fall information from the e-SS using fuzzy logic. This fuzzy logic based algorithm resides within all the e-SS modules and if a valid fall has been detected by one or more e-SS modules, each respective module notifies the e-BS of a valid fall occurrence.

In a quiet residential environment, the typical indoor SPL is measured to be in the range of 30dB - 50dB SPL. 30dB is a typical bedroom SPL, 40dB typically represents a person whispering, and 50dB represents a typical person talking SPL. A group of people doing an intense discussion can have a moderate

SPL of 60dB. 70dB SPL represents a noisy office, restaurant or street noise, and 80dB SPL is very loud, representing the sound of a heavy street noise and an average factory floor [189].

Sound signal sampled by the uni-directional microphone is directly processed by the MCU within the e-SS to determine its SPL value and its duration of occurrence. The SPL (in dB) is calculated by using Equation 5.2 [190] [191]. Microphone sensitivity is defined as -46 dB/Pa and $V_{ref} = 10^{-\frac{46}{20}}$. V_{MIC} is the RMS sound signal voltage level.

$$SPL(dB) = MIC\ Sensitivity\ (dB) + 20 \cdot log_{10}(\frac{V_{MIC}}{V_{ref}}) + 94 \tag{5.2}$$

Sound generated from a fall usually emits from an elderly body impacting the floor or a hard object. An experiment was conducted where a volunteer emulates several occurrences of falls (front fall, back fall, side fall, and fall from a chair) on a hard floor overlayed with soft rubber foam. The recorded SPL for each fall is within the range of 50dB to 70dB with a sound duration of $\leq$ 500ms. A short burst sound with SPL of $>$ 70dB and duration of $\leq$ 500ms can also be associated with an occurrence of a fall, where the large SPL can be associated with the elderly person's body shattering a glass object during impact. Based on this conducted experiment, sound can be used as an indicator to detect or estimate an elderly person's fall occurrence.

Having established a possible scenario where sound can be used to identify a valid fall, the next step is to use fuzzy logic to fuse the IFA message and sound information. The proposed fuzzy logic based fall detection algorithm has three inputs and a single output. The defined fuzzy logic function inputs are:

1. IFAINFO: IFA message received when an inertial fall is detected by an e-WM resulting in IFA message being broadcasted (by e-WM) and received by an e-SS. e-SS sets IFAINFO = HIGH when it receives an IFA message from e-WM, otherwise e-SS clears IFAINFO = LOW.

2. DURATION: signal represents the length of a sound event sampled by the e-SS, where DURATION = LOW if the length of the sound event is $\leq$ 500ms, and DURATION = HIGH if the length is $>$ 500ms

3. SPLVALUE: signal represents the SPL of the sampled sound event, where SPLVALUE = LOW if SPLVALUE $\leq$ 30dB, SPLVALUE = MID if 30dB $<$ SPL $\leq$ 50dB, and SPLVALUE = HIGH if SPL $>$ 50dB.

The fuzzy logic function has only a single output FOUTPUT where it produces FALL for a valid fall occurrence, and NOFALL for otherwise. Thus, the Mamdani fuzzy rule system [192] for detecting a valid fall has five rules:

1. IF **IFAINFO** is LOW then **FOUTPUT** is NOFALL
2. IF **IFAINFO** is HIGH and **DURATION** is LONG then **FOUTPUT** is NOFALL
3. IF **IFAINFO** is HIGH and **DURATION** is SHORT and **SPLVALUE** is LOW then **FOUTPUT** is NOFALL
4. IF **IFAINFO** is HIGH and **DURATION** is SHORT and **SPLVALUE** is MID then **FOUTPUT** is FALL
5. IF **IFAINFO** is HIGH and **DURATION** is SHORT and **SPLVALUE** is HIGH then **FOUTPUT** is FALL

The constructed membership functions for IFAINFO, DURATION and SPLVALUE inputs are respectively depicted in Figure 5.11 to 5.13, and the membership function for FOUTPUT is depicted in Figure 5.14.

By using the constructed membership functions that define the fuzzy logic rules, the IFA message and sound information can be fused for an effective

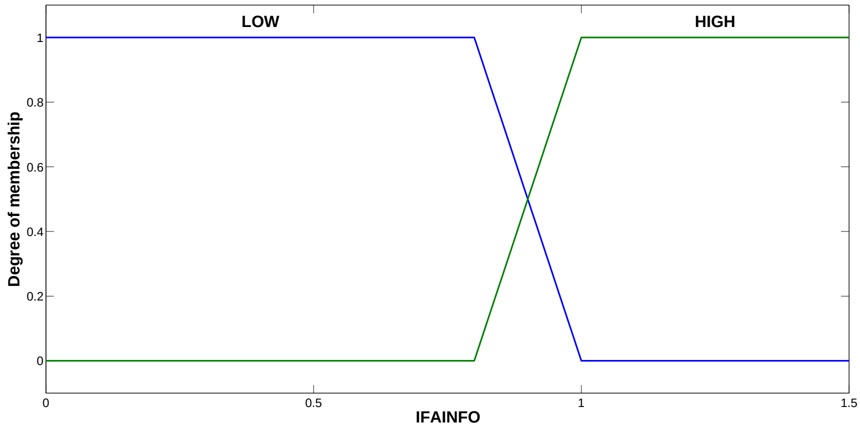

Figure 5.11: Membership Function for IFAINFO input.

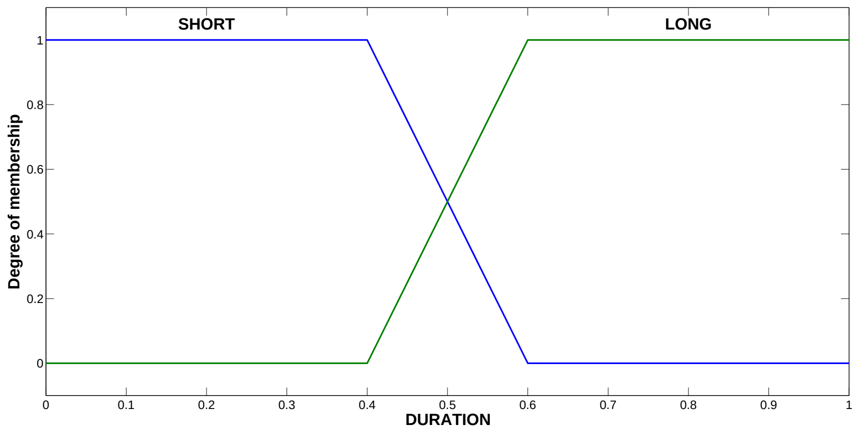

Figure 5.12: Membership Function for DURATION input.

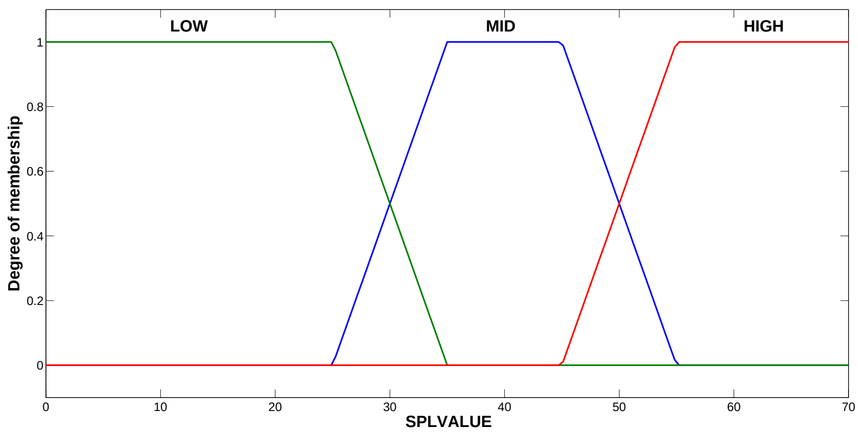

Figure 5.13: Membership Function for SPLVALUE input.

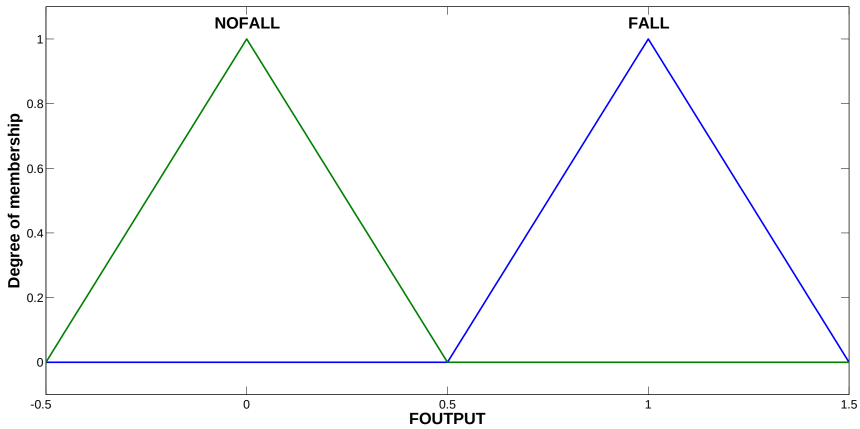

Figure 5.14: Membership Function for FOUTPUT.

detection of an elderly person's fall occurrence. The accuracy of the fall detection algorithm will be verified in Section 5.6 in the later part of the chapter.

5.5 Pseudo-Binaural Hearing Aid Feature

This section highlights the need to include an addition hearing aid feature into the e-WM. Hearing loss is one of the common chronic health conditions among senior citizens. Age-related and noise induced hearing loss are the leading causes of hearing loss. An elderly person who is over 60 years old have a 40% likelihood of hearing loss. Unattended hearing loss results in reduced quality of life, social integration, communications with friends and families. Un-rehabilitated hearing loss has been associated with reduced cognition and memory, and increased falls and accidents [193–195]. Hearing loss can be unilateral or bilateral. A candidate diagnosed with unilateral hearing loss will normally be prescribed a monaural hearing aid for the affected ear. A hearing loss candidate will be recommended for binaural hearing aid if bilateral hearing loss is being diagnosed. The binaural hearing aid has the main advantage of being able to independently customize hearing levels for each ear.

Hearing aids are currently handled as highly specialized devices [196]. A prospective user has to go through hearing loss calibration at a specialized clinic, and get a hearing aid customized to their hearing level, including a mould made to conform to the outer ear to reduce feedback and interference. These aids run on special and small low voltage batteries which have to be replenished on a regular basis at limited number of places. Clearly, apart from the trouble making one and maintaining it, the cost associated with a pair of hearing aids is very high, from the perspective of an elderly person with no or limited income.

Hearing aids are small and require effort to store them when not in use and to remember where they are kept. They contain digital components which are sensitive to moisture and require regular caretaking. Retuning the aids for regular maintenance require another specialized process with associated costs. To some, these may be trivial problems; to the elderly people, these are quite a chore. Elderly people with poor vision and poor mobility of fingers have difficulties handling the current small, cosmetic, sophisticated hearing aids. They have difficulty with the small controls sited on the hearing aids. These hearing aids are also easily lost. There is a need for simple and effective hearing aids that are easy to use and comfortable.

Current hearing aids are fitted as single pieces into the ears, including the microphone which is likely to be a directional one. The sound source to discern is typically where the user is facing. This highly constrains the use of more efficient noise cancelation schemes. A non-negligible proportion of elderly people or patients who have purchased hearing aids are not accustomed to hearing sound components in the new proportions prescribed by the hearing aids. Some persists; others may leave many pairs that do not work well with them in the drawers. The negative or unpleasant users feedbacks result in many others not giving hearing aids a fair trial. It is not unusual for vendors to push the small sophisticated hearing aids for better sales, even if they are not always suitable for the elderly people.

Thus, pushing the state of the art assistive hearing technology to those needing one has not resulted in a large segment of these people now fitted with a hearing aid. In fact, the same features that hearing aids companies may pride themselves on are turning out to be deterrence to a senior citizen sector of the group and the less financially bestowed sector. In this section, the objective to include a hearing aid capability into e-WM is based on the real needs of this bigger group of users of hearing aids and to be driven and pulled by a frugal objectivity.

5.5.1 Hearing Aid Design

The basic function of a hearing aid is as follow: sound waves enter through the microphone, which converts acoustic signals into electrical signals. The amplifier increases the strength of the electrical signal. The amplified signal is then transformed back to an acoustic signal by the receiver. From the receiver, the signal is channeled into ear canal either through a small tube or through an ear mold. A battery is required to power the hearing aid and enable the amplification process.

Binaural hearing can provides better sense of balance and sound quality. With binaural hearing, a person benefits from wider range of hearing and tone quality is smoother and more natural. Wearing binaural hearing aid keeps both ears active and avoids auditory deprivation effect. Research has shown that the unaided ear tends to lose its ability to hear and understand when only one hearing aid (monaural) is worn.

A digital pseudo binaural hearing aid is designed to add binaural features in which the frequency components equalizer setting with individual frequencies bands adjustments are independent for both ears. Binaural hearing aid has the advantages of increased speech clarity, enhanced overall sound quality, improved comfort level while listening, and improved ability to locate sources and directions of sound.

The proposed digital pseudo binaural hearing aid with signal conditioning, filtering and amplification is implemented by using standard of-the-shelf electronics components. It does not have expensive features and refined electro-acoustic, so as to keep the circuit simple for ease of manufacturing in bulk quantity. The hearing aid requires low maintenances as it minimizes the requirement of being serviced by the manufacturer or trained professionals. A simple acoustic calibration and programming can be done on-site to keep the hearing aid functioning for long term usage. Figure 5.15 depicts the functional block diagram of the implementation of a digital pseudo binaural hearing aid.

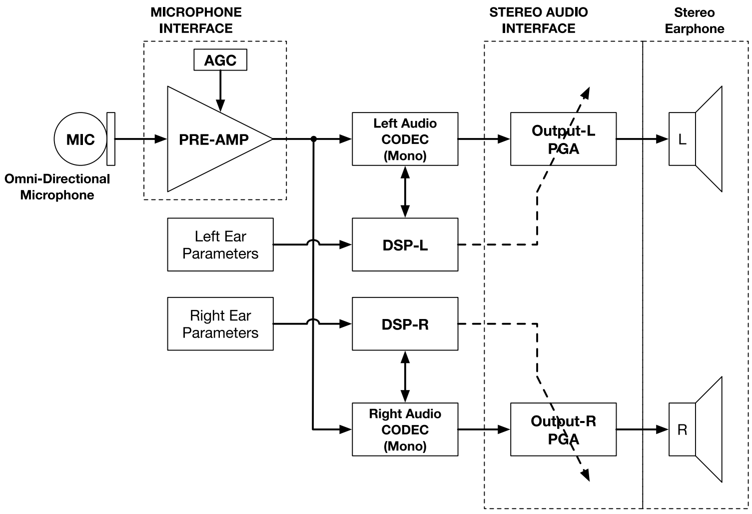

Figure 5.15: e-WM Pseudo-Binaural Hearing Aid Functional Block Diagram

5.5.1.1 Microphone Interface (Pre-Amplifier with AGC)

The Microphone Interface (Pre-Amplifier with Automatic Gain Control (AGC)) functional sub-block is included to provide proper interface to the external omni-directional microphone, and to prevent clipping at the pre-amplified output when a too high gain is applied at the microphone input. The automatic gain control (AGC) function of the pre-amplifier adjusts the gain by detecting if the output voltage level has exceeded the preset threshold value. It consists of several distinct functional sub-blocks: a low noise preamplifier, a Variable Gain Amplifier (VGA), an output amplifier, a microphone-bias-voltage generator, and AGC control circuitry as depicted in Figure 5.16. This Pre-amplifier sub-block amplifies the input over three distinct stages. In the first stage, the input is buffered and amplified through the low-noise preamplifier with a fixed gain of 12dB. The second stage consists of the VGA controlled by the AGC. The VGA/AGC combination is capable of varying the gain from 0dB to 20dB. The output amplifier is the final stage in which a fixed gain of 28dB. With no compression from the AGC, the Pre-Amplifier is capable of providing up to 60dB gain.

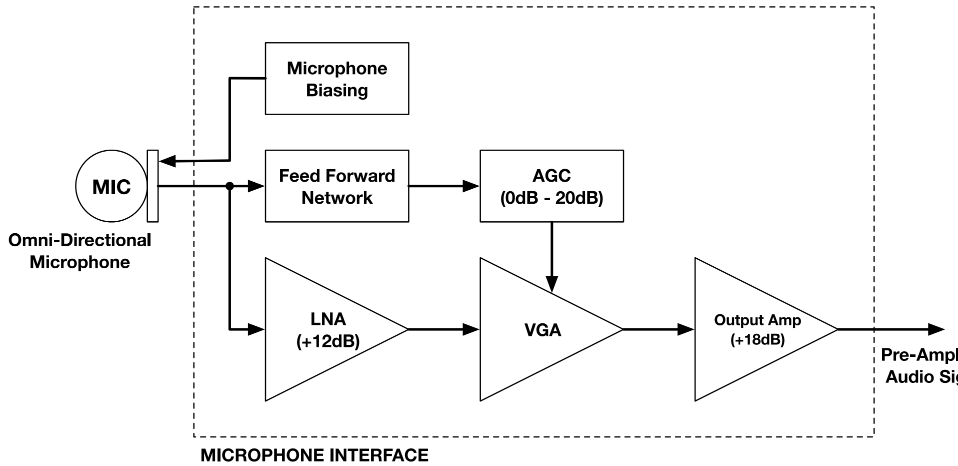

Figure 5.16: Pre-Amplifier with AGC (Microphone Inteface) Functional Sub-Block Diagram.

5.5.1.2 Digital Audio Signal Processing

The 32 bit MCU hosts the digital signal processing (DSP) algorithm for each individual left ear and right ear. This approach presents a proper adjusted audio signal output for each individual ear. The two DSP algorithms implemented are: (a) Noise Suppression, and (b) Individual Frequency Bands Adjustment (Equalizer Function).

The Noise Suppression (NS) algorithm is required in the hearing aid design, in which the incoming audio (speech) signal is susceptible to ambient noise. The NS function removes noise from a 10ms block of 16-bit speech data sampled at 8kHz. The algorithm operates in the frequency domain in which Fast Fourier Transform (FFT) is performed on each 10ms block of digitized speech data to analyze its frequency components. A Voice Activity Detection (VAD) algorithm is included to determine if the individual 10ms audio block is speech or noise. The NS algorithm maintains a profile of the detected noise within each block, and updates it every time a noise segment is detected by the VAD. Every frequency band of the block is then scaled according to proportion of noise contained in the frequency band, thereby causing a significant degree of noise suppression of the block. The algorithm adapts to changes in the nature and level of noise and does not require a separate noise reference input [197].

Each ear frequency response differs with each individual with hearing loss. As such the Individual Frequency Band Adjustment (Equalizer Function) of the hearing aid is crucial to cater to individuals with different hearing losses levels where individual speech frequency components can be pre-emphasized or de-emphasized based on the different characteristics of hearing loss. Signal processing functions and related operations within the hearing aid may suppress or boost certain frequencies of a signal. This manifests as a change in the tonal properties of the output signal as compared to the input. Additionally, input and output devices (microphone and speaker) may emphasize or de-emphasize certain frequencies in an audio (speech) signal due to their mechanical characteristics and limitations.

A digital audio (speech) equalizer that allows the spectral characteristics of a digital speech signal to be changed is incorporated into the hearing aid. Figure 5.17 shows the conceptual block diagram of the digital equalizer implementation. The equalizer splits the input signal into different frequency bands (component signals) using a set of digital band-pass filters. The center frequency for these filters is fixed at 250Hz, 500Hz, 1000Hz, 2000Hz, and 4000Hz respectively [198]. The gain of each of this frequency component is user adjustable from −18dB to +12dB determined based on the frequency bands attenuator values and by the master gain. The component signals are then summed up and provided as the equalized output audio (speech) signal.

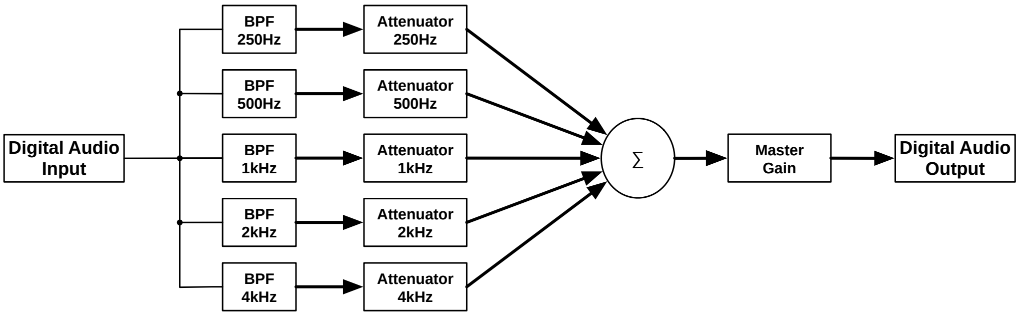

Figure 5.17: Equalizer Functional Sub-Block Diagram.

5.5.1.3 Stereo Audio Interface (Output Amplifier)

The Stereo Audio Interface (Output Amplifier) serves as a driver for the earphone speakers (or miniature headphone speaker) where it is able to provide the driving current. Due to the low current driving requirement of the earphone speakers, a programmable gain earphone amplifier with a standard high output slew rate with rail-to-rail voltage swing output, which is available in the audio CODEC is being used for this purpose. The amplifier is designed for driving of earphone speakers with minimal output noise, and has the advantage of implementing volume control features on the hearing aid without additional components.

An alternative implementation using a standard high output slew-rate operational amplifier (OP-AMP) with rail-to-rail voltage swing output can also be used for this purpose. In this approach, the volume control is implemented via software manipulating the digital speech output data. An OP-AMP with high internal noise is thus not recommended as such OP-AMP will further introduce the unwanted noise to the complete system which will electronically introduce unwanted frequencies components to the otherwise clean regenerated audio signals. This will result in the degradation of the intended audio signals and the user will experience hearing fatigue when using this product. Based on sampling of few OP-AMPs from different manufacturers, an OP-AMP with an internal noise of at most (or maximum of) 3.9 nV/vHz was chosen. The chosen OP-AMP will introduce the acceptable level of output noise to the system while still maintaining the audio fidelity.

5.5.2 Hearing Aid Calibration

The completed digital pseudo binaural hearing aid functional feature for e-WM has to be calibrated to match its configurable gains to the desired output sound pressure level. Figure 5.18 depicts the setup for calibrating the hearing aid. The calibration setup consists of an Audiometer, Audiometric Headphone, an Acoustic Damper, Digital Hearing Aid, an Earphone, and a Simulated Human Ear.

The audiometer and the audiometric headphone are calibrated to generate pure-tones at the desired frequency and sound pressure level. The acoustic

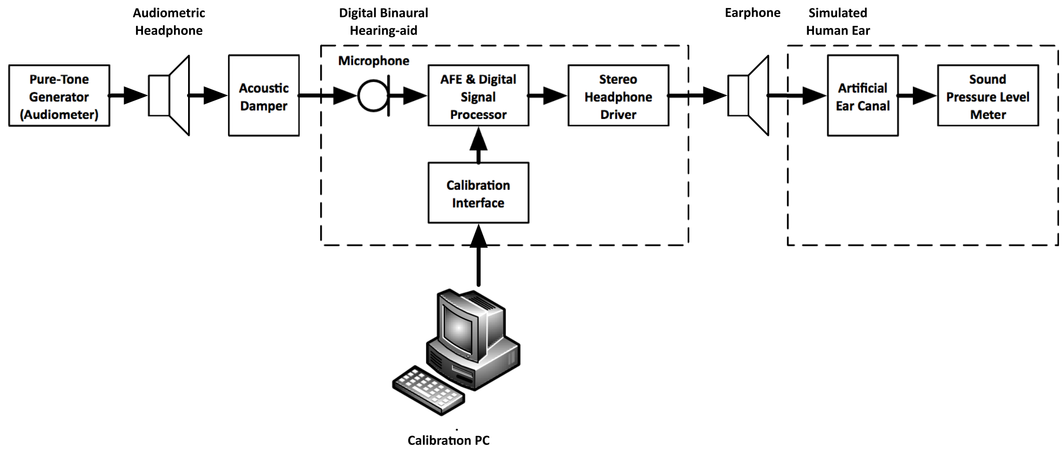

Figure 5.18: Hearing aid calibration setup diagram.

damper is included to simulate the free-to-air audio transmission channel. The damper guides the pure-tone audio signal acoustically to the microphone within the digital hearing aid, and at the same instance provides some form of acoustic resistance which is commonly encountered in the free-to-air transmission. The digital hearing aid is calibrated via a built-in I2C based calibration interface connected to a calibration PC via a serial to I2C protocol converter. The individual left and right audio channels discrete frequencies and gains are fully configurable via this calibration interface.

The processed audio from the hearing aid is output via a standard earphone. The earphone is attached to a simulated human ear. The simulated human ear consists of an artificial human ear canal, and a sound pressure level meter. The artificial human ear canal is constructed using silicone material which mimics the performance of a real human ear canal. The sound pressure level meter is used to measure the sound pressure level picked up from the ear canal.

In this setup, only one audio channel is calibrated as the performance of both audio channels are identical. The setup and the calibration as depicted in Figure 5.18 are carried out in an enclosed room with an ambient noise sound pressure level measured to be at 46 - 50dB. Only certain pure-tone frequencies of interest at 500Hz, 1kHz, 2kHz and 4kHz are being calibrated, the reason for such limitation is pertained to the surrounding ambient noise; hence SPL measurements at frequencies of lower than 500Hz are not deterministic given the setup was not in a proper sound-proof chamber.

Based on the calibration result, the hearing aid gain-output SPL results for each frequency bands are plotted and curve-fitted using Matlab curve fit polynomial functions. Figure 5.19 depicts the plots for the gain settings for the digital hearing aid and its desired sound pressure levels output. The required gains of the desired output SPLs of the hearing aid for the 500Hz, 1kHz, 2kHz and 4kHz frequencies bands can be independently adjusted based on Figure 5.19 respectively. As such, Figure 5.19 served as a calibration and adjustment chart for the hearing aid.

5.6 Experiment and Verification

5.6.1 Fall Detection Algorithm Verification

In this section, the developed accelerometer based algorithm and the fuzzy logic based algorithm are tested for false human fall occurrences detection. Five volunteers are engaged to emulate elderly physical behaviors in per-

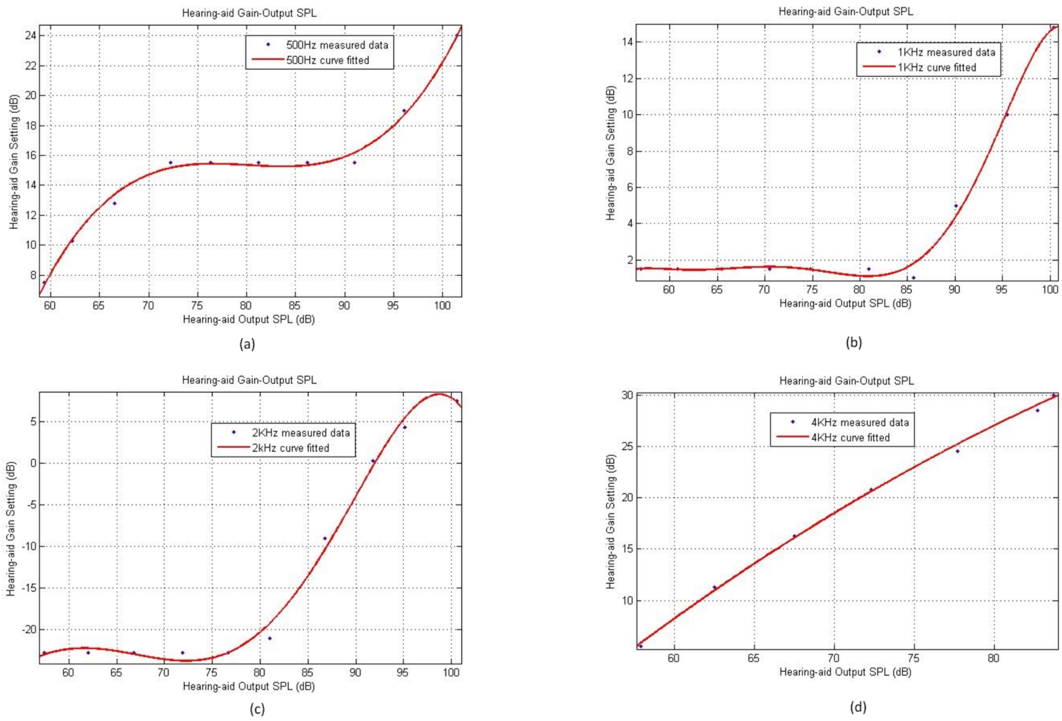

Figure 5.19: Gain SPL output plots (a) 500Hz (b) 1kHz (c) 2kHz (d) 4kHz.

forming common daily motion activities such as: (a) Walking and using stairs, (b) Sitting down, (c) Standing up, and (d) squatting. Each of the volunteer hangs an e-WM around their neck, is required to perform all the defined motion activities, and each activity requires 10 repeats.

Table 5.1 depicts the false fall occurrence detection results using only the accelerometer based algorithm in the e-WM, and Table 5.2 depicts the detection results using the fuzzy logic based algorithm in the e-SS. Based on the results, without fuzzy logic, the accelerometer based algorithm has the maximum false fall detection of 20%. With fuzzy logic, the false fall detection is further reduced to $\leq 2.5\%$, thus greatly improves in the false fall detection problem.

The same volunteers are tasked to emulate four types of falls namely: (a) Front fall, (b) Back fall, (c) Side fall, and (d) Fall from a chair. The exper-

Table 5.1: Accelerometer based algorithm in detecting false fall occurrences.

Volunteer	Motion Type				Error
	Walking	Sitting Down	Standing Up	Squatting	(%)
1	2	3	0	0	12.5
2	3	3	0	1	12.5
3	3	4	0	1	20
4	2	3	1	0	15
5	3	3	0	0	15

Table 5.2: Fuzzy logic based algorithm in detecting false fall occurrences.

Volunteer	Motion Type				Error
	Walking	Sitting Down	Standing Up	Squatting	(%)
1	1	0	0	0	2.5
2	0	0	0	0	0
3	1	0	0	0	2.5
4	1	0	0	0	2.5
5	0	0	0	0	0

iment was conducted in a lab with a tiled floor overlaid with a 1.5" thick soft rubber foam mat to cushion the emulated falls. Each fall is executed 10 times by each volunteer. Table 5.3 depicts the detection results using only the accelerometer based algorithm (e-WM), and Table 5.4 depicts the detection results using the fuzzy logic based algorithm (e-SS). To detect a valid fall, the accelerometer based algorithm is sufficient as it presents at least 95% accuracy in detecting the various emulated falls scenarios. Thus, the accelerometer based algorithm is sufficiently accurate in detecting a valid fall but is prone to false falls detections. The fuzzy logic algorithm is very effective in reducing the false falls detections but does not improves on the overall accuracy of the valid fall detection.

Table 5.3: Accelerometer based algorithm in detecting valid fall occurrences.

Volunteer	Fall Type				Accuracy
	Front	Back	Side	From a Chair	(%)
1	10	10	10	10	100
2	10	10	10	10	100
3	10	10	9	10	97.5
4	10	10	9	9	95
5	10	10	10	9	97.5

Table 5.4: Fuzzy logic based algorithm in detecting valid fall occurrences.

Volunteer	Fall Type				Accuracy
	Front	Back	Side	From a Chair	(%)
1	10	10	10	10	100
2	10	10	10	10	100
3	10	10	9	10	97.5
4	10	10	9	9	95
5	10	10	10	9	97.5

5.6.2 e-HealthCM Trial Deployments

e-HealthCM systems have been tested in selected homes of lone senior citizen. Several conditions must be met before an elderly person is selected for the trial:

(a) $\geq$ 70 years of age and lives alone in a studio apartment.

(b) With mild to moderate hearing difficulty on one of both ears.

(c) Have accessed to caregivers who are family members or friends.

(d) Able body, healthy and without any known chronic and mental illness.

(e) Allows motion activity data to be collected during the trial period.

The trial was conducted on four lone elderly persons households (S1 - S4) meeting the requirements, located in various parts of Singapore, for a period of 30 days. Two caregivers were assigned to each household. e-

HealthCM system consisting of an e-BS and several e-SS modules installed in each of the elderly person's apartment and adjusted to ensure maximum area coverage within the apartment. Each elderly person is also assigned an e-WM attached to a lanyard and worn around the neck during daytime within the apartment. Each elderly person was informed to remove the e-WM only when leaving the apartment and during sleeping.

The e-WM hearing aid feature was tailored to each elderly person's hearing level by performing on the spot simple hearing loss calibrations for the elderly persons. During the period of the trial, the elderly persons were advised to press on the alert button on the e-WM if help was required, and in the event of false fall detection alarm, they were to note down the date, time, frequency of the motion activity (Walk, Sit Down, Stand Up or Squat) they were performing that caused the false fall alerts on the provided log books. They were also briefed on the simple way to reset e-HealthCM after each false fall detection, and designated caregivers will call and check on them when fall alerts were triggered. During the trial, the four elderly volunteers did not experienced any form of valid fall, hence the collected results reflected only the occurrences of false fall occurrences from the performed daily activities. Figure 5.20 - 5.23 depict the false fall detections data (from daily motion activities) for the 30 days trial period for the respective elderly volunteers. The detailed data is tabulated in a Table form and is depicted in Appendix B.

In order to benchmark the effectiveness of the e-HealthCM fuzzy logic algorithm in minimizing false fall detection, an able bodied volunteer (V1)

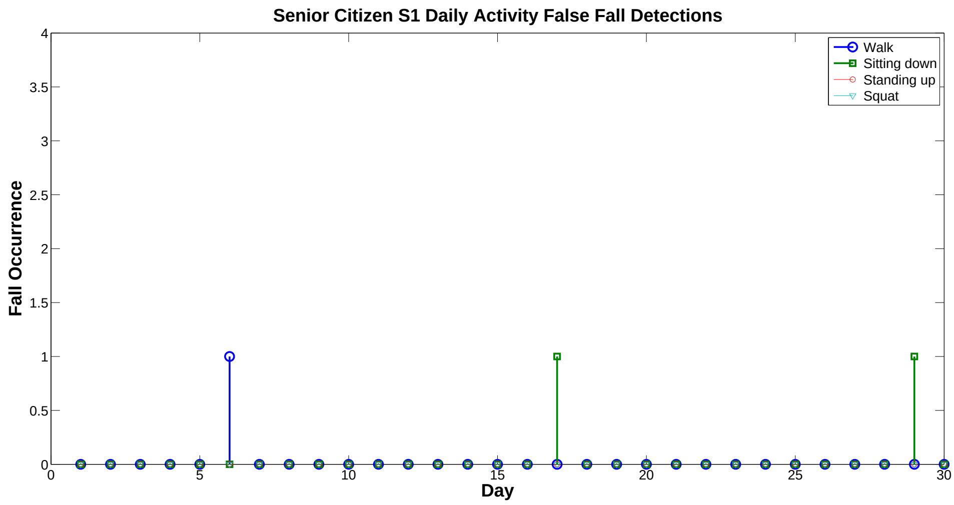

Figure 5.20: Senior Citizen S1 false fall occurrences from daily activities.

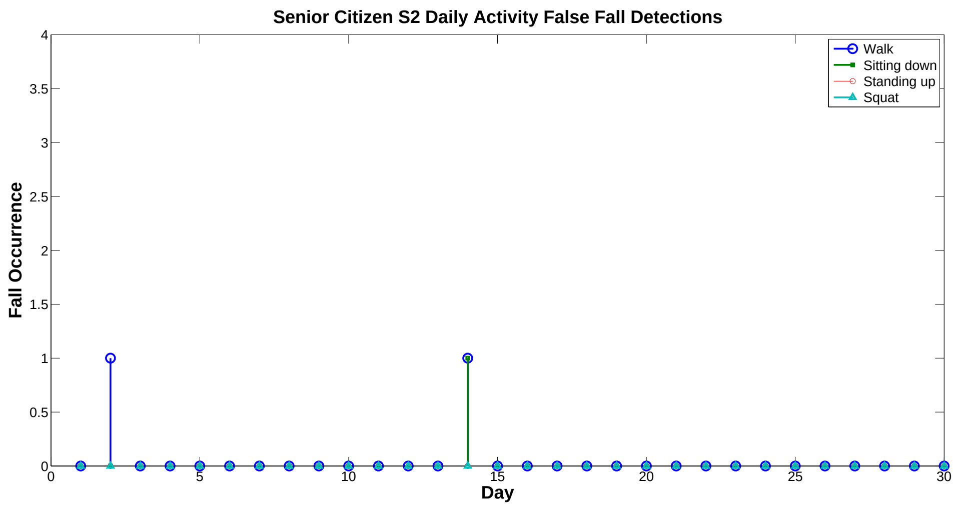

Figure 5.21: Senior Citizen S2 false fall occurrences from daily activities.

was designated as a reference and tasked to wear a specially modified e-WM that operated in a stand-alone mode and retro-fitted with a small audible speaker. This modified e-WM used only the accelerometer based algorithm to detect an occurrence of a fall. This volunteer was tasked to wear the modified e-WM for the same 30 days trial duration. During the trial, the volunteer wore the modified e-WM throughout the day and only removed it while sleeping. The modified e-WM generated a low audible

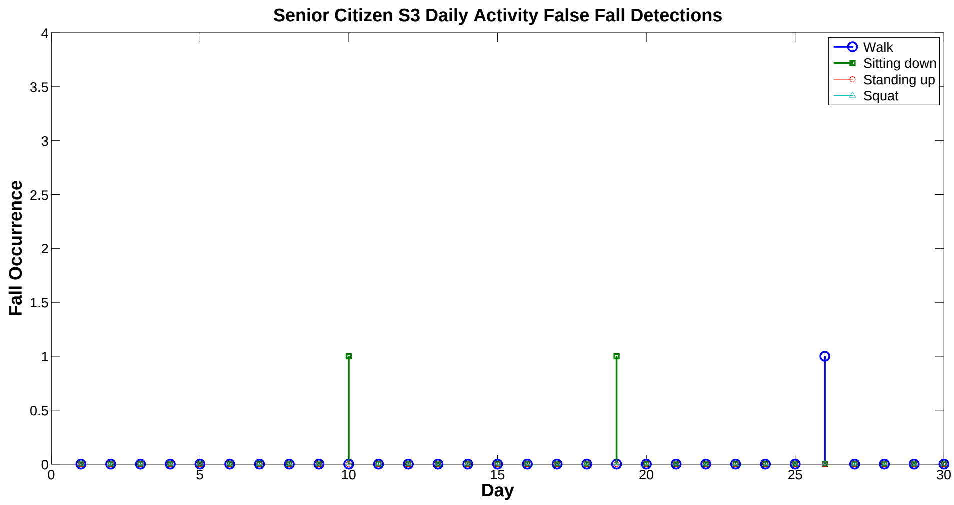

Figure 5.22: Senior Citizen S3 false fall occurrences from daily activities.

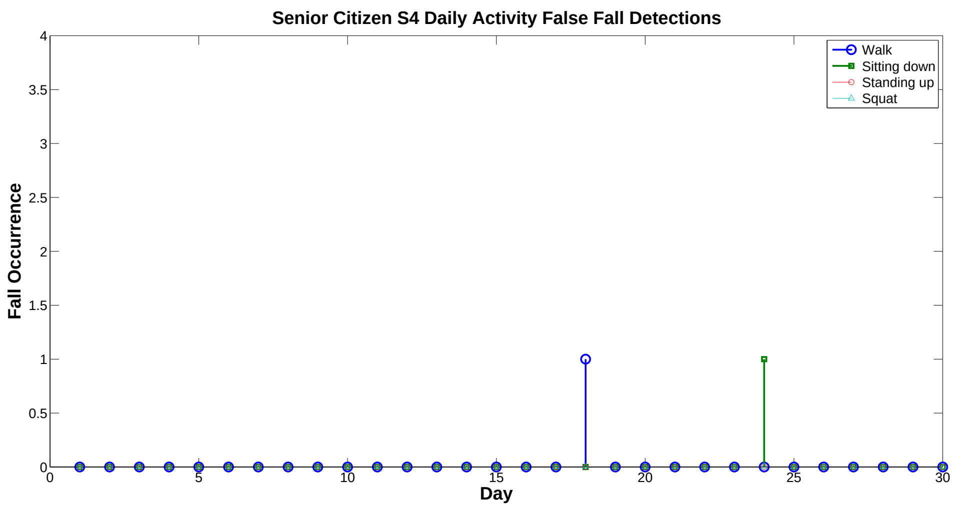

Figure 5.23: Senior Citizen S4 false fall occurrences from daily activities.

sound once a fall was detected, and the volunteer was tasked to record down the date, time, frequency of the motion activity (Walk, Sit Down, Stand Up or Squat) he was performing that caused the false fall alerts on the provided log book. This trial was executed concurrently with the trial involving the four elderly volunteers.

Figure 5.24 depicts the trial results (detail data in Table form is provided in Appendix B) for the number of false fall detections using the modified e-WM. By comparing the results against Figure 5.20 - 5.23 of the elderly volunteers, it is very obvious that the fuzzy logic algorithm in the e-HealthCM (deployed to the elderly volunteers) is capable of minimizing false fall detections. The trials were considered successful with the fuzzy logic based algorithm verified to be effective in reducing false fall alerts.

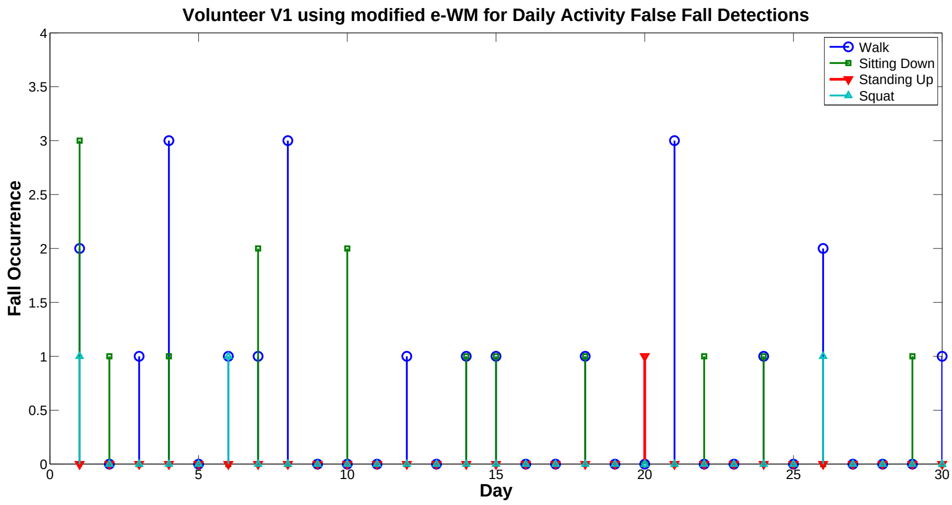

Figure 5.24: Volunteer V1 using a modified e-WM to detect false fall occurrences from daily activities.

At the end of the 30 days trial, each elderly was also asked to fill up a simple usage satisfaction survey pertaining to the low cost hearing aid feature of the e-WM. The survey was conducted to gauge on the usefulness of the low cost hearing aid in addressing the mild to moderate hearing impairment without the need to use an expensive commercial hearing aid. The sample survey forms and collated results are includes in Appendix A. In general, the trial participants were satisfied with the performance of the hearing feature of the e-WM.

5.7 Discussion

This chapter has demonstrated non-feasibility of using only a digital triaxial accelerometer to detect a valid human fall. The accelerometer based fall detection algorithm is highly accurate in detecting a real human fall process. However, the algorithm is also sensitive to human motion attributed to daily movements (sitting, standing, etc.) and each human motion is person dependent. Thus, the algorithm also generates false alarm by detecting falls due to non-fall related daily movements. From the conducted experiments, the algorithm is shown to produce between 12.5% to 20% false alarms from normal daily movements. This error rate is unacceptable as it will cause un-necessary workload to any caregiver. With this shortfall of the accelerometer based fall detection algorithm, an additional form of fall detection by using sound sensing is developed. A newly developed fuzzy logic based fall detection algorithm is used to fuse the result from the accelerometer based fall detection algorithm and the result from the sound based fall detection system. This newly developed fuzzy logic algorithm has been demonstrated in experiments to effectively reduce the false alarm to a minimum level of $\leq 2.5\%$. Thus, making the e-HealthCM to be a reliable system suitable for field deployment. Fuzzy logic can also be applied to other types of CM system and not restricted to application in health based CM. Fuzzy logic has been shown to help to increase the monitoring accuracy of the industrial based CM system. Fuzzy logic based CM system is well-known and has already been developed for CM of metal cutting machines [199] [200].

Chapter 4 depicts an artificial neural network (RBF) based method for acoustic based CM for a precision cutting machine. Precision metal cutting operations constitute a large percentage of industrial activity. By using traditional CM strategies, machine is usually maintained after a fixed number operational time, or the engineer would perform the required maintenance when he thought it to be no longer capable of performing normally. However, it is also possible for a partially faulty machine to be continuously used in the machining process so the parts produced do not meet the required accuracy standard. It is therefore necessary that a CM system (in Chapter 4) be devised to monitor the machine state during cutting operations so that impending machine faults can be detected and the machine being maintained at the optimum time. The RBF based acoustic based CM produces errors between 2% - 8% for detecting the various documented machine conditions. The machine conditions are determined solely via the emitted machine sound during production process. It would be beneficial if low level machine health parameters (e.g., machine vibration, current consumption, lubrication level, operating temperature, etc.) can be included as part of the machine CM process. The additional low level parameters will greatly improve on the overall CM experience. By using the experience of the fuzzy logic algorithm developed in this chapter, its method for decision making can be adopted to further reduce the errors produced.

Yumak *et al* [199] and Pan *et al* [200] have independently demonstrated the feasibility of combining artificial neural network with fuzzy logic for tool and machine CM. Thus, it is highly possible to introduce fuzzy logic into the works in Chapter 4. An additional layer of high level fuzzy logic based decision making system can be introduced to process the output from the CM system developed in Chapter 4, along with additional sensor inputs measuring low level machine health parameters. The introduction of the fuzzy logic layer is intended to fuse the artificial neural network (RBF) based CM result together with the low-level machine health parameters to produce a highly accurate machine CM output that is all inclusive.

5.8 Summary

e-HealthCM health CM system for monitoring of elderly person fall occurrence has been successfully constructed. The accelerometer based fall detection algorithm has been instrumental in detection valid fall occurrences. However, it has been shown that accelerometer alone is not sufficient to provide a reliable fall detection system, as the accelerometer also detects non valid falls from daily motion activities. Thus, a fuzzy logic algorithm is developed to assist in reducing the detection of non valid falls. Trials (internal and external) have been conducted to verify the accuracy of e-HealthCM in addressing valid and non-valid falls, and have successfully proved that the fuzzy logic algorithm works well.

Chapter 6

Conclusions

6.1 Main Contributions

In Chapter 2, the design and formulation of a unified condition monitoring framework with the identified common core components was presented. The framework defines the various requirements for a practical implementation of condition monitoring systems for industrial and healthcare.

The framework presented in Chapter 2 formed the foundation to develop the optimal sensor placement method and two type of condition monitoring systems for industrial and healthcare. In Chapter 3, the optimal sensor placement method covers the sensory set selection and fusion for continuous and real-time monitoring of machine conditions is implemented. The approach is scalable and it employs an architecture that is modular and amenable to parallel processing of incoming data to remain viable and sustainable for real-time applications without requiring large scale retrofitting to the system. A common machine monitoring problem is adopted to serve as the background problem for illustration of the proposed method and experiments. The main objective under the problem posed is to use a minimal number of vibration sensors mounted at key locations of a machine to infer the actual vibration spectrums at a critical point, where direct mounting of sensors at this location is not feasible. An example of such a critical point is at the tool tip of a machining center. The quality of the end-product is very much dependent on the tool condition, hence a real-time monitoring of the vibration spectrum at the critical point is necessary to allow various control and mitigation measures to be invoked when needed. The sensor placement locations are selected on the basis of a moderated sensitivity indicator which fuses the location sensitivity to a vibration frequency at the critical point, with the Fisher Information giving the measurement quality. Thus, each sensor/location is associated with a set of sensitive frequencies for which its measurement will be selected for inferring the specific vibration frequency at the critical point. A Radial Basis Function (RBF) is used to carry out the inferring process and the outputs of all the RBFs invoked yield the vibration spectrums of the critical point which is the basis for the condition monitoring. A comprehensive set of experimental results for verification of the proposed approach is provided.

Chapter 4 detailed a novel approach towards machine condition monitoring. The approach closely mimics the human ear listening process, and attempts to learn the machine operating conditions via the detected sound signatures. With proper machine learning, this approach is able to determine the machine operating conditions in an autonomous manner with minimal human intervention, and minimize the needs of skilled personnel to monitor the machine condition. The condition monitoring hardware has been successfully designed and developed based on the modular components framework defined in Chapter 2. Chapter 4 has demonstrated the feasibility of using only the machine generated sound for machine condition monitoring. The adaptive sound signal filtering algorithm has been demonstrated to be able to remove the unwanted ambient noise surrounding a machine in operation. The Mel Frequency Cepstral Coefficients (MFCC) based sound feature extraction algorithm has been demonstrated to be able to extract sound features that correctly distinguish the various machine operating conditions. The RBF based condition monitoring classifier is able to learn from the large amount of MFCC based sound features data sets for various machine operating conditions, and has the acceptable accuracy to identify the various machine operating conditions. All the algorithms have been successfully deployed to the respective hardware prototypes.

Chapter 5 highlighted the development of e-HealthCM, a health condition monitoring solution that detects an elderly accidental fall occurrence. e-HealthCM implements both accelerometer based and sound based detections for possible occurrence of fall by using fuzzy logic. The accelerometer based fall detection algorithm is instrumental in the detection of a valid fall occurrence. However, it has been shown that accelerometer alone is not sufficient to provide a reliable fall detection system, as the accelerometer also detects non valid falls from daily motion activities. Thus, a fuzzy logic algorithm is developed to assist in reducing the detection of non valid falls. e-HealthCM hardware has been successfully constructed based on the hardware framework defined in Chapter 2, and it's fuzzy logic based fall detection algorithm has been demonstrated to be able to reduce the number of false fall detections from daily motion activities.

6.2 Limitations and Suggestions for Future Work

Based on the prior research as well as the experience acquired while working on this thesis, the following deserves further consideration and investigation to improve the completed assistive healthcare systems.

(a) In Chapter 2, the developed hardware of the common framework only supports Wi-Fi wireless communication and GSM mobile network. Other competing wireless technologies developed for Internet of Things (IoT) (e.g., Bluetooth Low Energy, ZIGBEE, Z-Wave, 6LoWPAN, NFC, Sigfox, and etc.) should also be added as options to cater for deployments in different industrial and healthcare environments.

(b) In Chapter 3, the optimal sensor placement and fusion methodology only covers vibration based sensors. Other types of sensors (e.g., acoustic emission sensor, thermal infrared sensor, and etc.) should also be added as options to cater for deployments in different industrial scenarios or requirements. Fusion of different sensors yield the combination of sensory data with improvements to the resulting information. This has added advantages in the area of improving sensor reliability and redundancy, and increasing measurement resolution that will provide improvement in the machine condition monitoring accuracy.

(c) In Chapter 4, the developed hardware for machine condition monitoring using acoustics does not include pre-amplification with automatic gain control (AGC) feature for the microphones. Machine sound pressure level (SPL) $>$ 90dB causes signal clipping and this reduces the overall signal-to-noise ratio (SNR) and the feature extraction accuracy. At present, a sound level meter is used to determine the machine SPL. Manual microphone gain and position (or direction) adjustment are required to ensure no sound signal clipping. An AGC feature should be added to each microphone, which will be effective in equalizing the sound signal output level from the microphone to a predefined level, hence improving SNR and the resolution of the sound signal acquisition.

(d) In Chapter 5, the e-HealthCM system has been tested with a limited number of users. Although the test results are very good and they are helpful in validating all the implemented algorithms, it is essential to conduct another trial for a large number of users in wide geographical locations such as those in the developing countries whereby home based users are being monitored by distantly located healthcare professionals and care givers. Such a trial is necessary to detect potential short comings and to improve on it, so that the developed systems can be ready for field deployment.

In conclusion, this dissertation presented a practical condition monitoring framework, the design and development, and demonstration of the practical condition monitoring systems for industrial and healthcare. The proposed solutions have been demonstrated to perform satisfactory under various conditions imposed by trial users. It is important to have such a solution in the current situation, where condition monitoring is the key to minimize (or avoid) machine downtime and improving productivity in an industrial environment, and as an important real-time healthcare monitoring tool for the rapidly aging population.

Bibliography

[1] Jason Hill, Robert Szewczyk, Alec Woo, Seth Hollar, David Culler, and Kristofer Pister. System architecture directions for networked sensors. *ACM SIGOPS operating systems review*, 34(5):93–104, 2000.

[2] Anna Hac. Embedded systems and sensors in wireless networks. In *2005 International Conference on Wireless Networks, Communications and Mobile Computing*, volume 1, pages 330–335. IEEE, 2005.

[3] Kazem Sohraby, Daniel Minoli, and Taieb Znati. *Wireless sensor networks: technology, protocols, and applications*. John Wiley Sons, 2007.

[4] Alessandra Flammini, Paolo Ferrari, Daniele Marioli, Emiliano Sisinni, and Andrea Taroni. Wired and wireless sensor networks for industrial applications. *Microelectronics Journal*, 40(9):1322–1336, 2009.

[5] Arne Bröring, Johannes Echterhoff, Simon Jirka, Ingo Simonis, Thomas Everding, Christoph Stasch, Steve Liang, and Rob Lemmens. New generation sensor web enablement. *Sensors*, 11(2):2652–2699, 2011.

[6] Cui Li Ju Hailing, Miao Yong, Li Tianpu, Liu Wei, and Zhao Ze. Overview of wireless sensor networks. *Journal of Computer Research and Development*, 1:021, 2005.

[7] Charu C Aggarwal, Naveen Ashish, and Amit Sheth. The internet of things: A survey from the data-centric perspective. In *Managing and mining sensor data*, pages 383–428. Springer, 2013.

[8] Jayavardhana Gubbi, Rajkumar Buyya, Slaven Marusic, and Marimuthu Palaniswami. Internet of things (iot): A vision, architectural elements, and future directions. *Future Generation Computer Systems*, 29(7):1645–1660, 2013.

[9] Cristina Alcaraz, Pablo Najera, Javier Lopez, and Rodrigo Roman. Wireless sensor networks and the internet of things: Do we need a complete integration. In *1st International Workshop on the Security of the Internet of Things (SecIoT'10)*, volume 1, 2010.

[10] Jason Hill, Mike Horton, Ralph Kling, and Lakshman Krishnamurthy. The platforms enabling wireless sensor networks. *Communications of the ACM*, 47(6):41–46, 2004.

[11] Jose A Gutierrez, Edgar H Callaway, and Raymond L Barrett. *Low-rate wireless personal area networks: enabling wireless sensors with IEEE 802.15. 4*. IEEE Standards Association, 2004.

[12] John A Stankovic, TE Abdelzaher, Chenyang Lu, Lui Sha, and Jennifer C Hou. Real-time communication and coordination in embedded sensor networks. *Proceedings of the IEEE*, 91(7):1002–1022, 2003.

[13] Meijuan Gao, Kai Li, and Jingwen Tian. Wireless sensor network for community intrusion detection system based on embedded system. In *2008 Chinese Control and Decision Conference*, pages 4696–4699. IEEE, 2008.

[14] S Tadigadapa and K Mateti. Piezoelectric mems sensors: state-of-the-art and perspectives. *Measurement Science and technology*, 20(9):092001, 2009.

[15] Hejun Du and Robert Bogue. Mems sensors: past, present and future. *Sensor Review*, 27(1):7–13, 2007.

[16] Ian Sinclair. *Sensors and transducers*. Newnes, 2000.

[17] John Heidemann and Ramesh Govindan. Embedded sensor networks. In *Handbook of Networked and Embedded Control Systems*, pages 721–738. Springer, 2005.

[18] Shahin Farahani. *ZigBee wireless networks and transceivers*. Newnes, 2011.

[19] Ata Elahi and Adam Gschwender. *ZigBee wireless sensor and control network*. Pearson Education, 2009.

[20] Sewook Jung, Alexander Chang, and Mario Gerla. Comparisons of zigbee personal area network (pan) interconnection methods. In *2007 4th International Symposium on Wireless Communication Systems*, pages 337–341. IEEE, 2007.

[21] Dae-Man Han and Jae-Hyun Lim. Smart home energy management system using ieee 802.15. 4 and zigbee. *IEEE Transactions on Consumer Electronics*, 56(3):1403–1410, 2010.

[22] Kun Yang. *Wireless Sensor Networks Principles, Design and Applications*. Springer, 2014.

[23] Stanislav Safaric and Kresimir Malaric. Zigbee wireless standard. In *Multimedia Signal Processing and Communications, 48th International Symposium ELMAR-2006, Zadar, Croatia*, pages 259–262, 2006.

[24] Rob Flickenger. *Building wireless community networks*. O'Reilly Media, Inc., 2003.

[25] Steve Rackley. *Wireless networking technology: From principles to successful implementation*. Elsevier, 2011.

[26] Phill Smith. Comparisons between low power wireless technologies. *US Patent CS-213199-AN*, 2011.

[27] Hande Alemdar and Cem Ersoy. Wireless sensor networks for healthcare: A survey. *Computer Networks*, 54(15):2688–2710, 2010.

[28] Serbulent Tozlu. Feasibility of wi-fi enabled sensors for internet of things. In *2011 7th International Wireless Communications and Mobile Computing Conference*, pages 291–296. IEEE, 2011.

[29] Gerard Rudolph Mendez and Subhas Chandra Mukhopadhyay. A wi-fi based smart wireless sensor network for an agricultural environment. In *Wireless Sensor Networks and Ecological Monitoring*, pages 247–268. Springer, 2013.

[30] Stefan Aust, R Venkatesha Prasad, and Ignas GMM Niemegeers. Ieee 802.11 ah: Advantages in standards and further challenges for sub 1 ghz wi-fi. In *2012 IEEE International Conference on Communications (ICC)*, pages 6885–6889. IEEE, 2012.

[31] ECL Chan, G Baciu, and SC Mak. Using wi-fi signal strength to localize in wireless sensor networks. *Communications and Mobile Computing, 2009. CMC'09. WRI International Conference on*, 1:538–542, 2009.

[32] Serbulent Tozlu, Murat Senel, Wei Mao, and Abtin Keshavarzian. Wi-fi enabled sensors for internet of things: A practical approach. *IEEE Communications Magazine*, 50(6):134–143, 2012.

[33] Li Li, Hu Xiaoguang, Chen Ke, and He Ketai. The applications of wifi-based wireless sensor network in internet of things and smart grid. In *2011 6th IEEE Conference on Industrial Electronics and Applications*, pages 789–793. IEEE, 2011.

[34] Cai X., Wang Y., Zhang X., and Luo L. Internet of things (wf-iot). In *2014 IEEE World Forum on Design and implementation of a WiFi sensor device management system*, pages 10–14. IEEE, 2014.

[35] Serbulent Tozlu and Murat Senel. Battery lifetime performance of wi-fi enabled sensors. In *2012 IEEE Consumer Communications and Networking Conference (CCNC)*, pages 429–433. IEEE, 2012.

[36] Vitaly Petrov, Sergey Andreev, and Yevgeni Koucheryavy. An applicability assessment of ieee 802.11 technology for machine-type communications. In *Ad Hoc Networking Workshop (Med-Hoc-Net), 2012 The 11th Annual Mediterranean*, pages 24–31. IEEE, 2012.

[37] Benedikt Ostermaier, Matthias Kovatsch, and Silvia Santini. Connecting things to the web using programmable low-power wifi modules. In *Proceedings of the Second International Workshop on Web of Things*, page 2. ACM, 2011.

[38] Vinoth Gunasekaran and Fotios C Harmantzis. Towards a wi-fi ecosystem: Technology integration and emerging service models. *Telecommunications Policy*, 32(3):163–181, 2008.

[39] Weiping Sun, Okhwan Lee, Yeonchul Shin, Seongwon Kim, Changmok Yang, Hyoil Kim, and Sunghyun Choi. Wi-fi could be much more. *IEEE Communications Magazine*, 52(11):22–29, 2014.

[40] Markus Warsta and Timo Jokiaho. Mobile communication system and a method for connecting a remote workstation to a data communication network via a mobile communication network. *US Patent 5,896,369*, 1999.

[41] Jenny C Aker and Isaac M Mbiti. Mobile phones and economic development in africa. *The Journal of Economic Perspectives*, 24(3):207–232, 2010.

[42] Scott Motlik. Mobile learning in developing nations. *The International Review of Research in Open and Distributed Learning*, 9(2):1393, 2008.

[43] Christopher Drane, Malcolm Macnaughtan, and Craig Scott. Positioning gsm telephones. *IEEE Communications magazine*, 36(4):46–54, 59, 1998.

[44] Dr Aaron Quigley. Pervasive computing technology review. *Smart Internet Technology Research Group, Australia*, 12:1–37, 2004.

[45] Niclas Kempe and David Bystrm. Cellular devices in mechatronic applications: An evaluation from a sensor and communication perspective. *DIVA*, pages 1–101, 2012.

[46] JAL Riquelme, F Soto, J Suardiaz, and P Sanchez. Wireless sensor networks for precision horticulture in southern spain. *Computers and Electronics in Agriculture*, 68(1):25–35, 2009.

[47] K Romer and F Mattern. The design space of wireless sensor networks. *IEEE wireless communications*, 11(6):54–61, 2004.

[48] Niranjan Balasubramanian, Aruna Balasubramanian, and Arun Venkataramani. Energy consumption in mobile phones: a measurement study and implications for network applications. In *Proceedings of the 9th ACM SIGCOMM conference on Internet measurement conference*, pages 280–293. ACM, 2009.

[49] Bentley Banks, T Harms, S Sedigh Sarvestani, and Filippo Bastianini. A low-cost wireless system for autonomous generation of road

safety alerts. In *SPIE Smart Structures and Materials+ Nondestructive Evaluation and Health Monitoring*, pages 72920E–72920E. International Society for Optics and Photonics, 2009.

[50] Valerio Plessi, Filippo Bastianini, and Sahra Sedigh. A wireless system for real-time environmental and structural monitoring. In *IFIP International Workshop on Software Technologies for Embedded and Ubiquitous Systems*, pages 456–465. Springer, 2007.

[51] Volker Turau, Matthias Witt, and Marcus Venzke. Field trials with wireless sensor networks: Issues and remedies. In *ICWMC*, page 86. ICWMC, 2006.

[52] L Ruiz-Garcia, L Lunadei, P Barreiro, and I Robla. A review of wireless sensor technologies and applications in agriculture and food industry: state of the art and current trends. *sensors*, pages 4728–4750, 2009.

[53] Alexandros Pantelopoulos and Nikolaos G Bourbakis. A survey on wearable sensor-based systems for health monitoring and prognosis. *IEEE Transactions on Systems, Man, and Cybernetics, Part C (Applications and Reviews)*, 40(1):1–12, 2010.

[54] Liqun Hou and Neil W Bergmann. Novel industrial wireless sensor networks for machine condition monitoring and fault diagnosis. *IEEE Transactions on Instrumentation and Measurement*, 61(10):2787–2798, 2012.

[55] Hashem M Hashemian and Wendell C Bean. State-of-the-art predictive maintenance techniques. *IEEE Transactions on Instrumentation and measurement*, 60(10):3480–3492, 2011.

[56] Kay Soon Low, Win Nu Nu Win, and Meng Joo Er. Wireless sensor networks for industrial environments. In *International Conference on Computational Intelligence for Modelling, Control and Automation and International Conference on Intelligent Agents, Web Technologies and Internet Commerce (CIMCA-IAWTIC'06)*, pages 271–276. IEEE, 2005.

[57] Paul Wright, David Dornfeld, and Nathan Ota. Condition monitoring in end-milling using wireless sensor networks (wsns). *Transactions of NAMRI/SME*, 36:177–183, 2008.

[58] Bin Lu, Thomas G Habetler, Ronald G Harley, Jose A Gutierrez, and David B Durocher. Energy evaluation goes wireless. *IEEE Industry Applications Magazine*, 13(2):17–23, 2007.

[59] VMD Jagannath and B Raman. Wibeam: Wireless bearing monitoring system. In *2007 2nd International Conference on Communication Systems Software and Middleware*, pages 1–8. IEEE, 2007.

[60] V Sundararajan, Andrew Redfern, William Watts, and Paul Wright. Distributed monitoring of steady-state system performance using wireless sensor networks. In *ASME 2004 International Mechanical Engineering Congress and Exposition*, pages 23–29. ASME, 2004.

[61] Bary W Wilson, Norman H Hansen, Chester L Shepard, Timothy J Peters, and Frank L Greitzer. Development of a modular in-situ oil analysis prognostic system. In *Proceedings of the International Society of Logistics (SOLE) 1999 Symposium, August*, pages 1–6. SOLE, 1999.

[62] Paul K Wright, David Dornfeld, RG Hillaire, and Nathan K Ota. A wireless sensor for tool temperature measurement and its integration within a manufacturing system. *Laboratory for Manufacturing and Sustainability, Trans. North American Manufacturing Research Institute*, 34:1–8, 2006.

[63] V Sundararajan, Andrew Redfern, Michael Schneider, Paul Wright, and James Evans. Wireless sensor networks for machinery monitoring. In *ASME 2005 International Mechanical Engineering Congress and Exposition*, pages 425–433. ASME, 2005.

[64] P Jayaswal and AK Wadhwani. Machine fault signature analysis. *International Journal of Rotating Machinery*, 2008:1–11, 2008.

[65] MR Mehrjou, N Mariun, and MH Marhaban. Rotor fault condition monitoring techniques for squirrel-cage induction machinea review. *Mechanical Systems and Signal Processing*, 25(8):2827–2848, 2011.

[66] Richard H Lyon. *Machinery noise and diagnostics*. Butterworth-Heinemann, 2013.

[67] Cornelius Scheffer and Paresh Girdhar. *Practical machinery vibration analysis and predictive maintenance*. Elsevier, 2004.

[68] Y Altintas and E Budak. Analytical prediction of stability lobes in milling. *CIRP Annals-Manufacturing Technology*, 44(1):357–362, 1995.

[69] RJ Kuo and PH Cohen. Multi-sensor integration for on-line tool wear estimation through radial basis function networks and fuzzy neural network. *Neural Networks*, 12(2):355–370, 1999.

[70] N Ghosh, YB Ravi, A Patra, S Mukhopadhyay, S Paul, AR Mohanty, and AB Chattopadhyay. Estimation of tool wear during cnc milling using neural network-based sensor fusion. *Mechanical Systems and Signal Processing*, 21(1):466–479, 2007.

[71] Lakshman Krishnamurthy, Robert Adler, Phil Buonadonna, Jasmeet Chhabra, Mick Flanigan, Nandakishore Kushalnagar, Lama Nachman, and Mark Yarvis. Design and deployment of industrial sensor networks: experiences from a semiconductor plant and the north

sea. In *Proceedings of the 3rd international conference on Embedded networked sensor systems*, pages 64–75. ACM, 2005.

[72] Yusuf Altintas. *Manufacturing automation: metal cutting mechanics, machine tool vibrations, and CNC design*. Cambridge university press, 2012.

[73] Cuneyt Aliustaoglu, H Metin Ertunc, and Hasan Ocak. Tool wear condition monitoring using a sensor fusion model based on fuzzy inference system. *Mechanical Systems and Signal Processing*, 23(2):539–546, 2009.

[74] Huseyin M Ertunc, Kenneth A Loparo, Engin Ozdemir, and Hasan Ocak. Real time monitoring of tool wear using multiple modeling method. In *Electric Machines and Drives Conference, 2001. IEMDC 2001. IEEE International*, pages 687–691. IEEE, 2001.

[75] K Jemielniak and O Otman. Tool failure detection based on analysis of acoustic emission signals. *Journal of Materials Processing Technology*, 76(1):192–197, 1998.

[76] Qingbo He, Ruqiang Yan, Fanrang Kong, and Ruxu Du. Machine condition monitoring using principal component representations. *Mechanical Systems and Signal Processing*, 23(2):446–466, 2009.

[77] MLD Wong, LB Jack, and AK Nandi. Modified self-organising map for automated novelty detection applied to vibration signal monitoring. *Mechanical systems and signal processing*, 20(3):593–610, 2006.

[78] Jyoti K Sinha and Keri Elbhbah. A future possibility of vibration based condition monitoring of rotating machines. *Mechanical Systems and Signal Processing*, 34(1):231–240, 2013.

[79] A Jablonski and T Barszcz. Validation of vibration measurements for heavy duty machinery diagnostics. *Mechanical Systems and Signal Processing*, 38(1):248–263, 2013.

[80] David A Dornfeld and MF DeVries. Neural network sensor fusion for tool condition monitoring. *CIRP Annals-Manufacturing Technology*, 39(1):101–105, 1990.

[81] M Salama, T Rose, and J Garba. Optimal placement of excitations and sensors for verification of large dynamical systems. In *Proceedings of the 28th Structures, Structural Dynamics, and Materials Conference*, pages 6–8, 1987.

[82] Yung-Tseng Chung and J David Moore. On-orbit sensor placement and system identification of space station with limited instrumentations. In *Proceedings of the International Modal Analysis Conference*, pages 41–41. SEM SOCIETY FOR EXPERIMENTAL MECHANICS INC, 1993.

[83] DS Li, HN Li, and CP Fritzen. The connection between effective independence and modal kinetic energy methods for sensor placement. *Journal of sound and vibration*, 305(4):945–955, 2007.

[84] DS Li, HN Li, and CP Fritzen. Representative least squares methods for sensor placement. In *Proceedings of the 3rd International Conference on Structural Health Monitoring and Intelligent Infrastructure*, 2007.

[85] Daniel C Kammer. Sensor placement for on-orbit modal identification and correlation of large space structures. *Journal of Guidance, Control, and Dynamics*, 14(2):251–259, 1991.

[86] DC Kammer and L Yao. Enhancement of on-orbit modal identification of large space structures through sensor placement. *Journal of Sound and Vibration*, 171(1):119–139, 1994.

[87] Leehter Yao, William A Sethares, and Daniel C Kammer. Sensor placement for on-orbit modal identification via a genetic algorithm. *AIAA journal*, 31(10):1922–1928, 1993.

[88] Daniel C Kammer and Michael L Tinker. Optimal placement of triaxial accelerometers for modal vibration tests. *Mechanical systems and signal processing*, 18(1):29–41, 2004.

[89] Poul Henning Kirkegaard and Rune Brincker. On the optimal location of sensors for parametric identification of linear structural systems. *Fracture and Dynamics*, R9239(40):1–22, 1992.

[90] Ami Arbel. Sensor placement in optimal filtering and smoothing problems. *IEEE Transactions on Automatic Control*, 27(1):94–98, 1982.

[91] Sigeru Omatu, Satoni Koide, and Takasi Soeda. Optimal sensor location problem for a linear distributed parameter system. *IEEE Transactions on automatic control*, 23(4):665–673, 1978.

[92] Costas Papadimitriou, James L Beck, and Siu-Kui Au. Entropy-based optimal sensor location for structural model updating. *Journal of Vibration and Control*, 6(5):781–800, 2000.

[93] An-Pan Cherng. Optimal sensor placement for modal parameter identification using signal subspace correlation techniques. *Mechanical Systems and Signal Processing*, 17(2):361–378, 2003.

[94] R W Longman and K T Alfriend. Energy optimal degree of controllability and observability for regulator and maneuver problems. *Journal of the Astronautical Sciences*, 38:87–103, 1990.

[95] Ning Xu, Sumit Rangwala, Krishna Kant Chintalapudi, Deepak Ganesan, Alan Broad, Ramesh Govindan, and Deborah Estrin. A wireless sensor network for structural monitoring. In *Proceedings of the 2nd international conference on Embedded networked sensor systems*, pages 13–24. ACM, 2004.

[96] R Andrew Swartz, Jerome P Lynch, Stephan Zerbst, Bert Sweetman, and Raimund Rolfes. Structural monitoring of wind turbines using wireless sensor networks. *Smart structures and systems*, 6(3):183–196, 2010.

[97] Mo Li and Yunhao Liu. Underground coal mine monitoring with wireless sensor networks. *ACM Transactions on Sensor Networks (TOSN)*, 5(2):10, 2009.

[98] Frank Stajano, Neil Hoult, Ian Wassell, Peter Bennett, Campbell Middleton, and Kenichi Soga. Smart bridges, smart tunnels: Transforming wireless sensor networks from research prototypes into robust engineering infrastructure. *Ad Hoc Networks*, 8:872–888, 2010.

[99] Sukun Kim, Shamim Pakzad, David Culler, James Demmel, Gregory Fenves, Steven Glaser, and Martin Turon. Health monitoring of civil infrastructures using wireless sensor networks. In *2007 6th International Symposium on Information Processing in Sensor Networks*, pages 254–263. IEEE, 2007.

[100] M Picozzi, C Milkereit, C Zulfikar, K Fleming, R Ditommaso, M Erdik, J Zschau, J Fischer, E Şafak, O Özel, et al. Wireless technologies for the monitoring of strategic civil infrastructures: an ambient vibration test on the fatih sultan mehmet suspension bridge in istanbul, turkey. *Bulletin of Earthquake Engineering*, 8(3):671–691, 2010.

[101] Ning Jia. Fall detection application by using 3-axis accelerometer adxl345. *Analog Devices, Application Note*, 1023, 2012.

[102] Dana P Goldman, Paul G Shekelle, Jayanta Bhattacharya, Michael Hurd, and Geoffrey F Joyce. Health status and medical treatment of the future elderly. 2004.

[103] Shyamal Patel, Hyung Park, Paolo Bonato, Leighton Chan, and Mary Rodgers. A review of wearable sensors and systems with application in rehabilitation. *Journal of neuroengineering and rehabilitation*, 9(1):1, 2012.

[104] Tan X., Chen X., Hu X., Ren R., Zhou B., Fang Z., and Xia S. Emd-based electrocardiogram delineation for a wearable low-power ecg monitoring device. *Canadian Journal of Electrical and Computer Engineering*, 37(4):212–221, 2014.

[105] Elisa Spano, Stefano Di Pascoli, and Giuseppe Iannaccone. Low-power wearable ecg monitoring system for multiple-patient remote monitoring. *IEEE Sensors Journal*, 16(13):5425–5462, 2016.

[106] Dimitri Konstantas and Rainer Herzog. Continuous monitoring of vital constants for mobile users: the mobihealth approach. In *Engineering in Medicine and Biology Society, 2003. Proceedings of the 25th Annual International Conference of the IEEE*, volume 4, pages 3728–3731. IEEE, 2003.

[107] Paolo Bellavista, Giuseppe Cardone, Antonio Corradi, and Luca Foschini. Convergence of manet and wsn in iot urban scenarios. *IEEE Sensors Journal*, 13(10):3558–3567, 2013.

[108] Daniele Puccinelli and Martin Haenggi. Wireless sensor networks: applications and challenges of ubiquitous sensing. *IEEE Circuits and systems magazine*, 5(3):19–31, 2005.

[109] David Niewolny. How the internet of things is revolutionizing healthcare. *White paper, Freescale Semiconductor*, 2013.

[110] Ram Satish. Internet-of-things (iot) advances home healthcare for seniors. Online, April 2014.

[111] Ida. The internet of things (iot). Online, April 2015.

[112] Tadashi Castillo-Hi Mathias Cousin and Glenn Snyder. Devices and diseases: How the iot is transforming medtech. Online, September 2015.

[113] Bin Zhou, Chao Hu, HaiBin Wang, Ruiwen Guo, and Max Q-H Meng. A wireless sensor network for pervasive medical supervision. In *Integration Technology, 2007. ICIT'07. IEEE International Conference on*, pages 740–744. IEEE, 2007.

[114] Angelika Dohr, Robert Modre-Osprian, Mario Drobics, Dieter Hayn, and Gunter Schreier. The internet of things for ambient assisted living. *ITNG*, 10:804–809, 2010.

[115] Partha P Ray. Home health hub internet of things (h 3 iot): An architectural framework for monitoring health of elderly people. In *Science Engineering and Management Research (ICSEMR), 2014 International Conference on*, pages 1–3. IEEE, 2014.

[116] Richard Wootton. Telemedicine in the national health service. *Journal of the Royal Society of Medicine*, 91(12):614–621, 1998.

[117] Syed Farooq Ali, Muhammad Muaz, Alizaa Fatima, Fatima Idrees, and Noman Nazar. Human fall detection. In *Multi Topic Conference (INMIC), 2013 16th International*, pages 101–105. IEEE, 2013.

[118] Yaniv Zigel, Dima Litvak, and Israel Gannot. A method for automatic fall detection of elderly people using floor vibrations and sound proof of concept on human mimicking doll falls. *IEEE Transactions on Biomedical Engineering*, 56(12):2858–2867, 2009.

[119] Muhammad Mubashir, Ling Shao, and Luke Seed. A survey on fall detection: Principles and approaches. *Neurocomputing*, 100:144–152, 2013.

[120] L Cohen. A consumers' republic: The politics of mass consumption in postwar america. *Journal of Consumer Research*, 31(1):236–239, 2004.

[121] Mark C Eti, SOT Ogaji, and SD Probert. Reducing the cost of preventive maintenance (pm) through adopting a proactive reliability-focused culture. *Applied energy*, 83(11):1235–1248, 2006.

[122] H James Harrington. Performance improvement: a total poor-quality cost system. *The TQM Magazine*, 11(4):221–230, 1999.

[123] Andrew KS Jardine, Daming Lin, and Dragan Banjevic. A review on machinery diagnostics and prognostics implementing condition-based maintenance. *Mechanical systems and signal processing*, 20(7):1483–1510, 2006.

[124] Rosmaini Ahmad and Shahrul Kamaruddin. An overview of time-based and condition-based maintenance in industrial application. *Computers Industrial Engineering*, 63(1):135–149, 2012.

[125] Albert HC Tsang. Condition-based maintenance: tools and decision making. *Journal of Quality in Maintenance Engineering*, 1(3):3–17, 1995.

[126] Victor Chan, Pradeep Ray, and Nandan Parameswaran. Mobile e-health monitoring: an agent-based approach. *IET communications*, 2:223–230, 2008.

[127] Ziyu Lv, Feng Xia, Guowei Wu, Lin Yao, and Zhikui Chen. icare: a mobile health monitoring system for the elderly. In *Proceedings of the 2010 IEEE/ACM Int'l Conference on Green Computing and Communications Int'l Conference on Cyber, Physical and Social Computing*, pages 699–705. IEEE Computer Society, 2010.

[128] Wootton Richard. *Telehealth in the developing world*. IDRC, 2009.

[129] ICT Data and Statistics Division. Ict facts and figures. Online, May 2015.

[130] Robert L Rubinstein and Janet Capriotti Kilbride. *Elders living alone: Fraility and the perception of choice*. Transaction Publishers, 1992.

[131] Tai Janice. Old and home alone in singapore. Online, August 2015.

[132] Microchip. Microchip pic32mx5xx/6xx/7xx datasheet. Online, March 2013.

[133] Maggie K Delano and Charles G Sodini. A long-term wearable electrocardiogram measurement system. In *2013 IEEE International Conference on Body Sensor Networks*, pages 1–6. IEEE, 2013.

[134] Yang Hao and Robert Foster. Wireless body sensor networks for health-monitoring applications. *Physiological measurement*, 29(11):R27, 2008.

[135] Raghavendra V Kulkarni, Anna Forster, and Ganesh Kumar Venayagamoorthy. Computational intelligence in wireless sensor networks: A survey. *IEEE communications surveys tutorials*, 13(1):68–96, 2011.

[136] Microchip. Microchip rn171 2.4 ghz ieee std. 802.11 b/g wireless lan module datasheet. Online, March 2014.

[137] EIA Standard RS232-C. Interface between data terminal equipment and data communications equipment employing serial binary data interchange. 1969.

[138] Analog Devices. Adxl001 high performance, wide bandwidth accelerometer datasheet. Online, June 2015.

[139] Analog Devices. Adxl345 3-axis digital accelerometer datasheet. Online, June 2015.

[140] Yuan Xi, Chen Dong, Tian Xiang, and LV Jing. Three-axis digital accelerometer adxl345 and its application in sins design [j]. *Electronic Design Engineering*, 3:058, 2010.

[141] John T Roth, Dragan Djurdjanovic, Xiaoping Yang, Laine Mears, and Thomas Kurfess. Quality and inspection of machining operations: tool condition monitoring. *Journal of Manufacturing Science and Engineering*, 132(4):041015, 2010.

[142] Roy Frieden and Robert A Gatenby. *Exploratory data analysis using Fisher information.* Springer Science Business Media, 2010.

[143] Robert J Howlett and Lakhmi C Jain. *Radial basis function networks 2: new advances in design*, volume 67. Physica, 2013.

[144] Eric J Hartman, James D Keeler, and Jacek M Kowalski. Layered neural networks with gaussian hidden units as universal approximations. *Neural computation*, 2:210–215, 1990.

[145] Sunan Huang and Kok Kiong Tan. Fault detection and diagnosis based on modeling and estimation methods. *IEEE Transactions on Neural Networks*, 20(5):872–881, 2009.

[146] Kok-Zuea Tang, Kok-Kiong Tan, Tong-Heng Lee, and Chek-Sing Teo. Neural network-based correction and interpolation of encoder signals for precision motion control. In *Advanced Motion Control, 2004. AMC'04. The 8th IEEE International Workshop on*, pages 499–504. IEEE, 2004.

[147] Jinkun Liu. *Radial Basis Function (RBF) neural network control for mechanical systems: design, analysis and Matlab simulation.* Springer Science Business Media, 2013.

[148] SA Tobias. Machine tool vibration research. *International Journal of Machine Tool Design and Research*, 1:1–14, 1961.

[149] MSH Bhuiyan, IA Choudhury, and Y Nukman. Tool condition monitoring using acoustic emission and vibration signature in turning. In *Proceedings of the world congress on engineering*, volume 3, 2012.

[150] P Krishnakumar, K Rameshkumar, and KI Ramachandran. Tool wear condition prediction using vibration signals in high speed machining (hsm) of titanium (ti-6al-4v) alloy. *Procedia Computer Science*, 50:270–275, 2015.

[151] DR Salgado and FJ Alonso. An approach based on current and sound signals for in-process tool wear monitoring. *International Journal of Machine Tools and Manufacture*, 47(14):2140–2152, 2007.

[152] EJ Weller, Henry M Schrier, and Bjorn Weichbrodt. What sound can be expected from a worn tool. *Journal of Engineering for Industry*, 91(3):525–534, 1969.

[153] CH Shen. Acoustic based condition monitoring. *University of Akron*, 2012.

[154] ASY Heng. Intelligent prognostics of machinery health utilising suspended condition monitoring data. *Queensland University of Technology*, 2009.

[155] M Shiraishi. Scope of in-process measurement, monitoring and control techniques in machining processespart 1: In-process techniques for tools. *Precision Engineering*, 10(4):179–189, 1988.

[156] Z JunHong and H Bing. Analysis of engine front noise using sound intensity techniques. *Mechanical systems and signal processing*, 19(1):213–221, 2005.

[157] Alan Davies. *Handbook of condition monitoring: techniques and methodology.* Springer Science & Business Media, 2012.

[158] Neville Stanton, Paul M Salmon, and Laura A Rafferty. *Human factors methods: a practical guide for engineering and design.* Ashgate Publishing, Ltd., 2013.

[159] AKS Jardine, D Lin, and D Banjevic. A review on machinery diagnostics and prognostics implementing condition-based maintenance. *Mechanical systems and signal processing*, 20(7):1483–1510, 2006.

[160] G Dalpiaz and A Rivola. Condition monitoring and diagnostics in automatic machines: comparison of vibration analysis techniques. *Mechanical Systems and Signal Processing*, 11(1):53–73, 1997.

[161] Thomas W Parks and C Sidney Burrus. *Digital filter design.* Wiley-Interscience, 1987.

[162] Simon S Haykin. *Adaptive filter theory.* Pearson Education India, 2008.

[163] W Kim. Lms adaptive filter. *US Patent App. 10/927*, 2004.

[164] Simon Haykin and Bernard Widrow. *Least-mean-square adaptive filters*, volume 31. John Wiley & Sons, 2003.

[165] A Mesaros and J Astola. The mel-frequency cepstral coefficients in the context of singer identification. *ISMIR*, pages 610–613, 2005.

[166] A Srinivasan. Speaker identification and verification using vector quantization and mel frequency cepstral coefficients. *Research Journal of Applied Sciences, Engineering and Technology*, 4(1):33–40, 2012.

[167] AJM Houtsma. Pitch perception. *Hearing*, 6:262–262, 1995.

[168] MA Hossan and S Memon. A novel approach for mfcc feature extraction. *Signal Processing and Communication Systems (ICSPCS), 2010 4th International Conference on*, pages 1–5, 2010.

[169] V Tiwari. Mfcc and its applications in speaker recognition. *International Journal on Emerging Technologies*, 1(1):19–22, 2010.

[170] H Joseph Weaver. *Applications of discrete and continuous Fourier analysis.* Wiley-Interscience, 1983.

[171] Sigurdur Sigurdsson, Kaare Brandt Petersen, and Tue Lehn-Schiøler. Mel frequency cepstral coefficients: An evaluation of robustness of mp3 encoded music. *Seventh International Conference on Music Information Retrieval (ISMIR)*, pages 1–4, 2006.

[172] SH Chen and YR Luo. Speaker verification using mfcc and support vector machine. *Proceedings of the International MultiConference of Engineers and Computer Scientists*, 1(18-20), 2009.

[173] Yuhua Li, Michael J Pont, and N Barrie Jones. Improving the performance of radial basis function classifiers in condition monitoring and fault diagnosis applications where unknown faults may occur. *Pattern Recognition Letters*, 23(5):569–577, 2002.

[174] Tim Horberry, Robin Burgess-Limerick, and Lisa J Steiner. *Human factors for the design, operation, and maintenance of mining equipment.* CRC Press, 2016.

[175] Tan Theresa. More singaporeans living alone; trend seen rising. Online, March 2014.

[176] Tan Hwee Pink. Integrated approach to ageing in place. Online, January 2016.

[177] Yeo Sam Jo. Hdb elderly alert system well-received in test-bed. Online, March 2015.

[178] Lim Benjamin. Putting her mind at ease. Online, April 2014.

[179] Natthapon Pannurat, Surapa Thiemjarus, and Ekawit Nantajeewarawat. Automatic fall monitoring: a review. *Sensors*, 14(7):12900–12936, 2014.

[180] Yueng Santiago Delahoz and Miguel Angel Labrador. Survey on fall detection and fall prevention using wearable and external sensors. *Sensors*, 14(10):19806–19842, 2014.

[181] Raul Igual, Carlos Medrano, and Inmaculada Plaza. Challenges, issues and trends in fall detection systems. *Biomedical engineering online*, 12(1):1–24, 2013.

[182] Shomir Chaudhuri, Hilaire Thompson, and George Demiris. Fall detection devices and their use with older adults: a systematic review. *Journal of geriatric physical therapy (2001)*, 37(4):178–196, 2014.

[183] Shehroz S Khan and Jesse Hoey. Review of fall detection techniques: A data availability perspective. *arXiv preprint arXiv:1605.09351*, 2016.

[184] AK Bourke, JV O'brien, and GM Lyons. Evaluation of a threshold-based tri-axial accelerometer fall detection algorithm. *Gait & posture*, 26(2):194–199, 2007.

[185] Alan K Bourke, Pepijn WJ Van de Ven, Amy E Chaya, Gearóid M OLaighin, and John Nelson. Testing of a long-term fall detection system incorporated into a custom vest for the elderly. *2008 30th Annual International Conference of the IEEE Engineering in Medicine and Biology Society*, pages 2844–2847, 2008.

[186] Robert Burkard. Sound pressure level measurement and spectral analysis of brief acoustic transients. *Electroencephalography and clinical neurophysiology*, 57(1):83–91, 1984.

[187] Julia J Hindmarsh and E Harvey Estes. Falls in older persons: causes and interventions. *Archives of Internal Medicine*, 149(10):2217–2222, 1989.

[188] J Elizabeth Walker and Jonathan Howland. Falls and fear of falling among elderly persons living in the community: occupational therapy interventions. *American Journal of Occupational Therapy*, 45(2):119–122, 1991.

[189] W Babisch, G Dutilleux, M Paviotti, A Backman, B Gergely, B McManus, et al. Good practice guide on noise exposure and potential health effects. *European Environmental Agency, EEA Technical report*, (11):2010, 2010.

[190] John Eargle. *The Microphone Handbook.* Elar Publishing, 1981.

[191] Glen Ballou. *Handbook for sound engineers.* Taylor & Francis, 2013.

[192] Ebrahim H Mamdani. Application of fuzzy logic to approximate reasoning using linguistic synthesis. *IEEE transactions on computers*, 100(12):1182–1191, 1977.

[193] E Ihara, L Summer, and L Shirey. Challenges for the 21st century: chronic and disabling conditions. *Prescription drugs a vital component of health care.* , 5:1–6, 2002.

[194] Dayna S Dalton, Karen J Cruickshanks, Barbara EK Klein, Ronald Klein, Terry L Wiley, and David M Nondahl. The impact of hearing loss on quality of life in older adults. *The Gerontologist*, 43(5):661–668, 2003.

[195] Colin Mathers, Andrew Smith, and Marisol Concha. Global burden of hearing loss in the year 2000. *Global burden of Disease*, 18(4):1–30, 2000.

[196] Henning Puder. Compensation of hearing impairment with hearing aids: Current solutions and trends. *Voice Communication (SprachKommunikation), 2008 ITG Conference on*, pages 1–4, 2008.

[197] Er Poi Voon, Tan Kok Kiong, Arun S Narayanan, Clarence W de Silva, and Lim Hsueh Yee. Development of digital pseudo binaural hearing aid. *Control and Intelligent Systems*, 41(3), 2013.

[198] R Gao, S Basseas, and DT Bargiotas. Next-generation hearing prosthetics. *IEEE robotics & automation magazine*, 10(1):21–25, 2003.

[199] Onder Yumak and H Metin Ertunc. Tool wear condition monitoring in drilling processes using fuzzy logic. In *International Conference on Neural Information Processing*, pages 508–517. Springer, 2006.

[200] Pan Fu and Anthony Hope. Fuzzy logic data fusion for condition monitoring. In *Applications of NDT Data Fusion*, pages 59–89. Springer, 2001.

Appendix A: Hearing aid features survey

e-HealthCM contains a built-in hearing aid function for its wearable module. A survey was conducted on the trial users of e-HealthCM system in order to better understand their usage experiences and expectations of the current hearing aid implementation. The survey forms are depicted Figure A1 and A2.

Summaries of users response to the survey questions:

(a) Question 1: None of the participants have ever used a commercial hearing aid. All the participants highlighted that cost is a major concern.

(b) Question 2: None of the participants use any form of hearing aids due to concern highlighted in Question 1.

(c) Question 3: Not Applicable.

(d) Question 4: Not Applicable.

(e) Question 5: Not Applicable.

(f) Question 6: Not Applicable.

(g) Question 7: Not Applicable.

(h) Question 8: All participants answered "NO". It is their first time using the hearing aid feature of the e-HealthCM.

(i) Question 9: All participants choose "Independent ears amplification adjustment" feature, three participants also choose "Fall Detection Alert" and "Panic Button for Help Request", and two participants also choose "Rechargeable battery".

(j) Question 10: All the participants choose "Excellent". Question 11: All the participants choose "S$100-S$200" price range.

In general, all the participants are very satisfied with the hearing aid function of the e-HealthCM wearable module.

Dear trial participant, we are doing a survey on hearing aids products. This survey takes about 10 minutes. Thank you for your participation.

Personal Particular				
Name			**NRIC**	
Date of Birth			**Age**	
Address		**Postal Code**	**Gender**	**Male / Female**
			Race	
			Tel	
Email			**Handphone**	
Occupation			**Monthly Income**	

Questionnaire (General)					
1	**Have you ever used hearing aids before?**	**Yes / No**		**Brand**	
				Cost	
		If "No", what are the reason(s) for not using a hearing aid (tick where applicable)			
		Lack of awareness			
		Troublesome having to see doctor			
		Troublesome of fitting a hearing aid			
		Cost concern			
		Not useful after trial			
		Others (please specify)			
2	**How long have you worn your Hearing Aids?**			**Start date of 1st used**	
3	**How long do you wear your hearing aids each day?**				
4	**Are you satisfied with your current hearing aids product?**	**Yes / No**		**If no, please specify reasons:**	
5	**What is the battery type and lifetime**	**Lifetime (hours)**		**Rechargeable / Non-rechargeable**	
6	**Where did you get your hearing aids from? (Please tick the appropriate)**	**Doctor**		**Hearing loss at:**	**left ear / right ear / both ears**
		Audiologist		**Location of Hearing test conducted:**	
		Hearing Aids Dealer			

Figure A1: Hearing aid survey form.

<table>
<tr><td rowspan="7">7</td><td rowspan="7">Do you feel like your hearing aids have lived up to what your audiologist or hearing aid dealer told you they would do?</td><td colspan="2">Yes / No</td><td colspan="4">If “No”, please indicate the reason(s) of dissatisfaction. (tick where applicable)</td></tr>
<tr><td colspan="2" rowspan="6">If “No”, please indicate when you stopped using it:</td><td colspan="2">Sound Unnatural</td><td colspan="2"></td></tr>
<tr><td colspan="2">Sound Unclear</td><td colspan="2"></td></tr>
<tr><td colspan="2">Acoustic Feedback</td><td colspan="2"></td></tr>
<tr><td colspan="2">Ear Discomfort</td><td colspan="2"></td></tr>
<tr><td colspan="2">Cost</td><td colspan="2"></td></tr>
<tr><td colspan="2">Others</td><td colspan="2"></td></tr>
<tr><td colspan="8">Questionnaire (e-WM Hearing Aid Function)</td></tr>
<tr><td>8</td><td>Have you seen or try out low cost hearing aids ?</td><td colspan="6">Yes / No</td></tr>
<tr><td rowspan="2">9</td><td rowspan="2">What features would you like to have in an elderly friendly watch hearing aid (Please tick the appropriate)</td><td>Fall Detection Alert</td><td></td><td>Rechargeable battery</td><td></td><td rowspan="2">Independent ears amplification adjustment</td><td rowspan="2"></td></tr>
<tr><td>“Panic Button” for Help Request</td><td></td><td>Water resistance</td><td></td></tr>
<tr><td rowspan="2">10</td><td rowspan="2">What do you think of this current design (Please tick the appropriate)</td><td>Excellent</td><td></td><td>Average</td><td></td><td colspan="2" rowspan="2"></td></tr>
<tr><td>Good</td><td></td><td>Poor</td><td></td></tr>
<tr><td>11</td><td>How much you willing to pay for this hearing aid</td><td>S$100-S$200</td><td></td><td>S$200-S$300</td><td></td><td>Above S$300</td><td></td></tr>
</table>

Figure A2: Hearing aid survey form (Continued).

Appendix B: e-HealthCM Trial Data Tabulation

Table B.1 - B.4 depict the trial results for the number of false fall detections respectively for each elderly volunteer. Table B.5 shows the trial results for the number of false fall detections using the modified e-WM by volunteer V1.

Table B.1: Volunteer S1 False Fall Occurrences.

Day	Motion Type				Error
	Walking	Sitting Down	Standing Up	Squatting	(Total/Day)
1	0	0	0	0	0
2	0	0	0	0	0
3	0	0	0	0	0
4	0	0	0	0	0
5	0	0	0	0	0
6	1	0	0	0	1
7	0	0	0	0	0
8	0	0	0	0	0
9	0	0	0	0	0
10	0	0	0	0	0
11	0	0	0	0	0
12	0	0	0	0	0
13	0	0	0	0	0
14	0	0	0	0	0
15	0	0	0	0	0
16	0	0	0	0	0
17	0	1	0	0	1
18	0	0	0	0	0
19	0	0	0	0	0
20	0	0	0	0	0
21	0	0	0	0	0
22	0	0	0	0	0
23	0	0	0	0	0
24	0	0	0	0	0
25	0	0	0	0	0
26	0	0	0	0	0
27	0	0	0	0	0
28	0	0	0	0	0
29	0	1	0	0	1
30	0	0	0	0	0

Table B.2: Volunteer S2 False Fall Occurrences.

Day	Motion Type				Error
	Walking	Sitting Down	Standing Up	Squatting	(Total/Day)
1	0	0	0	0	0
2	1	0	0	0	1
3	0	0	0	0	0
4	0	0	0	0	0
5	0	0	0	0	0
6	0	0	0	0	0
7	0	0	0	0	0
8	0	0	0	0	0
9	0	0	0	0	0
10	0	0	0	0	0
11	0	0	0	0	0
12	0	0	0	0	0
13	0	0	0	0	0
14	1	1	0	0	2
15	0	0	0	0	0
16	0	0	0	0	0
17	0	0	0	0	0
18	0	0	0	0	0
19	0	0	0	0	0
20	0	0	0	0	0
21	0	0	0	0	0
22	0	0	0	0	0
23	0	0	0	0	0
24	0	0	0	0	0
25	0	0	0	0	0
26	0	0	0	0	0
27	0	0	0	0	0
28	0	0	0	0	0
29	0	0	0	0	0
30	0	0	0	0	0

Table B.3: Volunteer S3 False Fall Occurrences.

Day	Motion Type				Error
	Walking	Sitting Down	Standing Up	Squatting	(Total/Day)
1	0	0	0	0	0
2	0	0	0	0	0
3	0	0	0	0	0
4	0	0	0	0	0
5	0	0	0	0	0
6	0	0	0	0	0
7	0	0	0	0	0
8	0	0	0	0	0
9	0	0	0	0	0
10	0	1	0	0	1
11	0	0	0	0	0
12	0	0	0	0	0
13	0	0	0	0	0
14	0	0	0	0	0
15	0	0	0	0	0
16	0	0	0	0	0
17	0	0	0	0	0
18	0	0	0	0	0
19	0	1	0	0	1
20	0	0	0	0	0
21	0	0	0	0	0
22	0	0	0	0	0
23	0	0	0	0	0
24	0	0	0	0	0
25	0	0	0	0	0
26	1	0	0	0	1
27	0	0	0	0	0
28	0	0	0	0	0
29	0	0	0	0	0
30	0	0	0	0	0

Table B.4: Volunteer S4 False Fall Occurrences.

Day	Motion Type				Error
	Walking	Sitting Down	Standing Up	Squatting	(Total/Day)
1	0	0	0	0	0
2	0	0	0	0	0
3	0	0	0	0	0
4	0	0	0	0	0
5	0	0	0	0	0
6	0	0	0	0	0
7	0	0	0	0	0
8	0	0	0	0	0
9	0	0	0	0	0
10	0	0	0	0	0
11	0	0	0	0	0
12	0	0	0	0	0
13	0	0	0	0	0
14	0	0	0	0	0
15	0	0	0	0	0
16	0	0	0	0	0
17	0	0	0	0	0
18	1	0	0	0	1
19	0	0	0	0	0
20	0	0	0	0	0
21	0	0	0	0	0
22	0	0	0	0	0
23	0	0	0	0	0
24	0	1	0	0	1
25	0	0	0	0	0
26	0	0	0	0	0
27	0	0	0	0	0
28	0	0	0	0	0
29	0	0	0	0	0
30	0	0	0	0	0

Table B.5: Volunteer V1 using modified e-WM for False Fall Occurrences.

Day	Motion Type				Error
	Walking	Sitting Down	Standing Up	Squatting	(Total/Day)
1	2	3	0	1	6
2	0	1	0	0	1
3	1	0	0	0	1
4	3	1	0	0	4
5	0	0	0	0	0
6	1	0	0	1	2
7	1	2	0	0	3
8	3	0	0	0	3
9	0	0	0	0	0
10	0	2	0	0	2
11	0	0	0	0	0
12	1	0	0	0	1
13	0	0	0	0	0
14	1	1	0	0	2
15	1	1	0	0	2
16	0	0	0	0	0
17	0	0	0	0	0
18	1	1	0	0	2
19	0	0	0	0	0
20	0	0	1	0	1
21	3	0	0	0	3
22	0	1	0	0	1
23	0	0	0	0	0
24	1	1	0	0	2
25	0	0	0	0	0
26	2	0	0	1	3
27	0	0	0	0	0
28	0	0	0	0	0
29	0	1	0	0	1
30	1	0	0	0	1

Author's Publications

Journal Papers

Poi Voon Er, and Kok Kiong Tan, "Development of Machine Condition Monitoring System based on Acoustics." *Submitted for publication in IEEE Sensors Journal.*

Poi Voon Er, and Kok Kiong Tan, "Development of a Non-Intrusive Fall Detection Monitoring System for the Elderly." *Submitted for publication in IEEE Sensors Journal.*

Kok Kiong Tan, Poi Voon Er, and Chek Sing Teo, "Machine Vibration Analysis based on Experimental Modal Analysis with Radial Basis Functions." *Submitted for publication in Elsevier Measurement Journal.*

Poi Voon Er, Chek Sing Teo, and Kok Kiong Tan, "Approach towards sensor placement, selection and fusion for real-time condition monitoring of precision machines." *Mechanical Systems and Signal Processing 68-69 (2016)*

Rui Yang, Poi Voon Er, Zidong Wang, and Kok Kiong Tan, "An RBF

neural network approach towards precision motion system with selective sensor fusion." *Neurocomputing 199: 31-39 (2016)*

Poi Voon Er, Rongmin Cao, Wenyu Liang, Rui Yang, Chek Sing Teo, and Kok Kiong Tan, "Selective approach towards robust control and accommodation of disturbances." *IJMA 4(3): 161-172 (2014)*

Conference Papers

Poi Voon Er, Chek Sing Teo, and Kok Kiong Tan, "An approach towards sensor selection and placement based on experimental modal analysis." *European Society for Precision Engineering and Nanotechnology's 15th International Conference and Exhibition*, Leuven, Belgium, 2015, pp. 237-238.

Chek Sing Teo, Poi Voon Er, and Kok Kiong Tan, "Finite element analysis validation of a novel experimental modal analysis method." *European Society for Precision Engineering and Nanotechnology's 15th International Conference and Exhibition*, Leuven, Belgium, 2015, pp. 239-240.

Kok Kiong Tan, Poi Voon Er, Rui Yang and Chek Sing Teo, "Selective precision motion control using weighted sensor fusion approach." *IEEE International Conference on Mechatronics and Automation*, Takamatsu, 2013, pp. 179-184.

Kok Kiong Tan, Rui Yang, Poi Voon Er, Arthur Tay and Chek Sing Teo, "RBF-based compensation method on displacement and thermal error."

IEEE International Conference on Mechatronics and Automation, Takamatsu, 2013, pp. 1039-1044.

Awards

Winner (Student Design Competition), *IASTED International Conference on Engineering and Applied Science (EAS 2012)*, Colombo, Sri Lanka, 27-29 Dec 2012.